Public Interest Energy Research (PIER) Program

White Paper

CLIMATE CHANGE EFFECTS ON THE HIGH-ELEVATION HYDROPOWER SYSTEM WITH CONSIDERATION OF WARMING IMPACTS ON ELECTRICITY DEMAND AND PRICING

A White Paper from the California Energy Commission's California Climate Change Center

Prepared for: California Energy Commission

Prepared by: University of California, Riverside
Lund University
University of Central Florida

JULY 2012

CEC-500-2012-020

Marion Guegan

Lund University

Kaveh Madani

University of California, Riverside
University of Central Florida

Cintia B. Uvo

Lund University

ACKNOWLEDGEMENTS

Most of this research was conducted during the time Kaveh Madani was a post-doctoral research scholar at the Water Science and Policy Center at the University of California, Riverside. The authors also thank the following individuals and entities for helping and facilitating this research:

- Ali Alaeipour, City of San Diego
- Karim Alizad, University of California, Riverside
- Shaahin Amini, University of California, Riverside
- Ariel Dinar, University of California, Riverside
- Guido Franco, California Energy Commission
- Haamun Kalaantari, University of California, Riverside
- Jay Lund, University of California, Davis
- Public Interest Energy Research (PIER) Program, California Energy Commission
- Water Science and Policy Center (WSPC), University of California, Riverside
- Water Resources Division, Lund University
- Hydro-Environmental and Energy Analysis (HEESA) Research Group, University of Central Florida

PREFACE

The California Energy Commission's Public Interest Energy Research (PIER) Program supports public interest energy research and development that will help improve the quality of life in California by bringing environmentally safe, affordable, and reliable energy services and products to the marketplace.

The PIER Program conducts public interest research, development, and demonstration (RD&D) projects to benefit California. The PIER Program strives to conduct the most promising public interest energy research by partnering with RD&D entities, including individuals, businesses, utilities, and public or private research institutions.

PIER funding efforts are focused on the following RD&D program areas:

- Buildings End-Use Energy Efficiency
- Energy Innovations Small Grants
- Energy-Related Environmental Research
- Energy Systems Integration
- Environmentally Preferred Advanced Generation
- Industrial/Agricultural/Water End-Use Energy Efficiency
- Renewable Energy Technologies
- Transportation

In 2003, the California Energy Commission's PIER Program established the California Climate Change Center to document climate change research relevant to the states. This center is a virtual organization with core research activities at Scripps Institution of Oceanography and the University of California, Berkeley, complemented by efforts at other research institutions.

For more information on the PIER Program, please visit the Energy Commission's website http://www.energy.ca.gov/research/index.html or contract the Energy Commission at (916) 327-1551.

ABSTRACT

While only about 30 percent of California's usable water storage capacity lies at higher elevations, high-elevation hydropower units generate, on average, 74 percent of California's in-state hydroelectricity. In general, high-elevation plants have small man-made reservoirs and rely mainly on snowpack. Their low built-in storage capacity is a concern with regard to climate warming. Snowmelt is expected to shift to earlier in the year, and the system may not be able to store sufficient water for release in high-demand periods. Previous studies have explored the climate warming effects on California's high-elevation hydropower system by focusing on the supply side (exploring the effects of hydrological changes on generation and revenues) but they have ignored the warming effects on hydropower demand and pricing. This study extends the previous work by simultaneous consideration of climate change effects on high-elevation hydropower supply and demand in California. Artificial Neural Network models were developed as long-term price estimation tools, to investigate the impact of climate warming on energy prices. California's Energy-Based Hydropower Optimization Model (EBHOM) was then applied, to estimate the adaptability of California's high-elevation hydropower system to climate warming, considering the warming effects on hydropower supply and demand. The model was run for dry and wet warming scenarios, representing a range of hydrological changes under climate change. The model's results relative to energy generation, energy spills, reservoir energy storage, and average shadow prices of energy generation and storage capacity expansion are examined and discussed. The modeling results are compared with previous studies to emphasize the need to consider climate change effects on hydroelectricity demand and pricing when exploring the effects of climate change on California's hydropower system.

Keywords: Hydropower, climate change, electricity, energy, generation, supply, demand, price, Artificial Neural Network, California, high-elevation, EBHOM, optimization

Please use the following citation for this paper:

Guegan M., K. Madani, and C. B. Uvo. 2012.***Climate Change Effects on the High-Elevation Hydropower System with Consideration of Warming Impacts on Electricity Demand and Pricing.*** California Energy Commission. Publication number: CEC-500-2012-020.

TABLE OF CONTENTS

LIST OF FIGURES

LIST OF TABLES

Section 1: Introduction

Hydropower facilities in California generated on average 37,000 gigawatt-hours (GWh), or 15 percent, of the annual in-state electricity generation between 1983 and 2001; ranging annually between 9 percent and 30 percent, depending on hydrological conditions (McKinney et al. 2003). When precipitation runoff is plentiful, hydroelectric generation is prioritized, while other power plants, mostly gas-fired facilities, may be shut down temporarily (McKinney et al. 2003). Hydroelectricity's very low cost, near-zero emissions, and load-following capacity are some of the reasons for its great popularity (McKinney et al. 2003; Pew Center on Global Climate Change 2009). The State of California has the second largest hydropower system in the United States, behind the state of Washington, with a total hydroelectric capacity over 14,000 megawatts (MW), representing 25 percent of California's electricity generation capacity (McKinney et al. 2003). California also relies on hydroelectricity imports from the Pacific Northwest, including Canada and the states of Oregon and Washington (Aspen Environmental Group and M. Cubed 2005).

California's statewide average temperatures are expected to rise between 3°F and 10.5°F (1.7°C and 5.8°C) by 2100 (CCCC 2006; Cayan et al. 2008 and 2009). This temperature increase is expected to decrease the state's snowpack reserve at high elevations and shift the runoff from snowmelt to an earlier period of the year than today (CCCC 2006). Variations in the annual runoff pattern may significantly alter hydropower generation, depending on the system's storage and generation capacities. California's state is currently encouraging active research on the adaptability of hydropower systems to climate change (e.g., Aspen Environmental Group and M. Cubed 2005; Tanaka et al. 2006; Madani and Lund 2007; Medellin-Azuara et al. 2008; Madani et al. 2008; Vicuña et al. 2008; Madani 2009; Duffy et al. 2009; Madani and Lund 2010; Madani 2011; Connell-Buck et al. 2011; Vicuña et al. 2011). Besides affecting the availability of water for electricity generation, higher temperatures will likely increase demand for cooling in warm periods (CCCC 2006; Franco and Sanstad 2006; Aroonruengsawat and Auffhammer 2009).

Rising energy demand, coupled with reduced hydroelectricity generation, could lead to a substantial impact on the electricity market. A rise in hydroelectricity prices is foreseeable, and electricity distributors will probably also have to shift to more-expensive, less-environmentally friendly energy sources to replace the lost hydropower generation (Union of Concerned Scientists 2006). To the best of the authors' knowledge, no study has addressed the impact of climate change on electricity prices in California by considering simultaneously changes in supply and demand of hydroelectricity.

California's Electricity Supply Industry (ESI) is a deregulated competitive market supervised by the state. It relies on long-term contracts regulated by the State to avoid market manipulations like those that happened during the California crisis of 2000–2001 (CBO 2001). The California Power Exchange (CalPX) operates the day-ahead market and sets the price that the generators will use to sell electricity, based on a bidding process. The California Independent System

Operator (CalISO) operates the region's power grid and wholesale electric markets, and deals with real-time imbalances of energy, ancillary services, and transmission usage.

The specificity of the electricity market compared to other commodities is that it requires a well-coordinated balance between generation and consumption, since storage of electricity remains limited and expensive (Amjady and Hemmati 2006). Therefore, accurate short-term price forecasting is crucial information for producers and retailers to develop their bidding strategy in a day-ahead electricity market; and has prompted many research works (e.g., Zhao et al. 2007; Zarezadeh et al. 2008; Amjady and Keynia 2010a). However, this is not an easy task, as price of electricity is a nonlinear, time-variant, and volatile signal owning multiple periodicity, high-frequency components, and significant outliers, i.e., unusual prices (especially in periods of high demand) due to unexpected events in the electricity markets (Amjady and Hemmati 2006). The application of Artificial Neural Network (ANN) models has provided a good ability to forecast normal electricity prices (Zhao et al. 2007). ANNs provide an appealing solution for relating nonlinear input and output variables in complex systems (ASCE 2000; Dawson and Wilby 2001).

The present research addresses the impacts of climate warming on California's high-elevation hydropower system, considering simultaneously the impact of climate change on the supply, demand, and pricing sides. The main contribution of this work is the development of a long-term price estimation model using Artificial Neural Networks. The novel long-term price estimation ANN model developed by Guégan et al. (2012) is used to estimate climate warming impacts on electricity prices. In this model price representation is based on the estimation of a relationship between temperature, electricity demand, time of year, and electricity price. The obtained results were finally fed into the model of Madani and Lund (2009) for hydropower operation optimization based on profit maximization to estimate statewide high-elevation hydropower system adaptability to climate change.

The paper is organized as follows: Section 2 describes California's hydropower system; Section 3 describes historical electricity demand and pricing trends in California; Section 4 is a literature review of climate change effects on hydropower supply and demand; Section 5 defines the research methodology;Section6presents the results from the hydropower optimization model simulations under climate warming scenarios; Section7discusses the limitations of the study and future direction; and Section8concludes the discussion. Details about the ANN models developed and the estimated effects of climate warming scenarios on electricity prices are provided in Appendix A.

Section 2: California and Hydropower

Climate across the California region can be very different, due to the great differences in altitude and in latitude of the state. According to Kauffman (2003), five major climate types can be observed in close proximity in California; namely Desert, Cool Interior, Highland, Steppe, and Mediterranean. As the objective of this research is to study the impacts of statewide climate change on California's high-elevation hydropower system, only major trends of temperature and precipitation distribution will be presented. Much of California has warm, dry summers and cool, wet winters (Zhu et al. 2005). In terms of electricity demands this corresponds to high demands in summer for air cooling (Figure 1) and in winter for heating; whereas, the lowest demands occur in spring and autumn, when neither great heating nor cooling is required. Precipitation is very uneven throughout the year, with around 75 percent of the annual 584 millimeters (mm) occurring between November and March (Zhu et al. 2005) and falling as snow in the Sierra Nevada mountain range (Moser et al. 2009). This situation results in spatially uneven runoff, with more than 70 percent of California's average annual runoff occurring in northern California (Madani and Lund 2009).

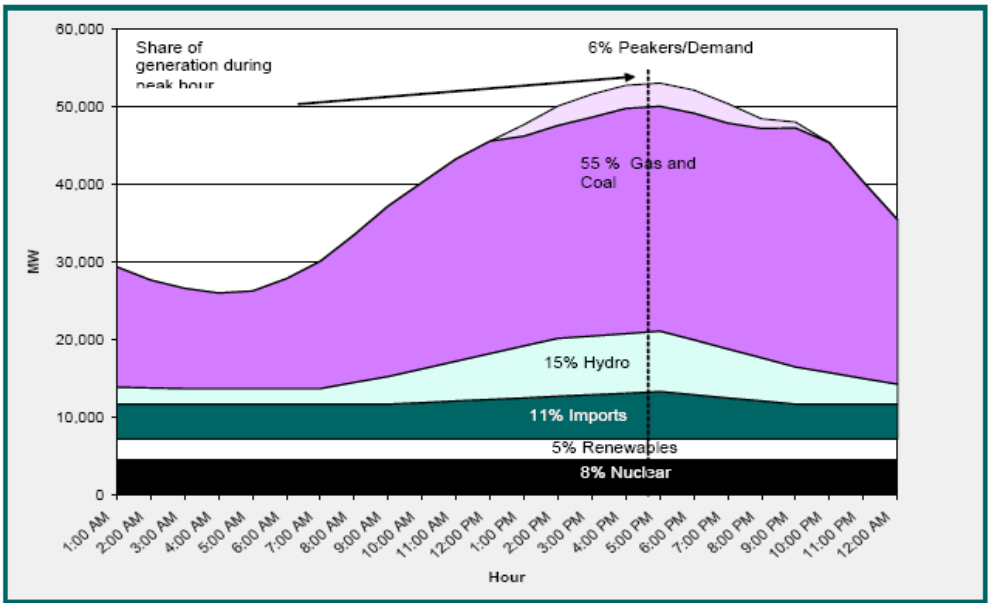

Source: Mc Kinney et al. 2003

Figure 1: Electricity Supply and Demand Profile for a Typical Hot Summer Day

California's hydroelectric system generated 15 percent, on average, of the annual in-state generation between 1983 and 2001 (McKinney et al. 2003). In-state hydropower is generated by four types of hydropower systems: high-head, low-storage hydropower plants; low-head multipurpose dams; pumped-storage plants; and run-of-the-river units (Pew Center on Global Climate Change 2009). Figure2 shows the distribution of California's hydropower system.

While only about 30 percent of the state's usable water storage capacity is at higher elevations, high-elevation hydropower units generate, on average, 74 percent of California's in-state hydroelectricity (Madani and Lund 2009). Madani and Lund (2009) have identified 156 high-

elevation hydropower plants above 1,000 feet (305 meters). Most are located in Northern California (Aspen Environmental Group and M. Cubed 2005). Hydroelectric generation is generally their only purpose, and only small amounts of water are necessary to produce substantial quantities of electricity with vertical drops of water of hundreds of feet (Pew Center on Global Climate Change 2009). They have been designed to take advantage of the snowpack acting as a natural reservoir and their human-made reservoir is usually small. Their limited storage capacity may make them sensitive to future snowpack volume and runoff timing variations (Madani and Lund 2010).

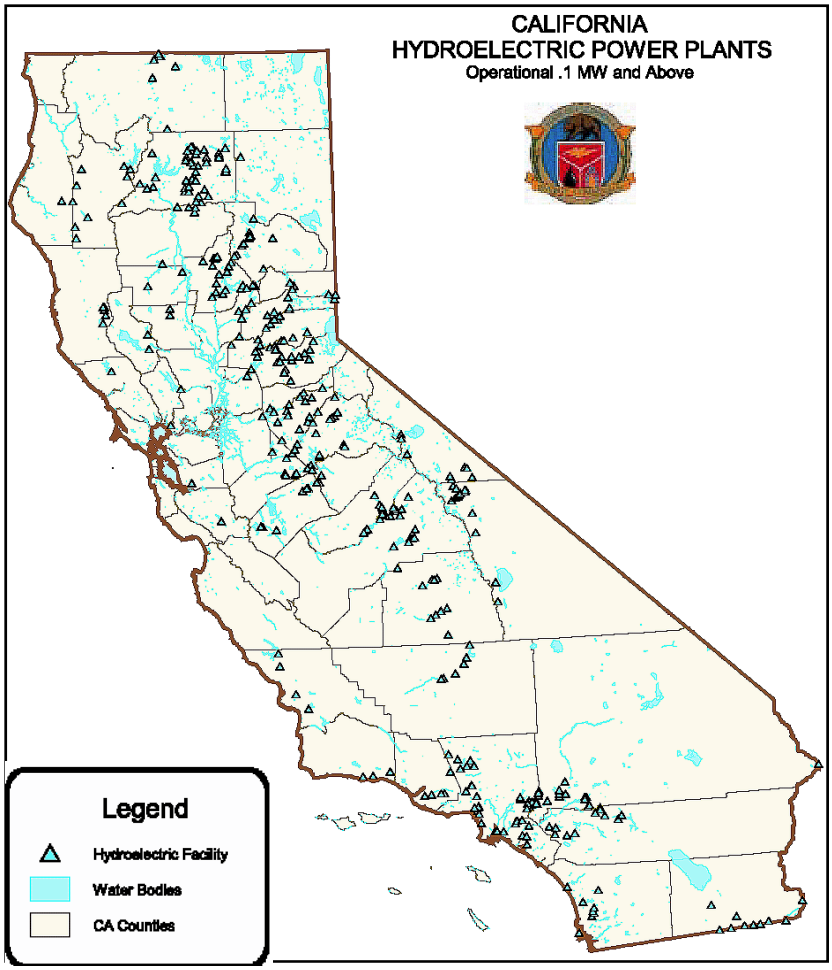

Source: California Energy Commission,www.energy.ca.gov/hydroelectric/hydro_power_plants.html

Figure 2: Hydroelectric Power Plant Distribution in California (Capacity > 1 MW)

Section 3: Electricity Demand and Pricing in California

The disparities between the trends in electricity demand in California and the United States have been of great interest to the scientific community (e.g., Kandel et al. 2008; Horowitz 2007; Rosenfeld 2006). California's aggregate electricity consumption per capita (ECP) remained almost flat since 1976, while it increased by around 50 percent nationwide, as shown in Figure 3. On a sector-by-sector basis, the main difference comes from the industrial and residential sectors. Between 1973 and 2005, California's residential per capita electricity consumption increased slowly (by 14 percent) compared to that in the United States overall, where it increased by 60 percent (Kandel et al. 2008). California's slow increase in residential ECP is related to many factors, including: its mild climate compared to other states, resulting in less heating and less cooling demand in winter and summer respectively (Kandel et al. 2008); the high concentration of urban areas with many multi-family units (Kandel et al. 2008); the higher-than-U.S. average energy prices (see Figure 5), encouraging consumers to save energy (Kandel et al. 2008); and probably the aggressive energy-efficiency programs launched around 1976 (Horowitz 2007). Between 1973 and 2005, California's industrial sector reduced its ECP by 39 percent, partly because there has been a structural change in California's economic structure since the late 1990s that has bartered energy-intensive manufacturing for less-energy intensive services (Tanton 2008).

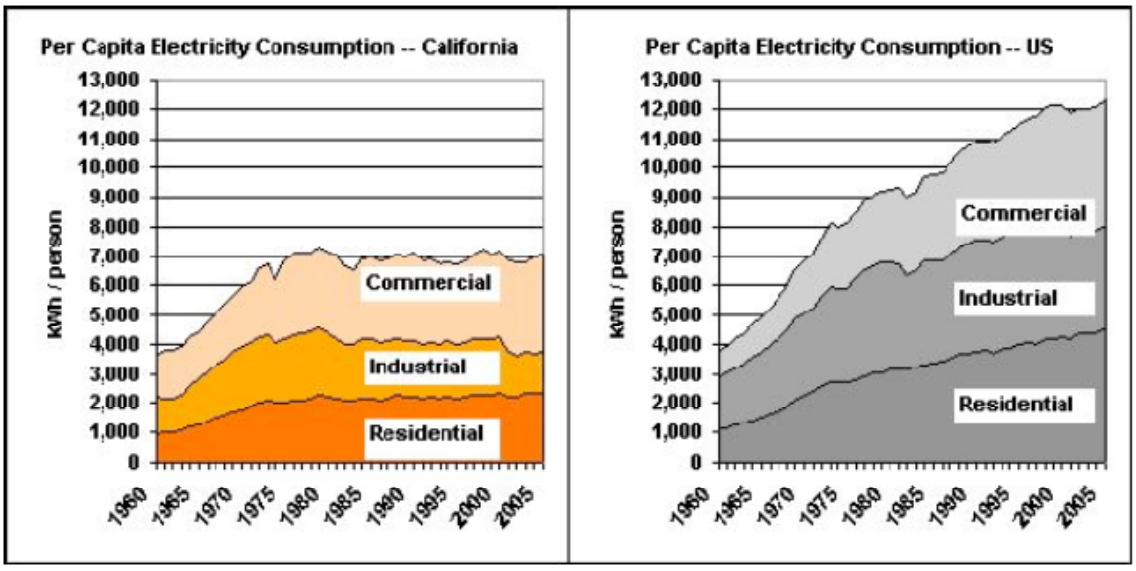

Source: Kandel et al. 2008

Figure 3: California and U.S. Per Capita Electricity Use by Sector, 1960–2008

Meanwhile, California's ECP has remained roughly flat. Its aggregate electricity consumption has increased by 65 percent between 1980 and 2008, as have its imports of electricity; with, for example, a 60 percent increase in coal-based electricity imports from 1983 to 2005 (Tanton 2008).

The electricity peak demand in California has also been increasing, as illustrated in Figure 4, but slowed after the initialization of energy-efficiency programs in 1976 (Rosenfeld 2006). California electricity peak demand reached 55 gigawatts (GW) in 2004.

Average nominal U.S. retail electricity prices have increased significantly since the 1970s, as shown in Figure 5, as a result of the 1970s fuel crisis (Bloom Energy 2010). On average, prices in California are higher than in the rest of the nation. The second energy crisis experienced by California in 2001 led to a retail price jump of30 percent between 1999 and 2002, and prices have not decreased significantly since then (Figure 5). In 2006, California had the second-highest retail sales in the United States, according to Kandel et al. (2008). A linear regression of the average retail prices for the period 1960–2005 corresponds to an annual growth rate of around 0.25cents/kilowatt-hour (KWh). If a similar linear increase is considered up to the end of the twenty-first century, this would lead to an increase of 25 cents/KWh by 2100, or an increase of more than 100 percent compared to 2005.

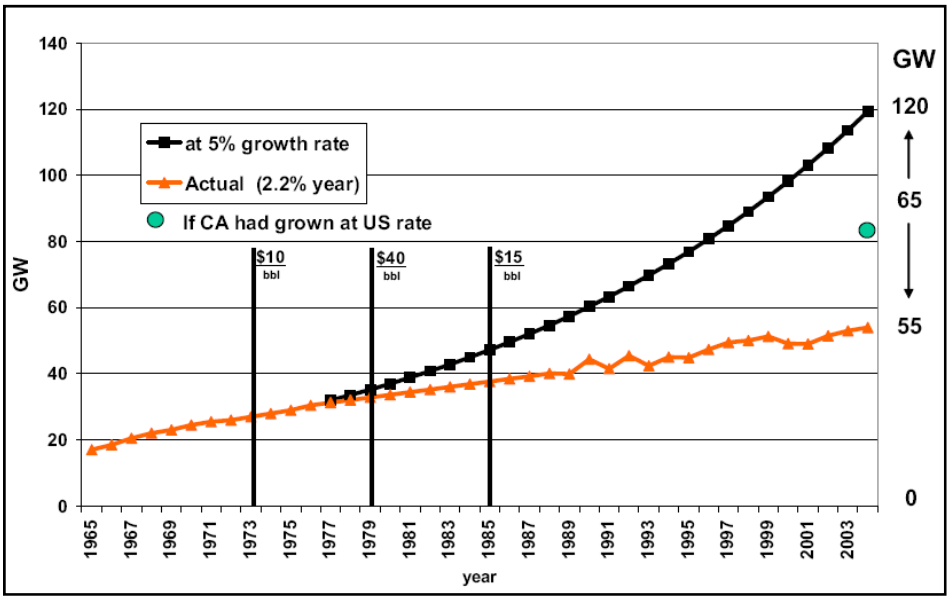

Source: Rosenfeld 2006

Figure 4: California Peak Electricity Demand, 1965–2004

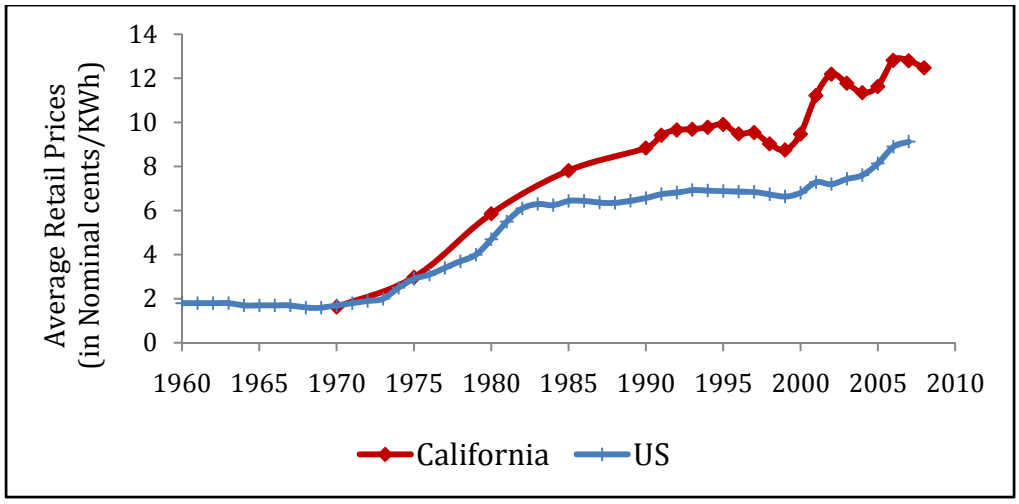

Source: EIA, data compiled from AER: Table 8.10; SEDS – California: Table 5.3 and California Electricity Profile: Table 8

Figure 5: Average Retail Price of Electricity to Ultimate Consumer in Nominal Dollars, for U.S. and California, 1960–2008

Section 4: California and Climate Change

Climate Change Scenarios for California

The scientific community agrees that the mean global temperature is expected to increase worldwide; whereas, the future hyetograph pattern is still uncertain (CCCC 2006; Cayan et al. 2008 and 2009). Cayan et al. (2008 and 2009) focused their study on changes in climate at the surface, mostly related to temperature and precipitation, and addressed plausible pathways for the California region. The climate change scenarios are produced by combining Global Climate Models (GCMs) to greenhouse gas (GHG) emission scenarios, as defined in the Intergovernmental Panel on Climate Change (IPCC) Fourth Assessment released in 2007. Three probable sets of projections of GHG emissions for California are the B1 (low emissions), A2 (medium-high emissions), and A1fi (high emissions) storylines (Figure 6) (Cayan et al. 2008 and 2009).

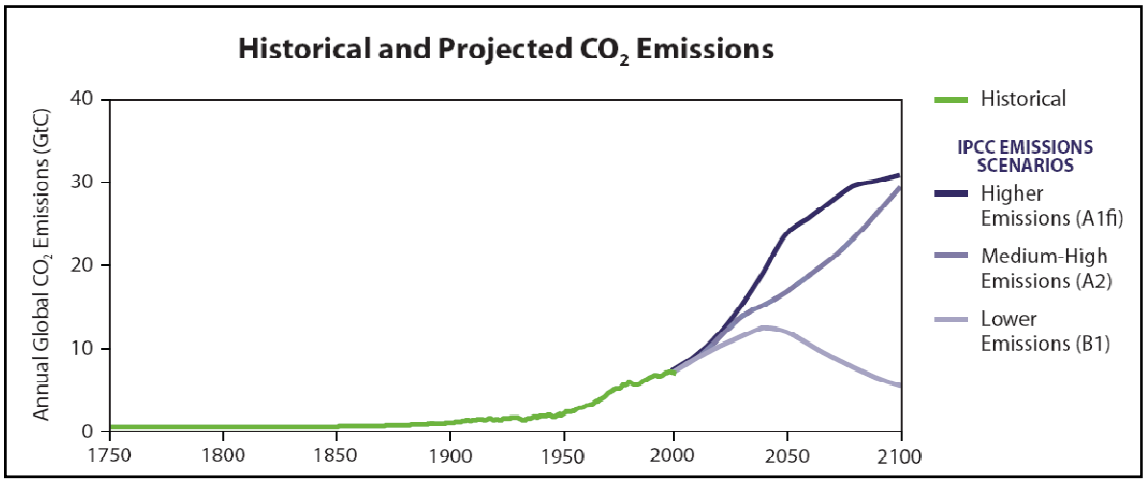

Source: CCCC 2006

Figure 6: Historical and Projected CO_2Emissions: Scenarios B1, A2, and A1fi

The magnitude of projected temperature rise over the twenty-first century varies between the model sensitivity and the emission scenarios, as illustrated in Figure 7. By 2100, temperature increases are estimated to range between 1.5°C and 4.5°C (2.8°F–8.0°F) under the lower-emission scenario B1 in the less-responsive GCM PCM (Parallel Climate Model)and under the higher-emission scenario A2 in the GFDL (Geophysical Fluid Dynamics Laboratory model), respectively (Cayan et al. 2009). Generally, warming is expected to be greater in summer than the rest of the year in all scenarios except the PCM B1 scenario (Cayan et al. 2008). Warming should affect both wet and dry days at about the same degree (Cayan et al. 2006). In their works, Cayan et al. (2008 and 2009) present different plausible temperature increases for both the Northern California region (NOCAL) and Southern California region (SOCAL).

Climate warming is likely to affect hydropower's supply/generation, demand, and pricing simultaneously. To the best knowledge of the authors, these issues have always been addressed independently. The following sections review recent research conducted in California on

climate warming impacts on hydropower supply (e.g., Vicuña et al. 2008 and 2011; Madani and Lund 2010) and demand (e.g., Franco and Sanstad 2006; Aroonruengsawat and Auffhammer 2009).

Previous works assessing climate change impacts in California have commonly used a range of plausible scenarios from an earlier work of Cayan et al. (2006) or directly based on the former IPCC Third Assessment (e.g., Medellín-Azuara et al. 2008; Vicuña et al. 2008; Aroonruengsawat and Auffhammer 2009; Madani and Lund 2010).

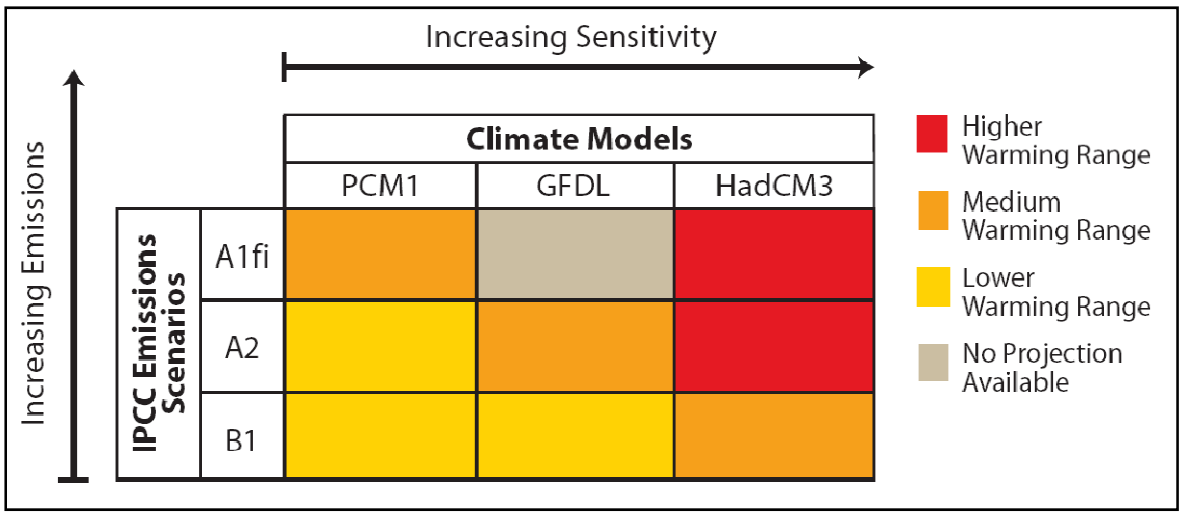

Source: CCCC 2006

Figure 7: Warming Ranges for Three Plausible GCMs Coupled with Three GHGs for California

Impacts on Hydropower Supply

Climate change will affect hydrological conditions. California's twenty-first century hydrology is expected to be altered in the following manner: part of the winter precipitation falling as snow will turn to rain; higher temperatures will lead to a shift in timing of the snowmelt peak flow; peak flow's intensity will be reduced; and winter runoff is increased (Moser et al. 2009).

Hydrological changes create a big concern for California's hydropower system, which may face water shortages in summer when the demand is the highest (Moser et al. 2009; Madani and Lund 2010). This issue should be less problematic for low-elevation multipurpose hydropower systems (less than 1,000 feet) benefitting from large human-made reservoirs, than it is for high-elevation units with small human-made reservoirs (Tanaka et al. 2006; Medellin-Azuara et al. 2008; Connell-Buck et al. 2011). Relying mainly on natural snowpack reserves, high-elevation hydropower systems have a limited flexibility in operation. If their storage capacity cannot accommodate hydrological changes, these high-elevation hydropower systems may be vulnerable to climate change (Madani and Lund 2010).

According to Madani and Lund (2010), most studies assessing the impacts of climate change on hydropower generation in California have focused on large-scale, low-elevation systems (e.g., Tanaka et al. 2006 and Medellin-Azuara et al. 2008) or on a few individual high-elevation

hydropower units (e.g., Vicuña et al. 2008 and 2011; Madani et al. 2008). High-elevation systems are nonetheless generating 74 percent of California's in-state hydroelectricity on average (Madani and Lund 2009), which has prompted recent research on the impacts of climate change on high-elevation hydropower systems (e.g., Vicuña et al. 2008 and Madani and Lund 2010).

Vicuña et al. (2008) studied the impact of four climate change scenarios on high-elevation hydropower system in the Upper American River, using a linear programming model that maximizes the system's revenue, subject to operational and physical constraints. The model ran under the historical scenario and replicated expected patterns of operation, with reservoir refilling in spring and electricity generated in priority when it is the most valuable. For the two drier scenarios, both power generation and energy revenue decreased, but generation decreased more than revenue, showing the system's ability to store water when prices are low for a later release when energy is more valuable (July-September). For the wetter scenarios, the increase in generation outpaced the increase in revenue, and the generation pattern was similar to the hydrograph. For all scenarios, the occurrence of spillage increased, caused by the inconvenient hydrograph.

The energy price representation considered by Vicuña et al. (2008) distinguished two constant on-peak and off-peak monthly prices; capturing some effects of non-constant energy prices. If fixed monthly prices were used, a model based on revenue maximization would suggest that there would be no generation in months with low energy prices, to allow maximum generation in months where energy is valuable (Madani and Lund 2007). Madani and Lund (2009) formulated a new approach, where the price representation was derived from the distribution of hourly real-time prices for each month. This allowed for capturing the hourly variability in energy prices—on a monthly basis—of the overall energy market that is responding mostly to on-peak and off-peak variability in energy demands. The energy price used was a function of the percent of the time that turbines are in operation, assuming that they operate in hours when the energy market offers higher prices (Madani and Lund 2009)[1].

Madani and Lund (2009) also introduced a novel approach to model the operations of a large number of high-elevation hydropower systems, using the Energy-Based Hydropower Optimization Model (EBHOM). EBHOM is the only one of its kind, allowing the modeling of an entire region's high-elevation hydropower system in a relatively straightforward manner, without the need to develop traditional stream flow and reservoir volume-based models for

[1] The suggested method develops monthly revenue curves to capture the considerable effects of on-peak and off-peak pricing on the revenues. Since in real electricity markets, prices fluctuate on an hourly basis and marginal revenues of generation decrease with increased hours of generation, fixed pricing methods fail to reflect the reality of the market. While capturing the fluctuating nature of the pricing in the hydropower market is possible through developing an hourly-based hydropower operations model, calculation effort for running such models can be burdensome. The suggested monthly revenue curves are developed based on the frequency distribution of hourly hydropower prices in the market. The revenue curves approximately represent hourly pricing within a monthly model, reducing the calculation effort. More details about the suggested method can be found in Madani and Lund (2009).

each plant in the system. To evaluate the reliability of EBHOM, this model was tested against the traditional hydropower optimization model developed by Vicuña et al. (2008) on the Upper American River system in a collaborative study by Madani et al. (2008). Both models predicted the same changes in generation and revenue with respect to the historical case[2]. Even if the EBHOM is very simplified compared to traditional optimization models, it produces reasonable results and is a step forward toward modeling global trends, including "the effects of climate change and energy prices on system-wide generation and hydropower revenues" (Madani and Lund 2010).

Madani and Lund (2010) applied EBHOM to estimate the impacts of climate warming on California's high-elevation hydropower system for the three following scenarios: warming-only, dry warming (GFDL-A2)[3], and wet warming (PCM-A2). Warming-only and dry warming scenarios show both reduced generation and revenue, while the wetter scenario has the opposite effect. Current storage and generation capacities are able to cope with some of the supply loss of the dry warming scenario. Compared with the base historical scenario, the 20 percent runoff decrease led to revenue losses of only 14 percent. Conversely, the 10 percent increase of annual runoff compared to the Base case led to an increase of only 6 percent in generation and 2 percent in revenues for the Wet case scenario. Spills increased for all scenarios except the Dry one.

The above-mentioned studies only considered that climate warming will change hydrologic conditions and alter hydropower water supply. Therefore, potential changes in electricity demand and prices, resulting from various climatic, economic, technologic, policy or market reasons (Madani and Lund 2010),were not accounted for.

Impacts on Hydropower Demand

On the demand side, climate warming is expected to increase the need for cooling in summer and reduce the need for heating in winter (CCCC 2006).

Franco and Sanstad (2006) examined the statewide correlation between daily average quantities (mean daily temperatures and base loads) and extreme quantities (maximum daily temperatures and peak loads). They determined a nonlinear convex relationship between average daily temperature and demand, and a linear relationship between summer peak load and maximum temperatures. Then they developed climate change scenarios for the twenty-first century and examined demand responsiveness (considering the relationships between demand and temperature invariant in the future). Relative to the base period 1961–1990, electricity demand increased in the range of 3.1–20.3 percent, and peak load increased in the range of

[2] Further details on validation of the EBHOM can be found in Madani et al. (2008) and Madani and Lund (2009).

[3] The dry warming scenario used in Madani and Lund (2010) may be considered as the worst case scenario as it is only one realization of multiple climate warming scenarios available for California.

4.1–19.3 percent by 2100. It is noteworthy that even a small increase in demand would result in a high increase in energy expenditures (Franco and Sanstad 2006).

Miller et al. (2008) estimated a potential for electricity deficits as high as 17 percent during peak electricity demand periods. To estimate the deficits, they mapped the projected extreme heat under climate warming and observed relationships between high temperature and electricity demand for California onto current availability, maintaining technology and population constant for demand-side calculations. They concluded that future increases in peak electricity demand can result in challenges to the current transmission and supply systems, especially when population and income growth are taken into account.

Aroonruengsawat and Auffhammer (2009) used a unique panel of household electricity billing data from California's three largest investor-owned utilities. They did not estimate demand as a function of statewide temperature, but divided California in 16 climate zones. They projected an increase in aggregate demand ranging from 18 percent to 55 percent by 2100 for a constant population. This represents an average annual growth rate of aggregate electricity demand ranging between 0.17 percent and 0.44 percent. In reality, these growth rates accelerate with time.

Aroonruengsawat and Auffhammer (2009) also coupled climate warming to economical future scenarios. They developed two scenarios that considered electricity price increases based on the projected impacts of AB 32 compliance combined with natural gas price increases: a discrete 30 percent increase by 2020 remaining to the same level until the end of the century, and two successive increases of 30 percent by 2020 and 20 percent by 2040. By 2100, the total change in demand ranged between +4 percent and +39 percent for the low price increase scenario and between -7 percent and +24 percent for the high price increase scenario. Higher prices result in a decreased demand compared to the Base case, where no price increase was considered.

Aroonruengsawat and Auffhammer (2009) also considered population increase scenarios. Combined to a low forcing climate warming scenario, a low projection of 0.18 percent population growth rate per year (equivalent to a population increase of 18 percent by 2100) predicts an increase of 65 to 70 percent in residential electricity demand by 2100. This increase is much higher than the 20 percent increase predicted for the climate warming-only scenario. The worst case they predicted coupled a high forcing scenario with a high growth rate (+1.47 percent per year) and suggested an increase in demand up to 478 percent. Demographic trends have substantial impacts on future energy demands and nearly outweigh the impact of climate change.

Many additional parameters are plausible drivers for future electricity demand changes: demographic trends (size and distribution of the state's population); economic growth (Aroonruengsawat and Auffhammer 2009); changes in the energy market (demand and pricing of resources such as gas, nuclear, or photovoltaic) (Franco and Sanstad 2006); new stringent environmental policies; human's adaptation to warmer conditions; energy use efficiency improvements; and others.

Section 5: Method

This section briefly describes the overall method used in this work, based on the flowchart in Figure 8. The following sections provide further details on the models selected and the choices and assumptions made.

The research team developed an artificial neural network (ANN) model to map the relationship between a set of inputs and the hourly electricity prices. Details about the developed ANN model have been provided in Appendix A and Guégan et al., (2012). The inputs to the ANN model include temperature, demand, and deterministic components (e.g., season, day of the week, hour). An ANN model was chosen because it is a powerful machine learning tool that provides an appealing solution for relating input and output variables in complex systems (Dawson and Wilby 2001). ANNs are capable of extracting information from systems even with little prior physical knowledge about the systems (Zhang et al. 1998). The ANN architecture chosen was a multilayer feedforward model using the Shuffle Complex Evolution (SCE-UA) global-search optimization method developed by Duan et al. (1992).

The ANN performance is reliant on the quantity and quality of the calibration data (Kingston et al. 2005). As described in Appendix A and Guégan et al., (2012) before calibration of the model, the researchers performed a preliminary statistical analysis of the collected data, to get an overview of existing trends and potential problems, and to allow for adequate data pre-processing. Once the ANN was trained, simulations with perturbed input data were run to account for the chosen climate warming scenarios. Scenarios were chosen from the work of Cayan et al. (2009) based on the IPCC Fourth Assessment. The outputs of the trained ANN are predicted hourly prices. The price representation chosen for the next modeling steps were based on the work of Madani and Lund (2009) capturing the hourly variability of energy prices.

The research team estimated the climate warming effect on California's high-elevation hydropower system using the Energy-Based Hydropower Optimization Model (EBHOM) developed by Madani and Lund (2009). Price frequency and revenue curves (integration over the price frequency curves) were drawn and used as inputs to EBHOM, together with historic monthly generation data and seasonal runoff distributions. The EBHOM results are monthly optimized generation, revenue and end-of-month storage data for the statewide high-elevation hydropower system, considering climate change effects on demand, supply, and pricing.

Previous findings from Madani and Lund (2010), assessing only the supply-side impacts of climate change, were compared to the results from this research.

Appendix A includes a description of existing ANN models, followed by data collection and analysis, ANN model selection, set up, and calibration. It includes the application of the trained ANN model to estimate future price scenarios. Section6 presents EBHOM and its results.

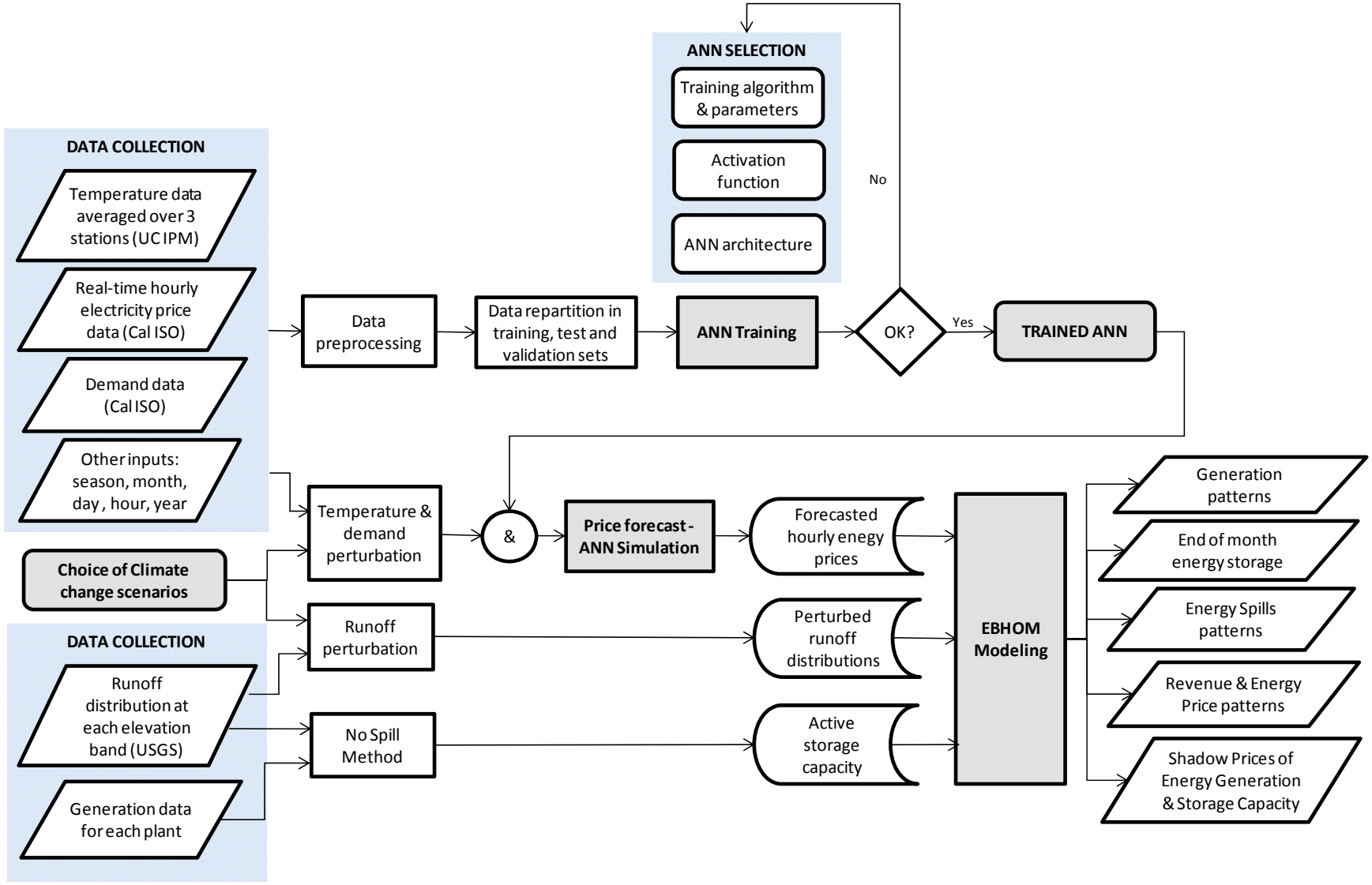

Source: Authors

Figure 8: Flow Chart of the Project's Methodology

Section 6: Energy-Based Hydropower Optimization Model (EBHOM)

Model Set Up

This study investigates the effects of climate change on California's high-elevation hydropower plants using the Energy-Based Hydropower Optimization Model (EBHOM) developed by Madani and Lund (2009). EBHOM is a monthly step model which performs all storage, release, and flow calculations in energy units (Madani and Lund 2009). It provides a big picture of the system and is an interesting alternative to conventional volume-based optimization models that usually require detailed information such as streamflows, turbine capacities, storage operating capacities, and energy storage capacities at each individual plant of the system.

Figure 9 is a flowchart of the EBHOM modeling procedure. The input data required to run EBHOM are: runoff data, available storage capacity at each power plant, and frequency of hourly electricity prices for each month of the year. See Madani and Lund (2009) for details on EBHOM's mathematical formulation.

Runoff data representative of three elevation ranges (1000–2000, 2000–3000 and >3000 feet) were gathered previously from several U.S. Geological Survey (USGS) gauges as described in Madani and Lund (2009). Three elevation bands were chosen to take into account the different value of the snowpack and precipitation in each band. Monthly runoff distributions in each range were then perturbed using monthly runoff perturbation ratios of the adopted climate change scenarios, as described by Vicuña et al. (2008). A perturbation ratio is "a simple ratio of average runoff predicted by a GCM for different eras for a given time period(e.g., $Q_{2070–99}/Q_{1960–90}$, where Q is average July streamflow)" (Vicuña et al. 2008).

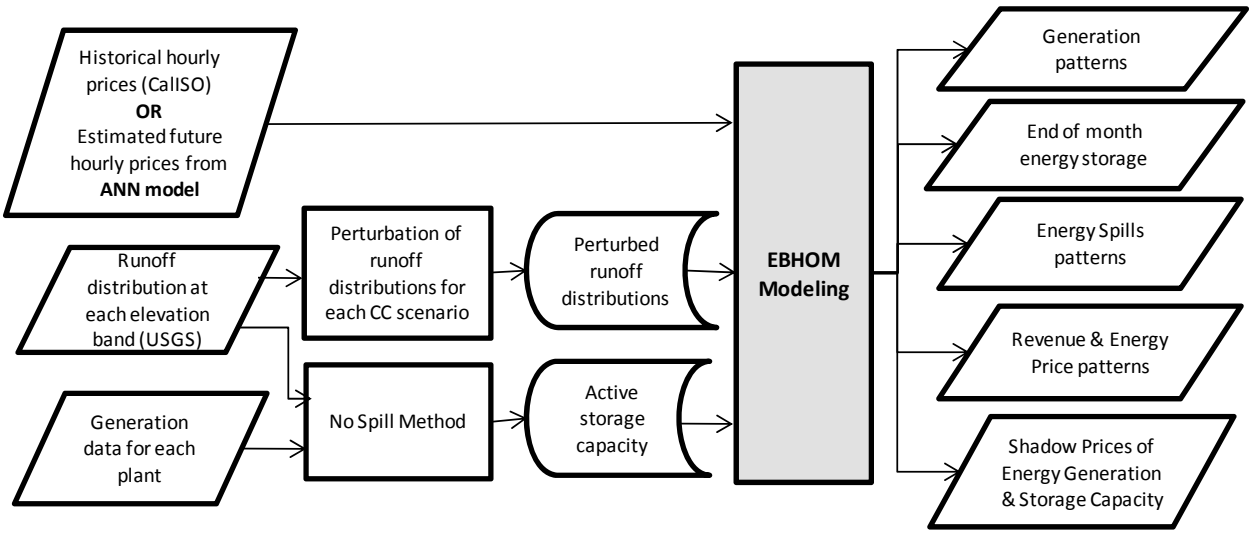

Source: Authors

Figure 9: Flowchart of EBHOM Modeling Procedure

The available energy storage capacity at each power plant is determined using the No Spill Method (NSM) developed by Madani and Lund (2009), which is applicable when: plants are operated for net revenue maximization, storage volumes do not significantly affect the head, and there is no over-year storage. These conditions are filled by California's high-elevation hydropower system (Madani and Lund 2009).

The price representation used to run is either historical prices or forecasted prices from the earlier ANNs developed, depending on the climate scenarios. Revenue curves were drawn by integration over the price frequency curves for each month and were then piecewise linearized into five segments to solve EBHOM through linear programming (Madani and Lund 2009).

Climate Warming and Price Increase Scenarios

Table 1 summarizes the scenarios selected to run EBHOM. A dry warming (GFDL-A2)[4], and a wet warming (PCM-A2) scenario were chosen to be consistent with the previous research of Madani and Lund (2010). Also chosen was an additional seasonal dry warming scenario considering high temperature increases in summer and low temperature increases in winter. For each climate scenario, EBHOM was run under historical price or price forecasts from either the monthly based ANN model (ANN1) or the annually based ANN model (ANN2). Running EBHOM based on price forecasts considers the changes in energy demand due to climate warming.

Two price increase scenarios (+30 percent or +100 percent by 2100) were defined. Inspired by the work from Aroonruengsawat and Auffhammer (2009), the first scenario assumes a discrete price increase of 30 percent by 2020 and remaining at that level until the end of the century. The second scenario is based on the historical trend of average retail prices in California described in Section 3. A constant annual growth rate of 0.25 cents/KWh (calculated for the period 1960–2005, see Figure 5) results in retail prices increase by 100 percent by 2100. Each price increase scenario is then coupled to each climate warming scenario, run under historical prices and the two ANN price models.

[4] This scenario was mainly selected for comparison of the results with results obtained by Madani and Lund (2010). Nevertheless, this scenario is only one realization of multiple climate warming scenarios available for California, and can be considered as the worst case scenario here.

Table 1: Scenarios Defined to Run EBHOM, Including Four Climate Scenarios and Three Price Models. Additional Scenarios Were Designed by Coupling Two Pure Price Increase Scenarios (+30 Percent and +100 Percent) to the Scenarios in this table.

Scenario Acronym	CC Scenario	Price Model	Price Increase
Base	Base Case	None: Historical prices	±0%
Dry	GFDL-A2-Annual		
Wet	PCM-A2-Annual		
Base ANN1	Base Case	ANN1: Monthly ANNs	
Dry ANN1	GFDL-A2-Annual		
Dry-Seas ANN1	GFDL-A2-Seasonal		
Wet ANN1	PCM-A2-Annual		
Base ANN2	Base Case	ANN2: Annual ANN for Normal Prices	
Dry ANN2	GFDL-A2-Annual		
Dry-Seas ANN2	GFDL-A2-Seasonal		
Wet ANN2	PCM-A2-Annual		

Results

Historical Prices and Climate Change Impact on Hydrology Only

EBHOM's results for 1985–1998 hydrologic conditions and 2005–2008 historical price dataset are presented here. Table 2 indicates how energy generation, energy spill[5], and annual energy revenue all change with the Dry, Wet, and Base case climate scenarios. In this section, results are discussed and compared to those obtained by Madani and Lund (2010), who did the same study but with a different price dataset. Hourly electricity prices from 2005–2008 are also used here but prices from the period September–December 2005 were removed from the set, as explained earlier. Other differences with the work of Madani and Lund (2010) are: a different piecewise linearization of the revenue curves was considered, and the solver may not always come up with the globally optimal solution, because the problem is relatively complex.

Energy generation, energy spills, and revenues increase under the Wet scenario but decrease under the Dry scenario relative to the Base case. Energy spills increase drastically under the Wet scenario, with eight times more spills than under Base case. Energy spills occur due to the limited storage capacity of the system and the abundant runoff available. These results are similar to those from Madani and Lund (2010). Even if average generation increases by nearly 6 percent under the Wet scenario relative to Base case, average revenues only increase by 2 percent. Under the Dry scenario, average generation decreases by 20 percent but revenues only decrease by 14 percent relative to Base case. The system adapts to the new climatic conditions to maximize profits. Revenues estimated in the present work are different from the ones obtained by Madani and Lund (2010).

[5]*Energy spill* represents the amount of potential energy which is lost in the system.

Table 2: EBHOM's Results (Average of Results over 1985–1998 Period) for Different Climate Scenarios

	Base	Dry	Wet
Generation (1,000 GWh/year)	22.3	17.9	23.6
Generation change with respect to the base case (%)		*-19.8*	*+5.8*
Spill (GWh/year)	130	96	1112
Spill change with respect to the base case (%)		*-26*	*+756*
Revenue (million $/year)	1,726	1,482	1,762
Revenue change with respect to the base case (%)		*-14.1*	*+2.1*

Generation Changes with Climate Warming

Figure 10 shows average monthly energy generation for 1985 to 1998 hydrologic conditions, modified for different climate changes. Results are summed from all 137 units modeled. On average, dry conditions led to less generation than under Base case except in January and February. The monthly generation peaks occur in January and in June, when demand is high and energy is valuable. Generation between January and April is highest for the Wet scenario due to increased runoff. In the rest of the year, average monthly generation is slightly less than under Base case.

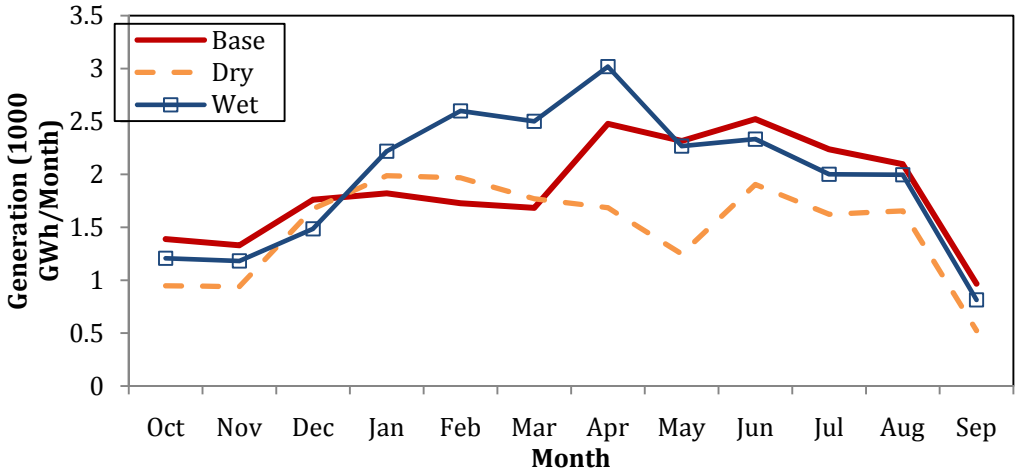

Source: Authors

Figure 10: Average Monthly Generation (1985–1998) under Different Climate Scenarios and Historical Prices

Figure 11 shows the frequency of optimized monthly generation for each month over the 14-year period (1985–1998) summed for all units, for the different climates. Over the entire study period, Dry climate leads to less generation than Base case and in contrast, Wet climate nearly always leads to more generation than found in the Base case. If more storage capacity

were available, the generation curve under the Wet scenario would be closer to the Base case curve, with higher revenues.

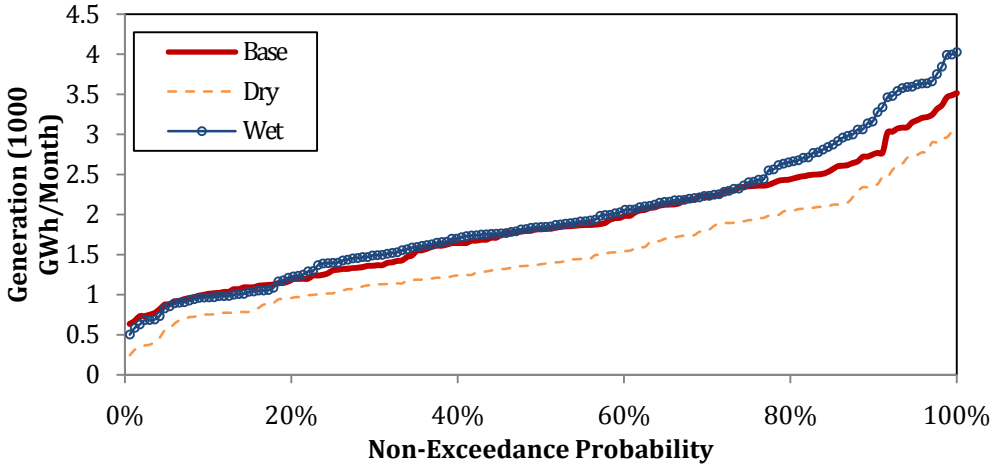

Source: Authors

Figure 11: Frequency of Monthly Optimized Generation (1985–1998) under Various Climate Scenarios (All Months, All Years, All Units) and Historical Prices

Reservoir Storage Changes with Climate Warming

Figure 12shows how average end-of-month energy storage in all of the reservoirs combined changes with climate when reservoirs are operated for energy revenues only. The starting month for reservoir refilling is January under the Base and Wet scenarios and November under the Dry climate. Under climate warming scenarios, reservoirs capture most of snowmelt water between January and May and release it progressively in months of high demand, maximizing profit. The timing of the patterns is similar to the monthly runoff distributions. The peak storage intensity is relative to the amount of water available; it is the largest under the Wet scenario, then the Base case, and finally the lowest under the Dry scenario. The peak intensity is also lower under Base case than Wet scenario because some of the water is directly released and not stored for later. For instance, the end-of-month storage capacity in June is about the same for these two scenarios.

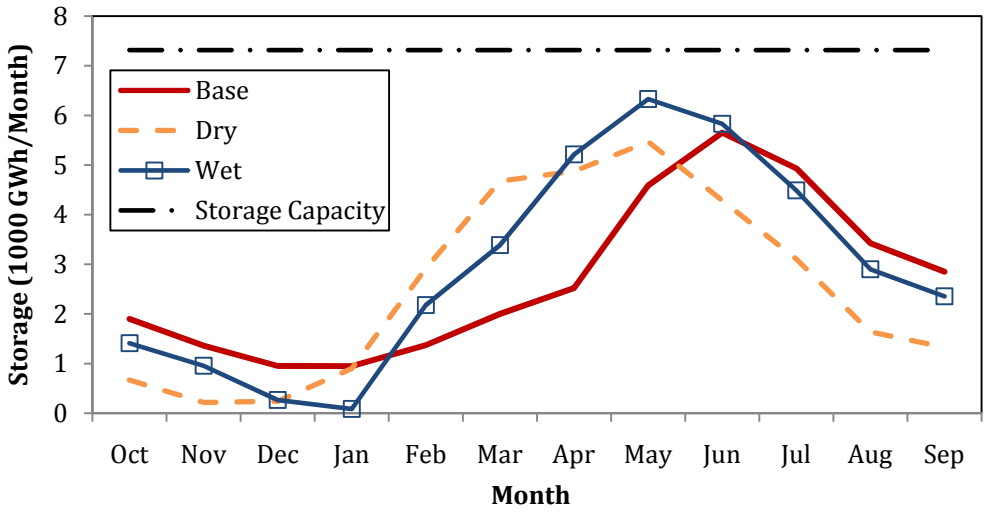

Source: Authors

Figure 12: Average Total End-of-Month Energy Storage (1985–1998) under Different Climate Scenarios and Historical Prices. The Black Line Is the System's Storage Capacity.

Energy Spills with Climate Warming

Figure 13 shows the frequency of total monthly energy spills from the system for the study period (1985–1998) when the system is optimized for revenue maximization. Energy spill is the equivalent energy value of the water that cannot be stored nor sent through turbines because of limited capacities. Energy is spilled by the system in 35 percent of months under Wet climate, in 20 percent of months under Base case, and in 10 percent of months under Dry climate. This study calculated energy spill as the increased energy spill with respect to the Base case, so zero spills under the Base case was expected. However, the results showed a minimal model error of 130 GWh, corresponding to 0.6 percent of total generation on average, under the Base case.

Figure 14 shows the distribution of total average monthly energy spill for different climates. Spills occur only between January and May in all cases. Substantial energy spills (850 GWh in total) occurred in February under the Wet scenario even though the total storage capacity is not met. EBHOM has perfect foresight into the future (because it is a deterministic model with fixed inflow and price distributions) and knows what will happen in the next months, so in this case it suggests spilling and emptying the reservoirs in advance.

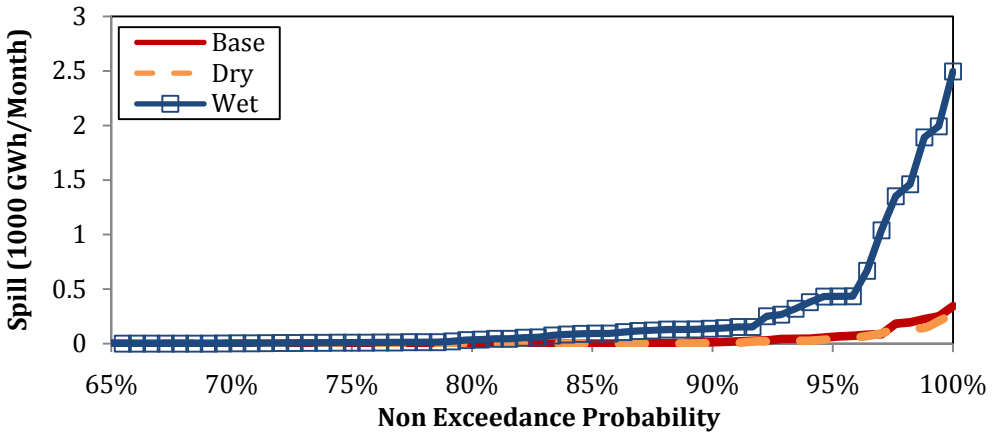

Source: Authors

Figure 13: Frequency of Total Monthly Energy Spill (1985–1998) Under Different Climate Scenarios (All Months, All Years, All Units) And Historical Prices

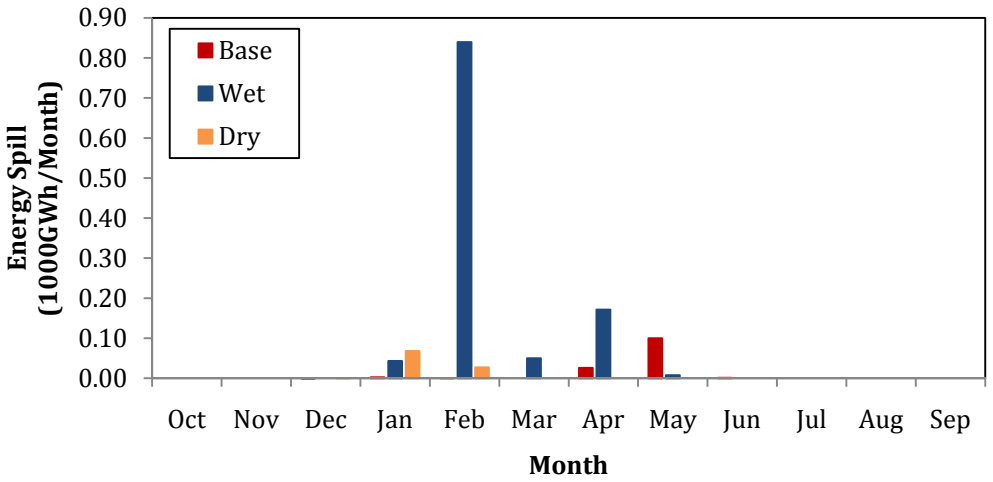

Source: Authors

Figure 14: Average Monthly Total Energy Spill (1985–1998) under Different Climate Scenarios and Historical Prices

Revenue and Energy Price Patterns under Climate Warming

Figure 15 shows climate warming effects on monthly average price received for generated energy in the period 1985–1998. Prices received under the Dry scenario exceed the Base case prices 85 percent of the time, but monthly generation is less 100 percent of the time. This is what was expected given the nonlinear relationship between electricity prices and generation. Prices received under Wet climate are similar to the ones under the Base case, but never exceed those prices. Average prices received here reach $175/MWh under the Dry climate, $150/MWh under the Wet climate, and $135/MWh under the Base case; whereas, those did not exceed $135/MWh, $120/MWh and $120/MWh, respectively, in Madani and Lund (2010).

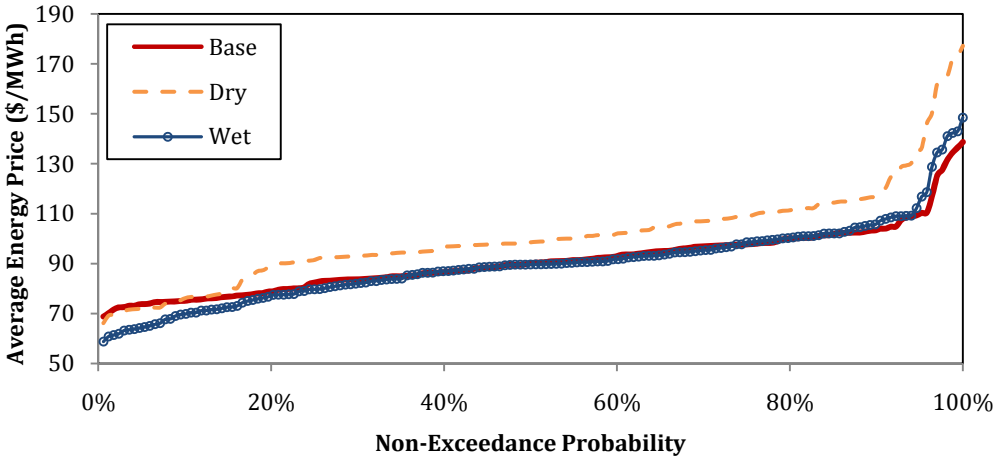

Source: Authors

Figure 15: Frequency of Monthly Energy Price (1985–1998) under Different Climate Scenarios (All Months, All Years, All Units) and Historical Prices

Figure 16 shows the effects of climate warming on the frequency of total annual revenues from the system for the 14-year period (1985–1998). Annual revenues are the highest 80 percent of the time under the Wet scenarios and the lowest 100 percent of the time under the Dry scenario. Although monthly average prices received for generated energy were higher under the Dry scenario, the increase in average prices received does not compensate for the Dry scenario reduction in energy generation. On average, annual revenues are $210 million lower than the Base case for the Dry scenario.

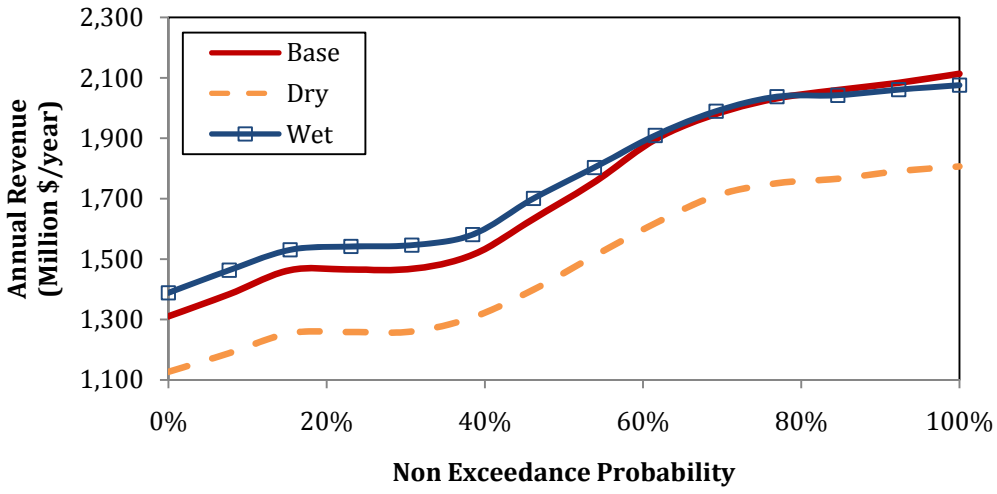

Source: Authors

Figure 16: Frequency of Total Annual Revenue (1985–1998) under Different Climate Scenarios and Historical Prices

Benefits of Expanding Energy Storage and Generation Capacity

Figure 17 shows, on average, how energy storage capacity expansion changes hydropower generation revenues for different climate scenarios over the 14-year study period. This figure indicates the average shadow price of energy storage capacity (the increase in annual revenue per 1 MWh energy storage capacity expansion) for all 137 reservoirs. For instance, increase in annual revenue per 1MWh energy storage capacity expansion is less than $29, $48, and $51 (compared to $35, $47, and $54 in Madani and Lund [2010]) for the 137 studied plants under the Base, Dry and Wet scenarios. Storage capacity expansion reduces spills and allows for more release in summer, when energy is the most valuable. Average annual revenues can be increased by expanding storage capacity in all plants (except for four plants under Base case), although such expansion might not be justified due to expansion costs. As expected, benefits of capacity expansion are greater for Wet scenario when the additional capacity can be more frequently used. Even with the historical hydrology, expanding storage capacity increases total annual revenues in all years.

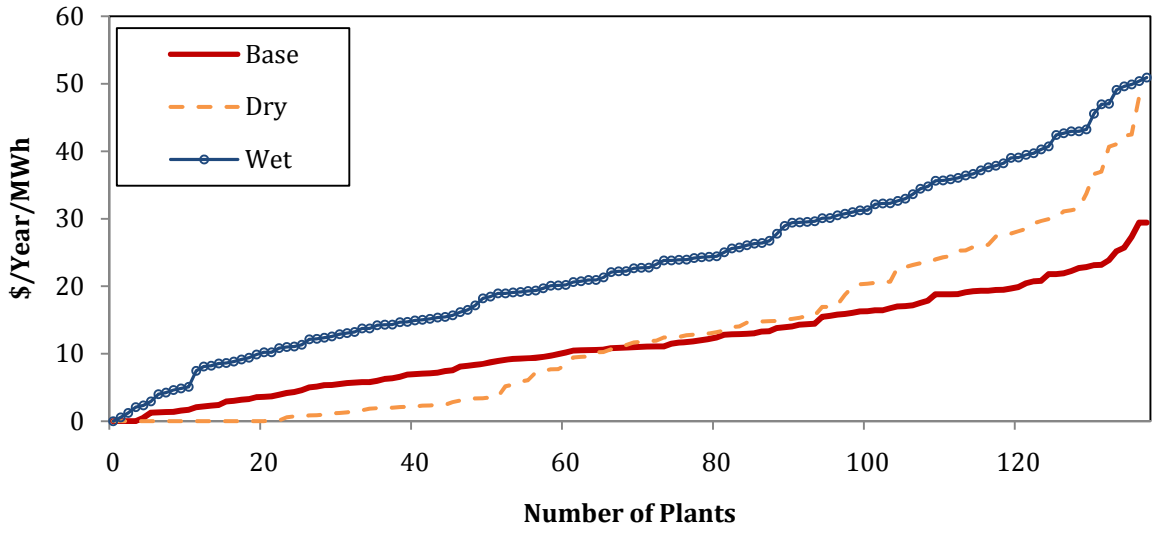

Source: Authors

Figure 17: Average Shadow Price of Energy Storage Capacity of 137 Hydropower Units in California for 1985–1998 Period under Different Climate Scenarios and Historical Prices

Figure 18 indicates the average shadow price of energy generation (turbine) capacity (increase in annual revenue per 1 MWh of annual energy generation capacity expansion) for all 137 plants under different climate scenarios. All scenarios benefit from an increase in generation capacity, reducing spills and allowing more energy to be generated when prices are high. Increase in annual revenue per 1MWh energy storage capacity expansion is around $22, $18, and $25 for the 137 studied plants under the Base, Dry, and Wet scenarios, respectively. Even though generation capacity expansion produces benefits, expansion costs might be prohibitive.

Figure 19indicates how the marginal benefits of energy storage and generation capacity expansion of power plants vary with climate (each point in the figure is a hydropower plant). It clarifies the relative importance of extra energy generation and storage capacity for each unit for

all climate scenarios. Under the Base scenario, half of the power plants benefit more from energy storage capacity expansion than from generation capacity expansion. However, storage capacity expansion is more beneficial in terms of revenue if the entire system is considered. Comparison of with the different diagrams in Figure 19 shows how storage capacity becomes more valuable under climate warming as the scatter in the figures expands to the right, highlighting the higher benefit from energy storage capacity expansion than generation capacity expansion. Under the Wet scenario, 86 percent of the units benefit more from storage capacity expansion. Finally, for the Dry scenario, 55 percent of the power plants benefit more from energy storage capacity expansion than from generation capacity expansion. However, nearly 40 percent of the plants increase their revenues by less than $5 per MWh from storage capacity expansion. The plants that do not spill are responsible for this low increase in average shadow prices.

Figure 20shows the changes of marginal benefits of energy storage and generation (turbine) capacities relative to the Base case with different climate warming scenarios. Under the Dry scenario, marginal benefits of energy generation capacity of all units are lower than the Base case, because water supply availability is the limiting factor. For about 50 percent of plants, the value of expanding energy storage under drier conditions is more than it is with the Base case, allowing more winter inflows to be shifted to high-value summer power generation (the maximum difference can be as high as $28). For the Wet scenario, almost all units benefit from energy storage capacity expansion, as well as from generation capacity expansion, reducing spills and shifting generation from low-value to high-value months. In this case, energy storage capacity expansion is more valuable than generation capacity expansion.

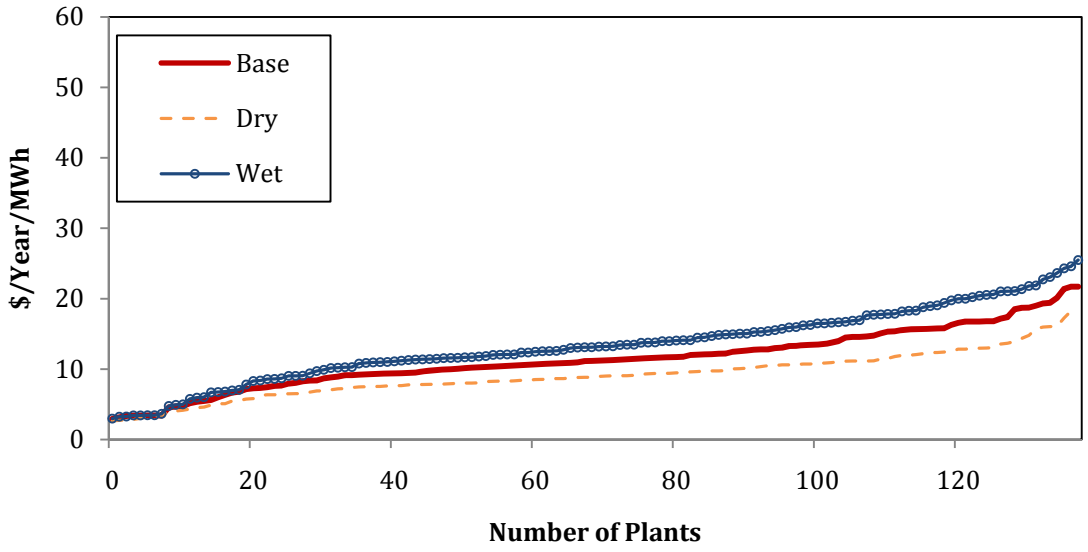

Source: Authors

Figure 18: Average Shadow Price of Energy Generation Capacity of 137 Hydropower Units in California for 1985–1998 Period under Different Climate Scenarios and Historical Prices

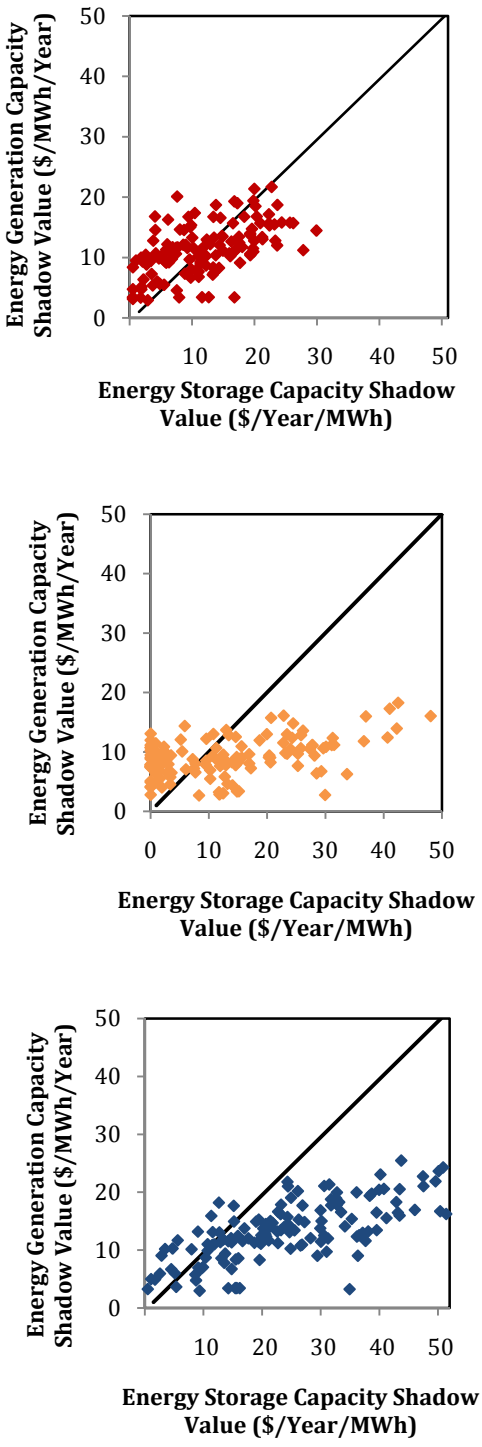

Source: Authors

Figure 19: Average Shadow Values of Energy Storage and Generation Capacity of 137 Hydropower Units in California in the 1985–1998 Period under the Base (Top), Dry (Middle), and Wet (Bottom) Climate Scenarios and Historical Prices

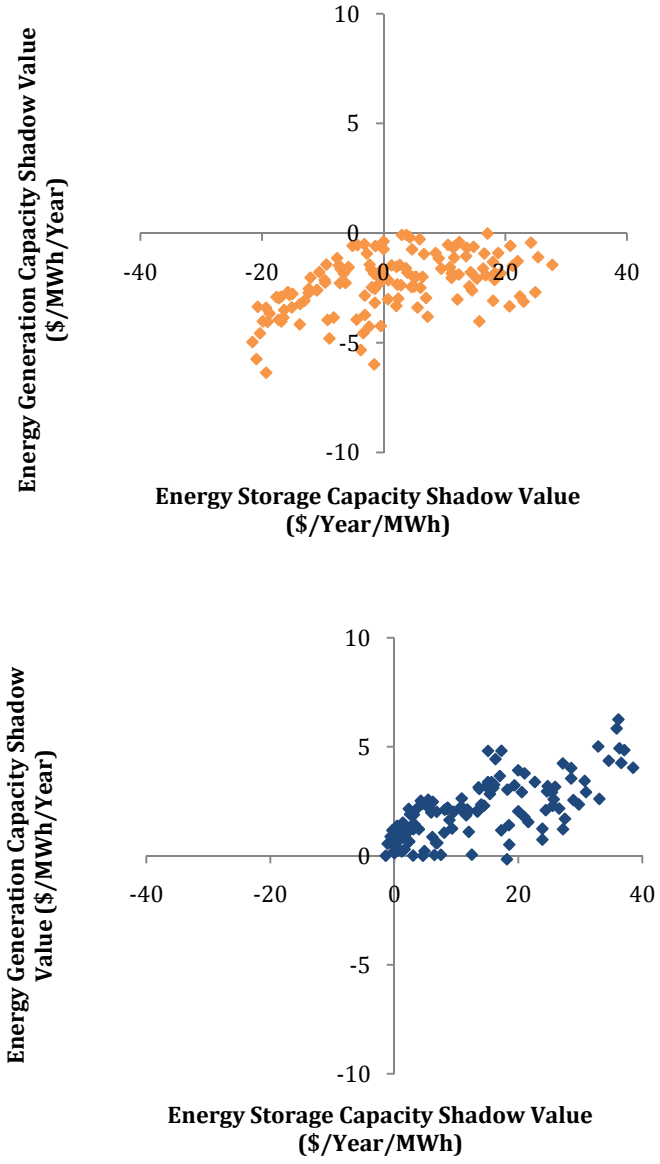

Source: Authors

Figure 20: Average Change of Energy Storage and Generation Capacity Shadow Values from the Base Case with Dry (Top) and Wet (Bottom) Climate Scenarios (for 137 Hydropower Units in California in the 1985–1998 Period) Based on Historical Prices

Climate Change Impact on Energy Demand, Pricing and on Hydrology

The previous section described climate warming effects on California's high-elevation hydropower system by focusing on the supply side (exploring the effects of hydrological changes on generation and revenues), ignoring the warming effects on hydropower demand and pricing. This section extends the previous results by simultaneous consideration of climate

change effects on high-elevation hydropower supply and demand in California. The research team used the ANNs as long-term price forecasting tools to estimate the impact of climate warming on energy prices. Two different ANN models were developed: 12 monthly based ANN models calibrated for all price ranges (ANN1), and a single annually based ANN model calibrated on Normal prices (ANN2).

Table 3 indicates how energy generation, energy spill, and annual energy revenue change relative to Base case for different climate scenarios and forecasted future energy pricing. For each climate warming scenario (Dry, Wet, or Dry-Seasonal), the average annual generation and energy spills are the same no matter what the price representation is. Generally, when warming effects on demand are considered, annual revenues decrease relative to the Base case for both drier and wetter conditions. Depending on the ANN model used to forecast prices, there can be significant differences in average revenues received, especially under drier conditions. Under Dry climate, the difference in revenues between models using ANN1 or ANN2 is about $130 million/year, and under Dry-Seasonal climate it reaches $180 million/year. Generally, ANN1 predicts higher annual average revenues than ANN2 under all climates. The Dry scenario estimates more important decreases in revenue than the Dry-Seasonal one.

Table 3: EBHOM's Results (Average of Results over 1985–1998 Period) for Different Climate Warming Scenarios Considering Simultaneously the Warming Effects on Hydropower Supply and Demand (ANN1: Monthly Based ANN Model; ANN2: Annually Based ANN Model Calibrated on Normal Prices)

Climate Scenario	Base	Dry	Wet	Dry		Dry-Seasonal		Wet	
Price Model	Historical			ANN 1	ANN 2	ANN 1	ANN 2	ANN 1	ANN 2
Generation (1,000 GWh/year)	22.3	17.9	23.6	17.9		17.9		23.6	
Generation change with respect to the Base case (%)		*-19.8*	*+5.8*	*-19.8*		*-19.8*		*+5.8*	
Spill (GWh/year)	130	96	1112	96		96		1112	
Spill change with respect to the Base case (%)		*-26*	*+756*	*-26*		*-26*		*+756*	
Revenue (million $/year)	1,726	1,482	1,762	1,533	1,400	1,587	1,408	1,718	1,660
Revenue change with respect to the Base case (%)		*-14.1*	*+2.1*	*-11.2*	*-18.9*	*-8.1*	*-18.4*	*-0.5*	*-3.8*

Generation Changes with Climate Warming

Figure 21 shows average monthly energy generation for 1985 to 1998 for different climate warming scenarios, considering climate warming effects on high-elevation hydropower supply and demand simultaneously. Results are summed from all of the 137 units modeled.

When climate warming effects on hydropower demand and pricing are considered, average monthly generation increases in June and July and decrease from November to February under all scenarios, compared to when those considerations were ignored. Less generation is necessary in winter since there is less need for heating, and more generation is necessary in the summer to satisfy the high cooling demand. Generation peaks in June or July (depending on the ANN model considered), but both ANN models result in a peak in summer. The highest peaks occur in June for ANN2 and reach 2,500GWh/month for Dry ANN2; 2,700GWh/month for Dry-Seasonal ANN2; and 2,900GWh/month for Wet ANN2. Dry-Seasonal scenarios estimate more generation in July and August than Dry scenarios. In the rest of the months, generation is not considerably sensitive to warming effects on energy demand.

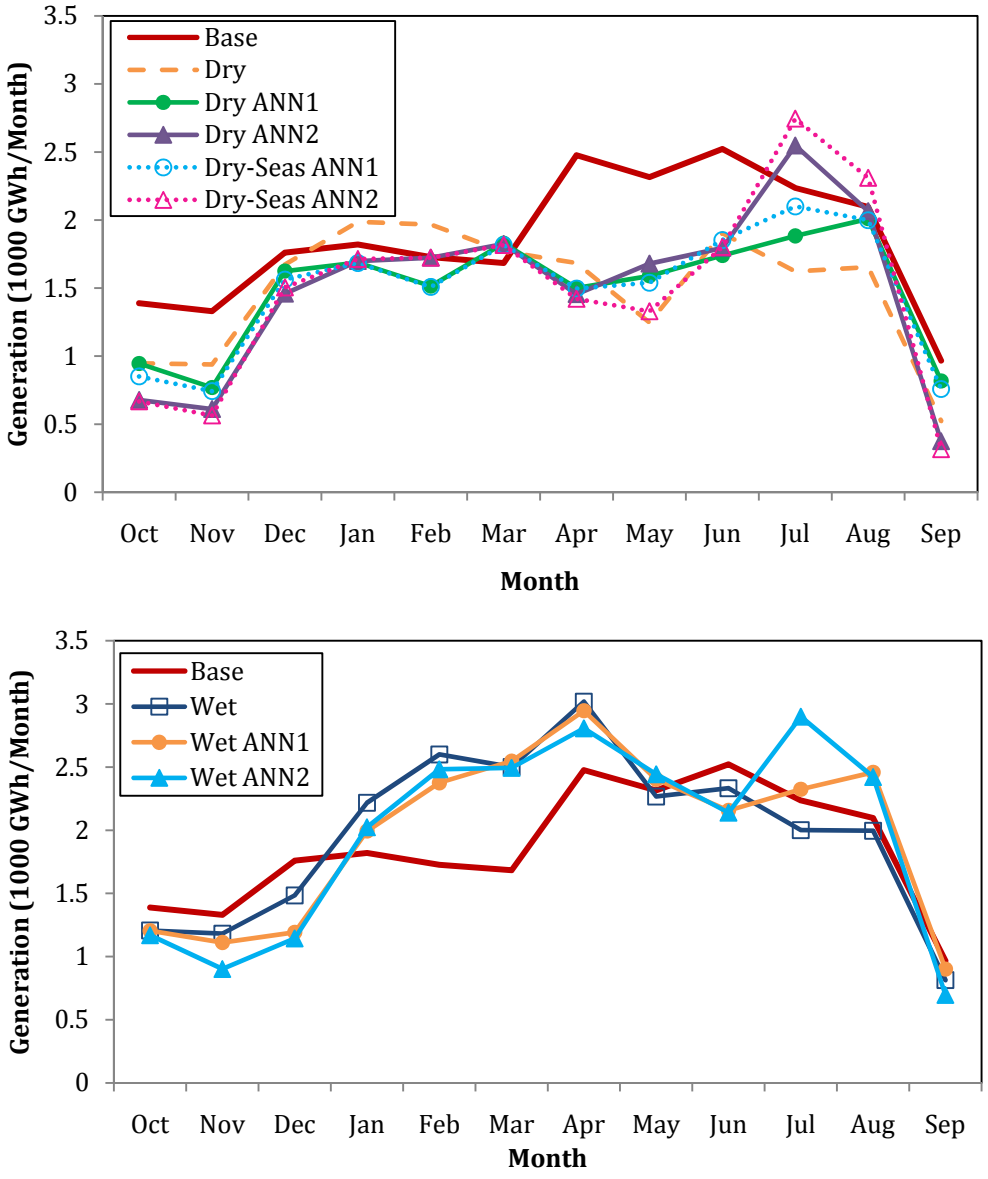

Source: Authors

Figure 21: Average Monthly Generation (1985–1998) under Dry (Top) and Wet (Bottom) Warming Scenarios, Considering the Warming Effects on Hydropower Supply and Demand Simultaneously (Future Energy Pricing Is Forecasted Using ANNs – ANN1: Monthly Based Model; ANN2: Annually Based Model Calibrated on Normal Prices)

Reservoir Storage Changes with Climate Warming

Figure 22 shows how average total end-of-month energy storage of the system (in all reservoirs combined) changes with drier and wetter scenarios respectively, with climate warming effects on hydropower demand is also considered.

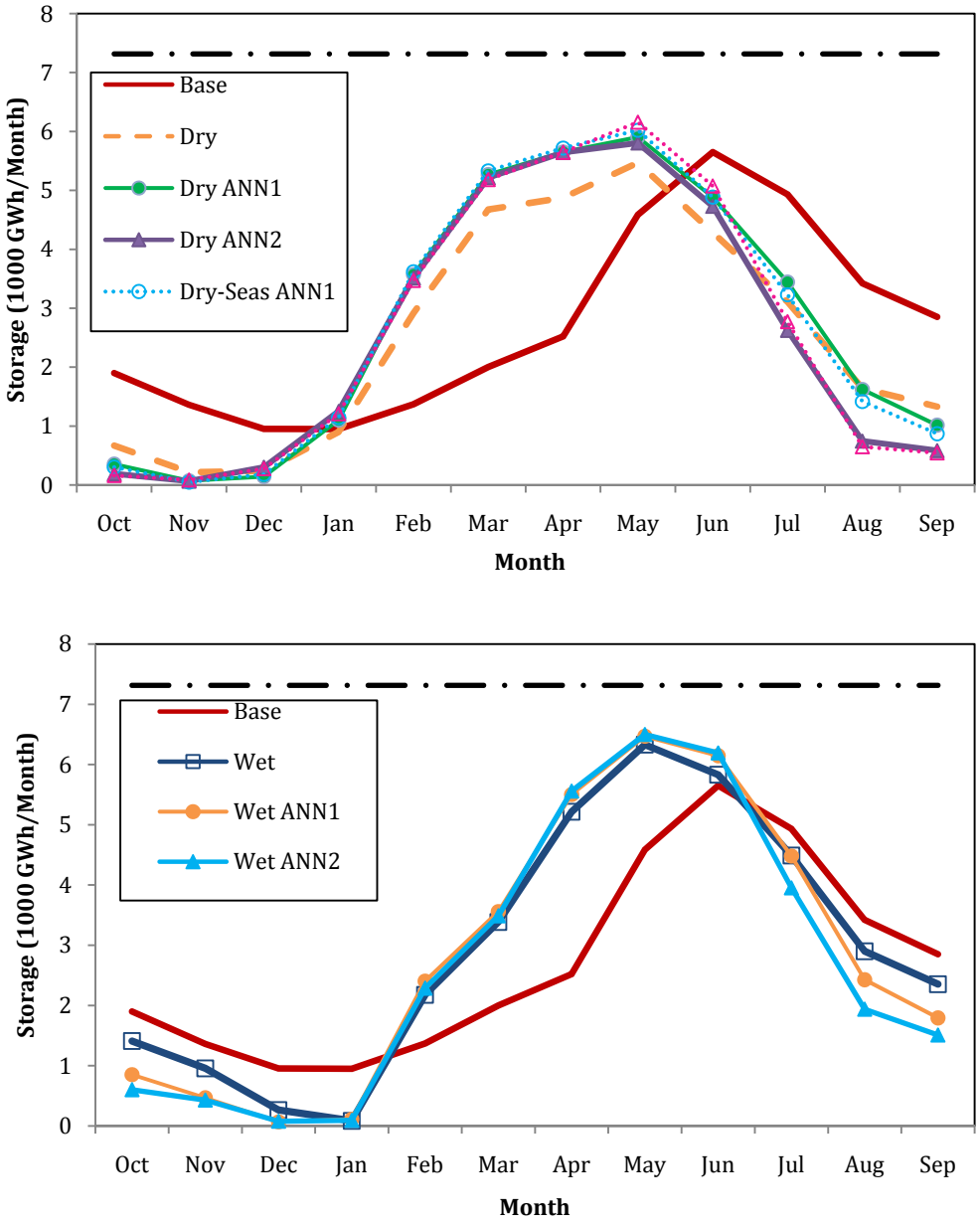

Source: Authors

Figure 22: Average Total End-of-Month Energy Storage (1985–1998) under Dry (Top) and Wet (Bottom) Warming Scenarios, Considering the Warming Effects on Hydropower Supply and Demand Simultaneously (Future Energy Pricing Is Forecasted Using ANNs – ANN1: Monthly Based Model; ANN2: Annually Based Model Calibrated on Normal Prices)

Reservoirs start refilling earlier in the Dry scenarios than they do in the Wet scenarios and the Base case. In the Dry scenarios, the system must take maximal advantage of the water available from late autumn to spring, to release it when prices are the highest, i.e. in summer. Between February and June, the system stores more water in its reservoirs when future changes in demand are considered than when they are ignored. This is true for both drier and wetter scenarios. Less energy is needed in cold months, so more water is available to be stored until

high-demand months. The peak storage occurs in May under all climate change scenarios. In the rest of the months, less energy is stored when changes in demand are considered. On average, the system's total storage capacity is never met. The main difference between the two ANN models is that on average less energy is stored in summer for ANN2 compared to ANN1. There is no significant difference between the Dry and Dry-Seasonal scenarios, except slightly less storage in summer for the latter scenario.

Energy Spills with Climate Warming

Figure 23shows the distribution of total average monthly energy spill for dry and wet climate scenarios, considering changes in future demands. All spills occur in the refilling season (December to May) before release when demand and prices are high. The energy spill patterns are similar between all dry scenarios and between all wet scenarios. Considering the warming effect on demand does not alter the average monthly spill pattern. Average energy spills of about 850GWh occur in February under Wet scenarios. EBHOM suggests emptying reservoirs in advance since it has perfect foresight into the future.

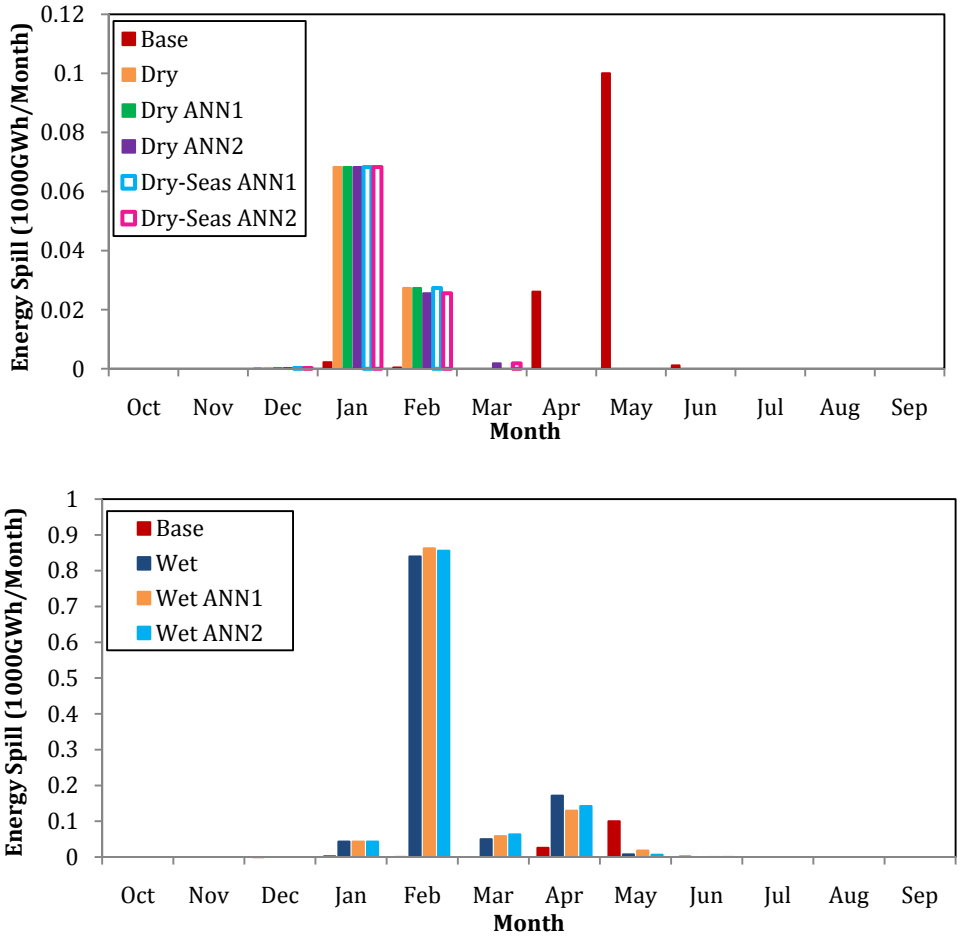

Source: Authors

Figure 23: Average Monthly Total Energy Spill (1985–1998) under the Dry (Top) and Wet (Bottom) Warming Scenarios, Considering the Warming Effects on Hydropower Supply and Demand Simultaneously (Future Energy Pricing Is Forecasted Using ANNs – ANN1: Monthly Based Model; ANN2: Annually Based Model Calibrated on Normal Prices)

Revenue and Energy Price Patterns under Climate Warming

Figure 24 shows climate warming's effects on the monthly average price received for generated energy, for drier (a) and wetter (b) scenarios, respectively, considering climate warming effects on hydropower supply and demand simultaneously.

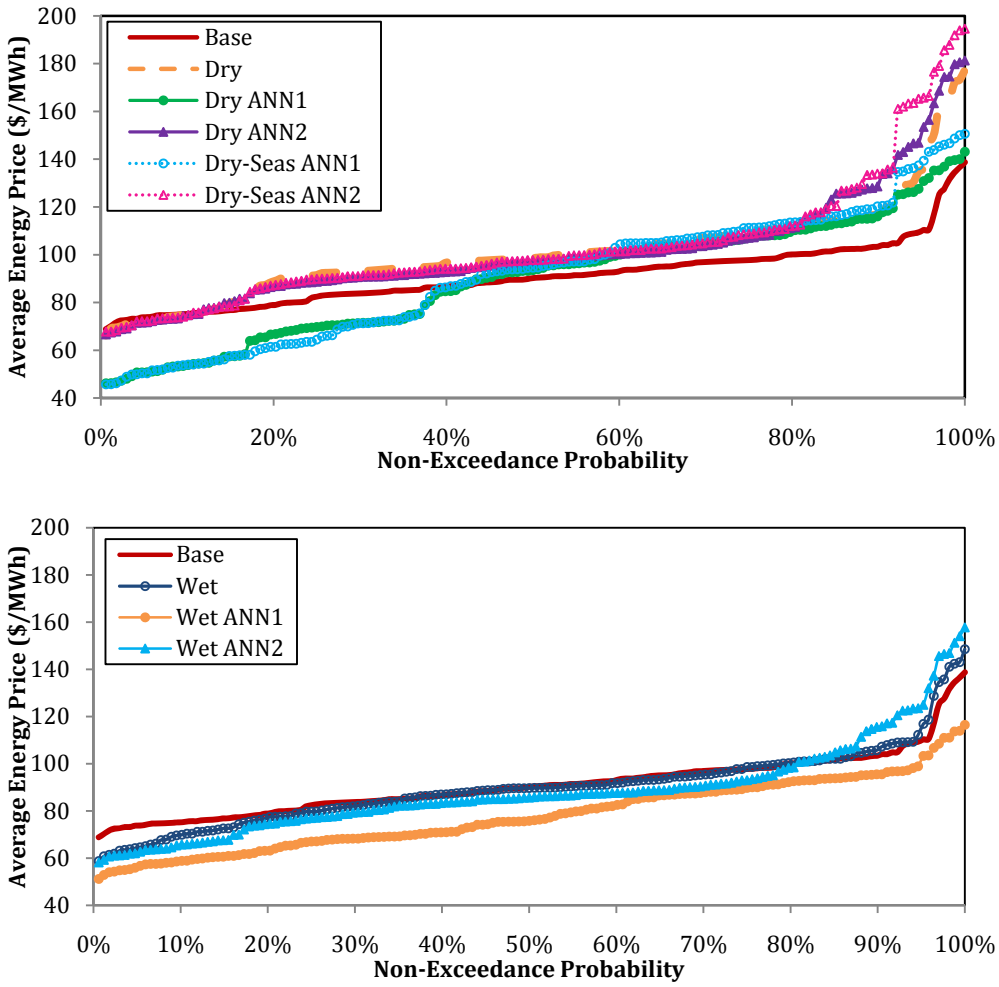

Source: Authors

Figure 24: Frequency of Monthly Energy Price (1985–1998) under Dry (Top) and Wet (Bottom) Warming Scenarios , Considering the Warming Effects on Hydropower Supply and Demand Simultaneously (All Months, All Years, All Units) (Future Energy Pricing Is Forecasted Using ANNs – ANN1: Monthly Based Model; ANN2: Annually Based Model Calibrated on Normal Prices)

Prices received under Dry ANN2 and Dry-Seasonal ANN2 exceed the monthly average Energy prices received under Base case (85 percent of the time under Dry ANN2 and Dry-Seasonal ANN2 and 60 percent of the time under Dry ANN1 and Dry-Seasonal ANN1). The aggregate monthly energy price received under both Dry-Seasonal scenarios exceeds those under their respective Dry scenario. Aggregate monthly energy prices for 1985–1998 are about $150–$160/MWh when ANN1 is used; whereas, they are about $180–$190/MWh when ANN2 is used under Dry scenarios. Generally, monthly energy prices when the scenario is based on ANN2 exceed those when ANN1 is used. Monthly energy prices under Wet ANN1 never exceed those received under the Base case scenario or other Wet scenarios. Prices received under Wet ANN2 are lower than those found under the Base case and Wet scenario (based on historical prices) 85 percent of the time, but exceed both of those the rest of the time. Generally dry scenarios increase monthly energy prices relative to the Base case; whereas, Wet scenarios decrease prices.

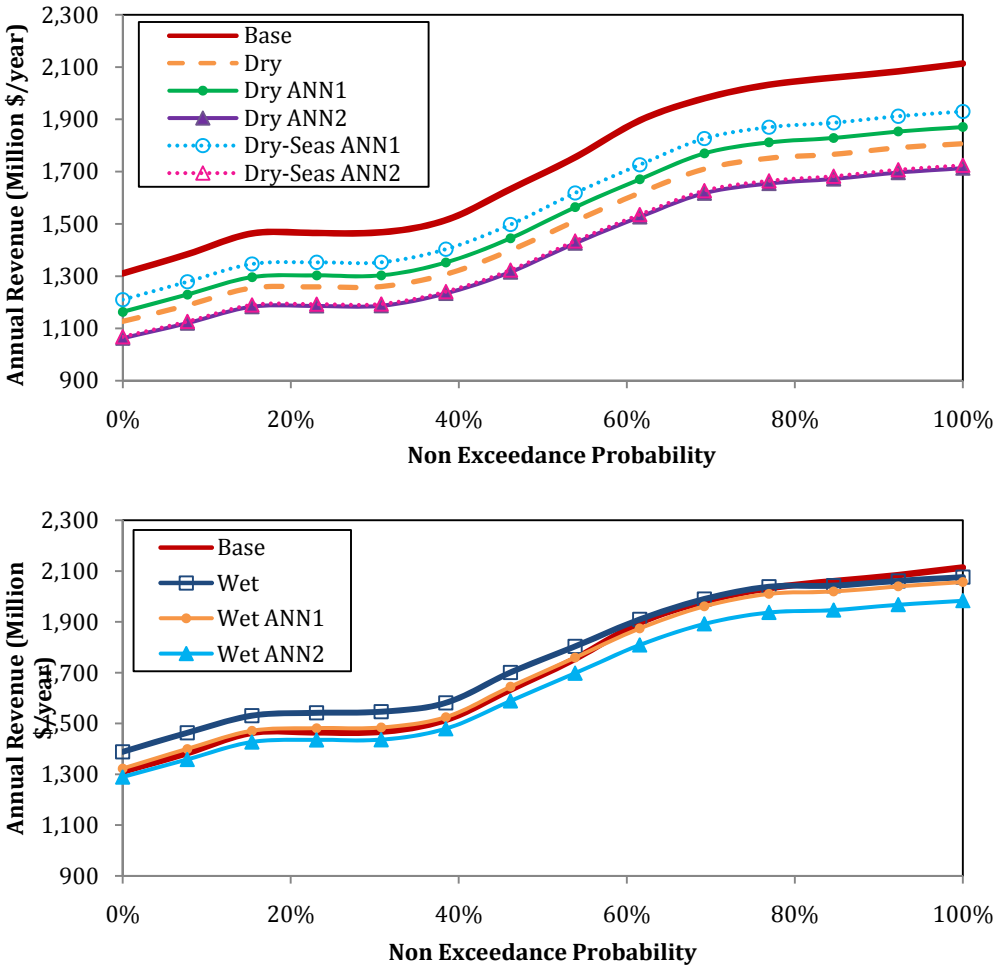

Source: Authors

Figure 25: Frequency of Total Annual Revenue (1985–1998) under Dry (Top) and Wet (Bottom) Warming Scenarios, Considering the Warming Effects on Hydropower Supply and Demand Simultaneously (Future Energy Pricing Is Forecasted Using ANNs – ANN1: Monthly Based Model; ANN2: Annually Based Model Calibrated on Normal Prices)

Figure 25shows the effects of climate warming on the frequency of total annual revenues from the system for the 14-year period (1985–1998) for drier (a) and wetter conditions (b), considering climate warming effects on hydropower supply and demand simultaneously. Under dry conditions, annual revenues received are always lower than those under Base case. Although monthly average prices received for generated energy were higher under the Dry scenarios, the increase in average prices received does not compensate for the Dry scenarios' reduction in energy generation. For drier climate, considering the simultaneous effects of climate warming on hydropower supply and demand leads to an increase in annual revenues when the model is based on ANN1, and a decrease when the model is based on ANN2. For wetter conditions, considering the simultaneous effects of warming on hydropower supply and demand decreases revenues compared to when those effects are neglected. For all climate warming scenarios ANN1 increases revenues compared to ANN2; this has already been discussed in reference to

long-term price forecasting; monthly based models (ANN1) are likely to overestimate future prices.

Benefits of Expanding Energy Storage and Generation Capacity

Figure 26 shows, on average, how energy storage capacity expansion changes hydropower generation revenues for drier (a) and wetter (b) climate scenarios over the 14-year study period. These figures indicate the average shadow price of energy storage capacity (the increase in annual revenue per 1 MWh energy storage capacity expansion) for all 137 reservoirs. Average annual revenues can be increased by expanding storage capacity in all plants (except for six plants under Dry ANN1 and Dry ANN2), although such expansion might not be justified due to expansion costs. In the summer, demand increases and energy is valuable, so the system benefits from storing more snowmelt water. Increase in annual revenue per 1MWh energy storage capacity expansion is between $45 and $81 for the 137 studied plants under drier scenarios considering changes in demand. Under wetter scenarios demand increase may not increase the benefit of storage capacity expansion. Expanding storage capacity can be more or less beneficial than when demand changes were ignored, depending on the ANN forecast model used. Under Dry ANN1, expanding energy storage capacity is more valuable for about 50 power plants than under wetter scenarios, which is surprising. Greater benefits of storage capacity expansion for Wet scenarios were expected since the additional capacity can be more frequently used. However the estimations from ANN2 seem more reasonable.

Figure 27 indicates the average shadow price of energy generation (turbine) capacity (increase in annual revenue per 1 MWh of annual energy generation capacity expansion) for the entire system, under drier (a) and wetter (b) climate warming scenarios. Considering climate warming effects on demand attenuates the benefits from expanding energy generation capacity under wetter scenarios relative to the Wet scenario, based on historical pricing. This is also true for drier conditions, except for the Dry-Seasonal ANN1 scenario. Increase in annual revenue per 1 MWh energy generation capacity expansion is $22, $15–17, and $22–24 for the 137 studied plants under the Base, drier, and wetter scenarios, respectively.

Figure 28indicates how the marginal benefits of energy storage and generation capacity expansion of power plants vary with the different scenarios (each point is a power plant). It clarifies the relative importance of extra energy generation and storage capacity for each unit for all climate scenarios. Under all climate warming scenarios, expanding energy storage capacity is typically more beneficial than expanding generation capacity if the expansion costs are the same. Expanding energy storage capacity allows water to be stored in off-peak months and then released through turbines when prices are higher. Depending on the ANN forecast model, between 45 and 52 plants under drier scenarios, and between 15 and 18 plants under wetter scenarios, benefit more from energy generation capacity expansion (out of 137 plants in total). Energy storage capacity shadow price is 1.81–2.32 and 1.93–2.27 times higher than the energy generation shadow price for all power plants under Dry and Wet scenarios considering warming effects on demand.

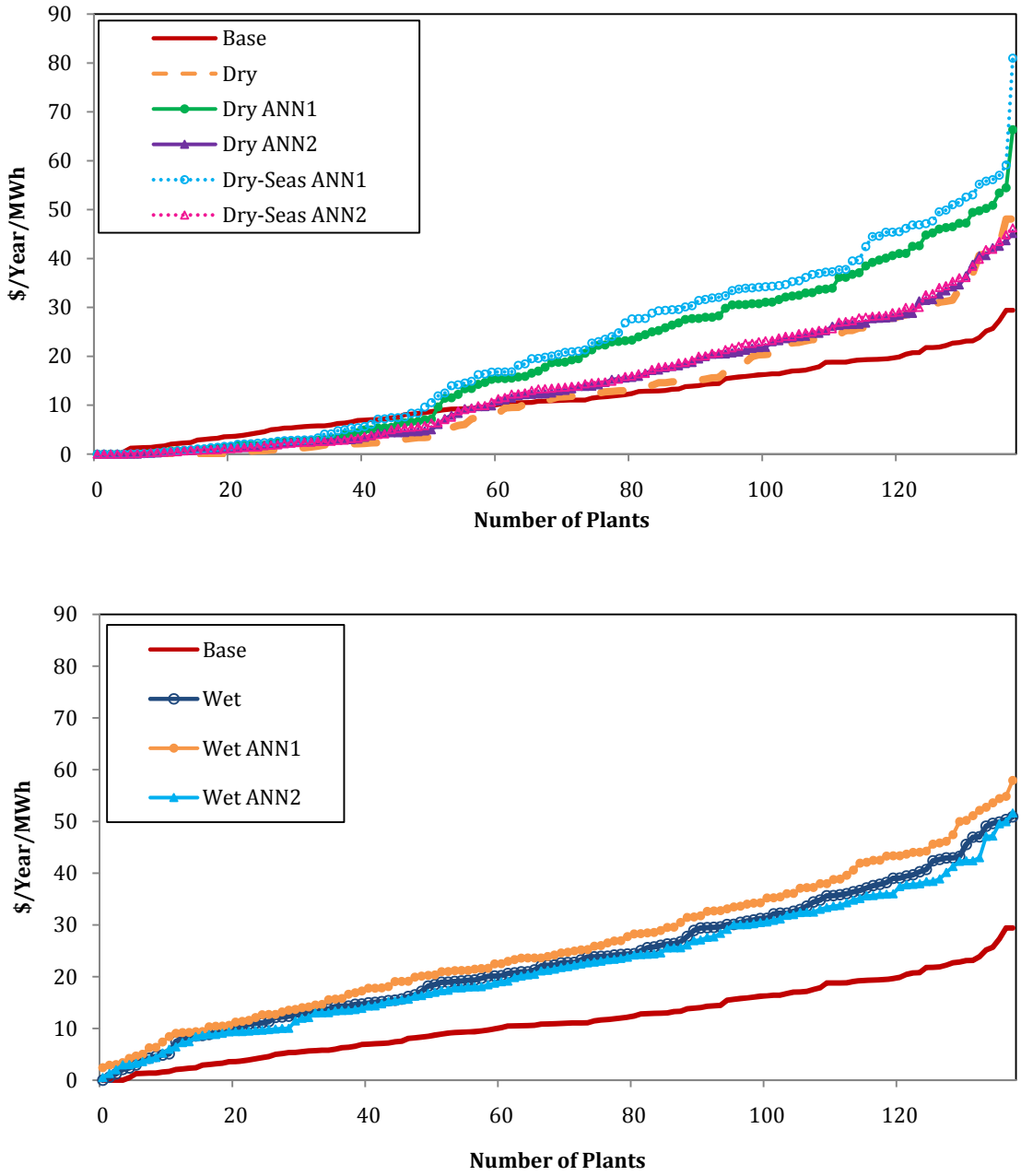

Source: Authors

Figure 26: Average Shadow Price of Energy Storage Capacity of 137 Hydropower Units in California in the 1985–1998 Period under Dry (Top) and Wet (Bottom) Warming Scenarios, Considering the Warming Effects on Hydropower Supply and Demand Simultaneously (Future Energy Pricing Is Forecasted Using ANNs – ANN1: Monthly Based Model; ANN2: Annually Based Model Calibrated on Normal Prices)

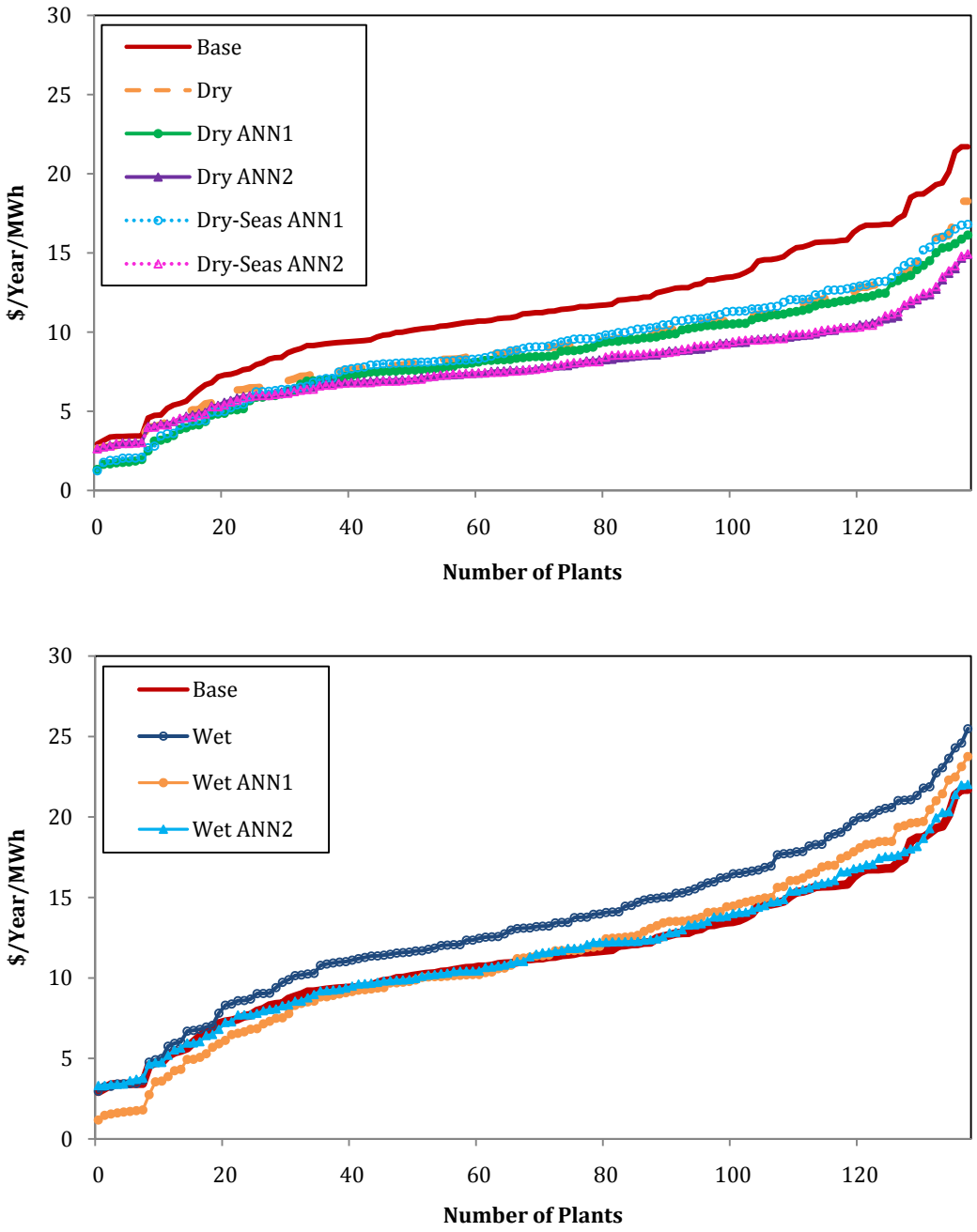

Source: Authors

Figure 27: Average Shadow Price of Energy Storage Capacity of 137 Hydropower Units in California in the 1985–1998 Period under Dry (Top) and Wet (Bottom) Warming Scenarios, Considering the Warming Effects on Hydropower Supply and Demand Simultaneously (Future Energy Pricing Is Forecasted Using ANNs – ANN1: Monthly Based Model; ANN2: Annually Based Model Calibrated on Normal Prices)

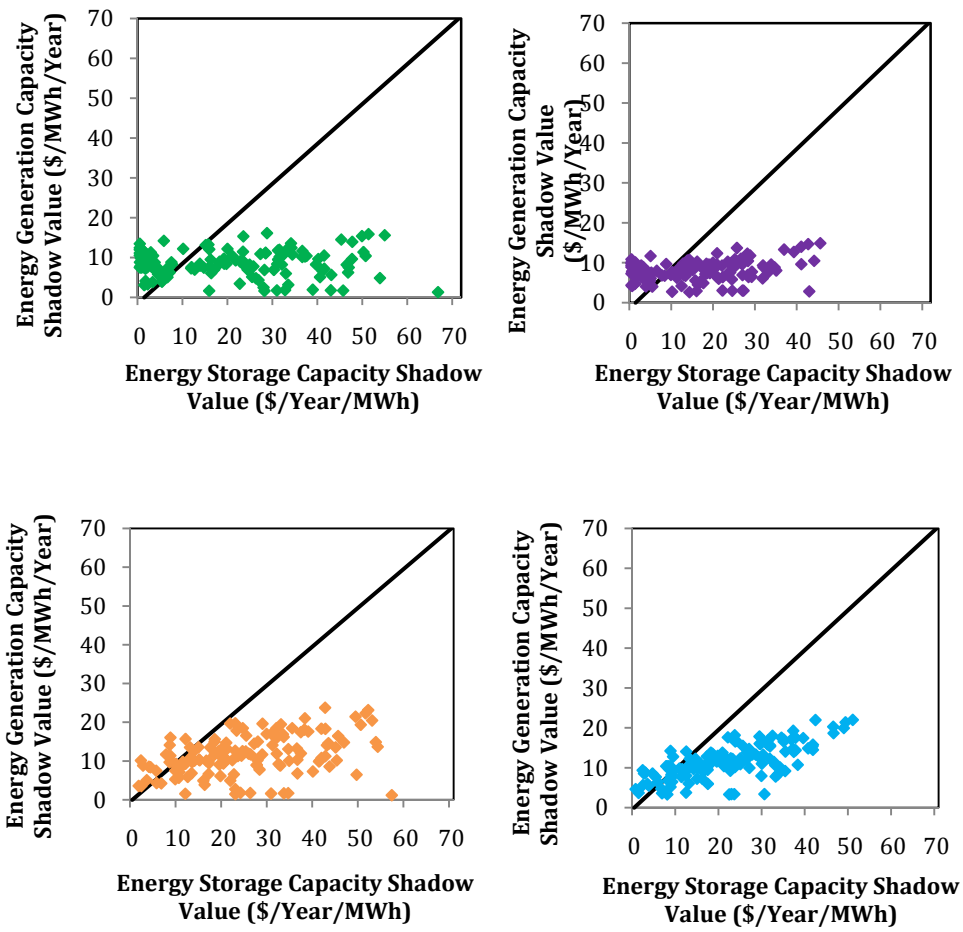

Source: Authors

Figure 28: Average Shadow Values of Energy Storage and Generation Capacity of 137 Hydropower units in California in the 1985–1998 Period under Dry (Top-Left = Dry-ANN1 and Top-Right = Dry-ANN2) and Wet (Bottom-Left = Wet-ANN1 and Bottom-Right = Wet-ANN2) Warming Scenarios, Considering the Warming Effects on Hydropower Supply and Demand Simultaneously (Future Energy Pricing Is Forecasted Using ANNs – ANN1: Monthly Based Model; ANN2: Annually Based Model Calibrated on Normal Prices)

Figure 29shows the changes of marginal benefits of energy storage and generation (turbine) capacities relative to the Base case with drier and wetter warming scenarios. Patterns for Dry-Seasonal scenarios are similar to the Dry scenarios, so they are not shown in the figure. Under Dry ANN1 and Dry ANN2, marginal benefits of expanding energy generation capacity for all units are lower than they are under the Base case. There is less inflow, so the existing generation capacity is more often sufficient to avoid spills. For between 75 and 87 of plants (55 to 63 percent), the value of expanding energy storage capacity under drier conditions is more than it is under the Base case. For Wet ANN1 and Wet ANN2 scenarios, most units (121 and 112, respectively) benefit more from energy storage capacity expansion than those under the Base case. Under the wetter scenarios, about 50 percent of plants benefit from expanding both generation and storage capacities, but energy storage capacity expansion is more valuable, as the scatter in Figure 29expands to the right.

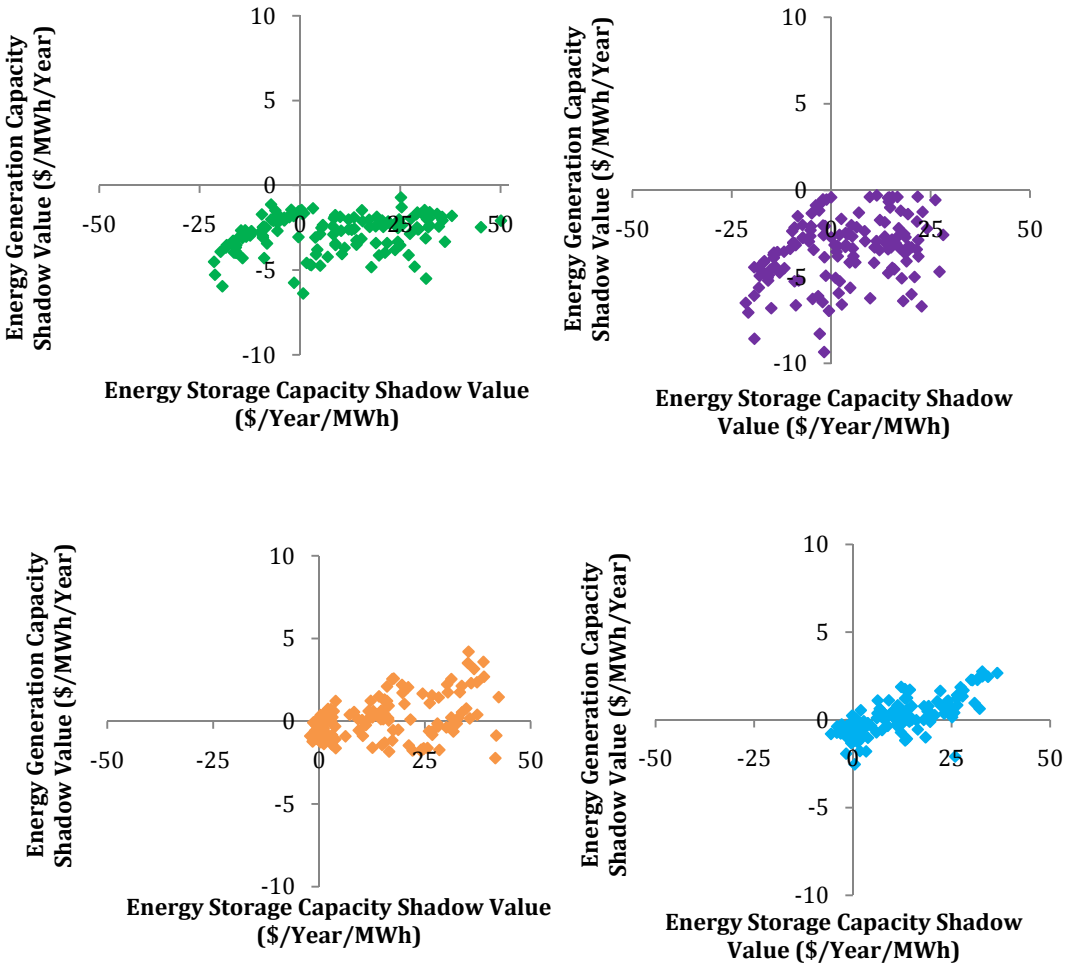

Source: Authors

Figure 29: Average Change of Energy Storage and Generation Capacity Shadow Values from the Base Case from Dry (Top-Left = Dry-ANN1 and Top-Right = Dry-ANN2) and Wet (Bottom-Left = Wet-ANN1 and Bottom-Right = Wet-ANN2) Warming Scenarios (for 137 Hydropower Units in the 1985–1998 Period), Considering the Warming Effects on Hydropower Supply and Demand Simultaneously (Future Energy Pricing Is Forecasted Using ANNs – ANN1: Monthly Based Model; ANN2: Annually Based Model Calibrated on Normal Prices)

Pure Price Increase Scenarios Coupled with Climate Warming Scenarios

Figure 30 shows the average annual revenues for each price increase scenario (±0 percent, +30 percent, and +100 percent by year 2100) coupled to warming scenarios. The inputs used with EBHOM are monthly revenue curves, which are the integration over the price frequency distribution. Therefore, a linear price increase by K percent increases annual revenues by K percent. For instance, a price increase of 100 percent under a Dry scenario increases average annual revenue by 100 percent relative to the initial Dry scenario. Revenues are increased by K percent (K=30 or 100) under each price increase scenario, and so are average shadow prices of energy generation expansion and energy capacity expansion. Energy storage expansion and

energy generation expansion become more valuable when price increase scenarios are considered.

Average annual energy generation and energy spills are identical whether or not a price distribution was increase by K percent for each climate warming scenario. The same behavior is observed for average monthly generation, average end-of-month storage, and energy spill patterns. The system optimized for revenue maximization responds in a similar manner to the price distribution increased by a constant percentage than to the initial price distribution.

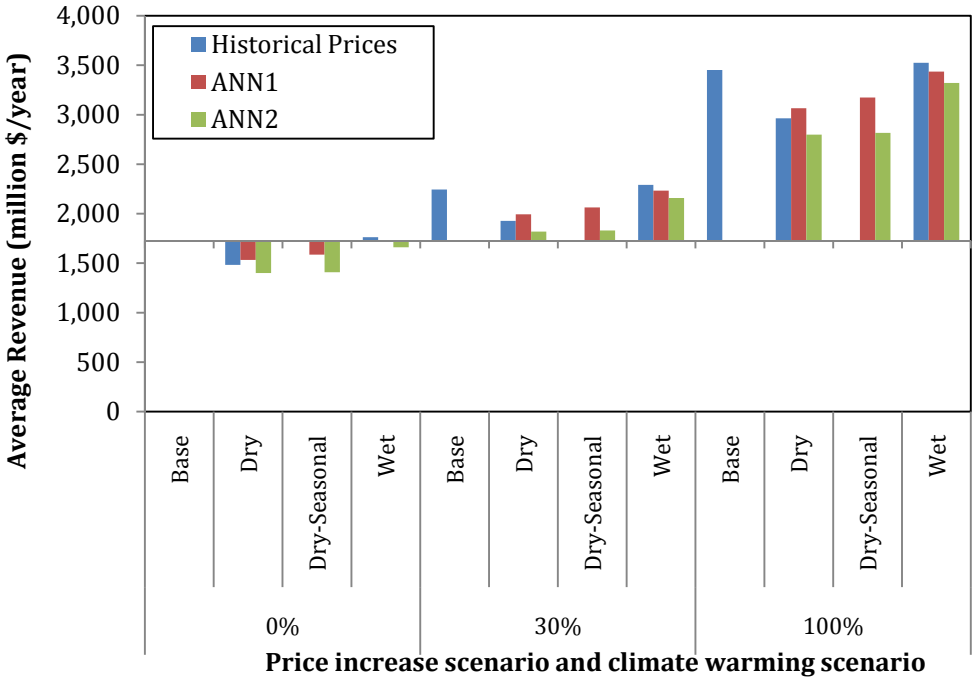

Source: Authors

Figure 30: EBHOM's Annual Revenue Results (Average of Results over 1985–1998 Period) for Different Climate Warming Scenarios Coupled to Price Increase Scenarios by 0%, 30%,and 100%. Scenarios Are Based on Historical Prices, or Forecasted Future Energy Prices from Monthly ANN Models (ANN1) or an Annual ANN Model (ANN2). The Horizontal Axis Crosses the Vertical Axis at the Base Case (+0%) Average Revenue Value.

Section 7: Limitations and Future Direction

Climate warming might have impacts on California's high-elevation hydropower system in the next century. This work is aiming to estimate the effects from a change in both hydrological conditions and energy demand and pricing. What we are interested in is the "big picture"; so many simplifying assumptions were necessary and should be considered in interpreting the results. Results from this work give, however, some insights on how the system works and how it might adapt to climate change.

Temperature data from several meteorological stations were averaged to define a temperature dataset for California, even if temperature varies consistently from area to area. As the big-picture study, this work also ignores the effects of climate variability on hydropower supply and demand. This is an important drawback of the study that may be addressed by future research. Furthermore, future studies may use hourly temperature data from other sources such as the National Climatic Data Center (NCDC) and Climate Reference Network.

Energy demand was included in ANN modeling as a third-order polynomial function of temperature. This function was estimated by Franco and Sanstad (2006) to correlate the daily mean demand to the average daily temperature. Estimating hourly demands through this function implies that the hourly demand follows the same pattern as the mean daily demand. This seems to be a reasonable assumption, knowing that we are interested in the big picture over California and that temperatures are also flattened. However, future studies may consider proper mapping of the hourly prices that contain the many peaks that may result from periods of peak demand. Historically, peak loads have been increasing year after year, and this was not considered in this modeling study. Future research could improve the experiment from this work by considering the development of two ANNs in series: the first to estimate a nonlinear response of demand from temperature, and the second to estimate a nonlinear response of price from demand.

Processing time for ANN calibration is a limiting factor. Using a more powerful computer system or opting for a simpler ANN optimization method, such as the Levenberg-Marquadt algorithm, could enhance the ANN architecture and accelerate the calibration process. Several independent calibration runs could then be performed to find the optimal set of weights (which should converge to identical values). However, even if the SCE-UA optimization algorithm is complex, it should have a high probability of finding the global optimum (Duan et al. 1992).

In the present research, two ANN models were developed; 12 parallel monthly models for all price ranges and one annual model for normal range prices (from which price spikes have been removed). Each approach presents advantages and drawbacks for mapping hourly prices accurately. Monthly models deal with all price ranges, and there is no arbitrary elimination of price intensities that could be abnormal (or not). However, it is possible that the ANN does not learn anything from these high prices, which might bias the learning phase.

One main drawback of the monthly models appears when using ANNs as forecast tools, and results from their inability to extrapolate. The temperature data samples are perturbed to

account for climate warming and then fed to the ANN. Some of these temperatures will be far off the range of the monthly calibrations datasets, and the ANN will face new examples. This might lead to overestimation of the prices. An annual ANN model may be more appropriate to deal with increases in temperature, because these temperatures might have occurred historically in other periods of the years, i.e., in other months. The annual ANN model trained on normal prices should model those with rather high accuracy according to Lu et al. (2005), who mention that it is necessary to remove price spikes from calibration to improve accuracy. When using this annual ANN model as a forecast tool, it is assumed that the future proportion of price spikes will remain the same as for 2005–2008. The future energy market was assumed to stay not ideally competitive, with operators giving priority to profit maximization, leading to possible manipulations of the market. However, it is worth mentioning that in an "ideal" or highly supervised energy market spikes should not occur, except when demand exceeds supply. Further research should deepen price spikes modeling.

The two ANN models developed here do not distinguish workdays from weekends or public holidays. This was seen in some works on short-term price forecasting (e.g., Gao et al. 2000; Amjady and Keynia 2010a) and should be considered in further research. Future research could develop two parallel ANNs: one for workdays and one for both weekends and holidays, since those have similar price patterns.

Real-time energy prices for the period 2005–2008 were employed to calibrate the ANN models and to model the Base case of EBHOM. Application of longer-period price datasets might improve the ANN mapping accuracy, as ANN models are reliant on the quantity and quality of data. The price set from 2005–2008 does not exactly match the energy prices from the runoff data period 1985–1998. This might cause some inaccuracies in EBHOM's estimation of revenues and energy prices but should not affect other results (generation, spills, and storage) much, as the energy price trends are similar between years (Madani and Lund 2010).

Calibration of EBHOM is likely to underestimate energy storage capacities (Madani and Lund 2009), and therefore also underestimate the adaptability of the system to climate changes. Availability of spill or energy storage capacity data would reduce this source of error (Madani and Lund 2010).

Population growth rate was not considered here for future scenarios. However, the work from Aroonruengsawat and Auffhammer (2009) showed that it had significant impacts on projected demand. Even a low population growth rate of 0.18 percent per year predicts an increase of 65 to 70 percent in residential electricity demand by 2100, which completely outpaces the increase resulting from climate change (Aroonruengsawat and Auffhammer 2009). Additional scenarios, including population increase scenarios, could be developed in future research work.

Finally, for problem simplification, price elasticity of demand was not included in this work. If energy prices start rising substantially, it is very probable that consumers will save money by saving energy. The consequent demand decrease will affect energy prices and so on. A recurrent ANN could be more suitable for modeling such phenomenon if compared to a

feedforward ANN, but a recurrent ANN is more complex to implement and time-consuming to train. An econometric model could also be built to estimate this price elasticity of demand.

Section 8: Conclusions

The main objectives of this research project were to develop a tool to model the effects of climate warming on future energy demand and pricing, and to estimate the consequent impacts of climate change on California's high-elevation hydropower system. An ANN model was chosen to map the nonlinear relationship between temperature, energy demand, and prices. This model was then used to forecast energy prices for different climate warming scenarios. Two ANN models were developed: a monthly based model calibrated on all price ranges, and an annually based ANN model calibrated on normal prices (with price spikes removed). Price spikes in the CalISO energy market were identified as prices exceeding $128/MWh, based on real-time energy prices for the period 2005–2008. For the model calibrated on normal prices, the same proportion of price spikes (with the same intensities) was assumed to occur in future. In this work, the energy market was assumed to remain not ideally competitive with priority given to profit maximization.

The ANN price forecast model estimated higher energy revenues in warm months for high-forcing climate scenarios than for low-forcing scenarios, and vice-versa in cold months. This corresponds to a higher demand for cooling in summer and a lower demand for heating in winter. The magnitude of changes in revenue is, on average, higher for the monthly based ANN models than for the annually based ANN model, but monthly models may overestimate prices.

The EBHOM model was run to examine Dry and Wet climate warming scenarios under historical prices. The results showed that energy generation increased from January to April under the Wet scenario; snowmelt water is plentiful, and the system has limited capacity to store the shift in peak runoff. Average monthly generation also increased under the Dry scenario from January to March, relative to Base case, but decreased in the rest of the months, since less inflow is available. For Dry warming scenarios (representing the worst-case), the month that the reservoirs refilled shifted to earlier in the year, to capture the shifted snowmelt. The peak end-of month storage was in May for both scenarios; whereas, it was in June under Base case. Under the Wet scenario, energy spills increased by nearly 1,000 GWh between January and April compared to the Base case. Energy spills occur when the system cannot store all the incoming runoff or send it through the turbines. Even if average generation increased by nearly 6 percent under the Wet scenario relative to Base case, average revenues only increased by 2 percent, because spills increase. Under the Dry scenario, average generation decreased by 20 percent, but revenues only decreased by 14 percent relative to Base case, showing that the system is able to adapt, to a certain extent, to changing hydrology. The system increases annual revenues if either energy storage or energy generation capacity is expanded under the Wet and Dry scenarios, relative to the Base case. Energy storage capacity expansion is more beneficial than generation capacity expansion, although such expansion might not be justified due to expansion costs. As expected, benefits of capacity expansion are greater for the Wet scenario, when the additional capacity can be more frequently used.

The study also compared the EBHOM model's results when climate change effects on high-elevation hydropower supply and demand in California are simultaneously considered to those

from studies that ignored demand changes. Energy generation increased in warm months when demand is high and energy is valuable, and decreased in winter, when less heating is needed and prices are off-peak. This held true for both climate warming scenarios and both ANN models. Between February and June, end-of-month storage increased under all scenarios relative to results from studies that ignored demand changes. Less energy is generated in warmer winters; therefore, it is available to be stored until the high-demand season. Energy spills are not much different from EBHOM's results based on historical pricing. Under the Wet scenarios, energy revenues decreased, because average energy price received decreased and average energy revenues were lower than in Base case. Under the Dry scenario, revenues were always lower than Base case, and the monthly based ANN model suggested more revenues than the annually based ANN model. The system under the Dry scenarios benefited more from energy storage capacity expansion than when historical prices were considered. The marginal benefits from energy generation expansion under both the Dry and the Wet scenarios that considered the effects of warming on demand are estimated to decrease relative to results of studies that did not consider those effects.

Finally, expanding the energy storage capacity of California's high-elevation hydropower system seems to be the most beneficial option to adapt to climate change and maximize the increase in revenue, although such expansion might not be justified due to expansion costs. The benefits gained range from $29 to $81/year/MWh when changes in demand are considered, depending on the climate scenario. Future research should conduct a case-by-case study of the benefits gained by each power plant to decide whether storage or generation capacities should be expanded at each unit.

The identified differences between the estimated impacts of climate change on California's high-elevation hydropower system with consideration and without consideration of climate change effects on hydropower demand and pricing have an important policy implication: "Studies that ignore the climate change effects on the demand side of hydropower systems do not provide a reliable picture of the system in the future and the positional effects of climate change effects on hydropower demand and pricing must be considered in future adaptation studies and policy making regarding hydropower."

References

Amjady, N., and Hemmati, M., 2006. Energy price forecasting - problems and proposals for such predictions. *IEEE Power Energy Mag. 4 (2)*, 20–29.

Amjady, N., and Keynia, F., 2010a. Electricity market price spike analysis by a hybrid data model and feature selection technique. *Electric Power Systems Research* 80, 318–327.

Aroonruengsawat, A., and Auffhammer, M., 2009. *Impacts of climate change on residential electricity consumption: evidence from billing data*. California. California Climate Change Center, CEC-500-2009-018-D, [Online] March 2009. Available at: www.energy.ca.gov/2009publications/CEC-500-2009-018/CEC-500-2009-018-D.PDF.

ASCE, 2000. Artificial Neural Networks in Hydrology. I: Preliminary Concepts. *Journal of Hydrologic Engineering*, 5 (2).

Aspen Environmental Group and M. Cubed. 2005. *Potential changes in hydropower production from global climate change in California and the western United States.* California Climate Change Center, CEC-700-2005-010, [Online] June 2005. Available at: www.energy.ca.gov/2005publications/CEC-700-2005-010/CEC-700-2005-010.PDF.

Bloom Energy, 2010. Understanding California's Electricity Prices. [Online] Available at: http://c0688662.cdn.cloudfiles.rackspacecloud.com/downloads_pdf_White_Paper_Calif_Elec_Prices.pdf [Accessed 10 April 2010].

California Climate Change Center, 2006. *Our Changing Climate – Assessing the Risks to California*. CEC-500-2006-077, [Online] Available at: www.energy.ca.gov/2006publications/CEC-500-2006-077/CEC-500-2006-077.PDF.

Cayan, D. Maurer, E. Dettinger, M. Tyree, M. Hayhoe, K. Bonfils, C. Duffy, P., and Santer, B.,2006. *Climate Scenarios for California*. California Climate Change Center, CEC-500-2005-203-SF, [Online] March 2006. Available at:www.energy.ca.gov/2005publications/CEC-500-2005-203/CEC-500-2005-203-SF.PDF.

Cayan, D. R. Maurer, E. P., Dettinger, M. D., Tyree, M. Hayhoe, K., 2008. Climate change scenarios for the California region. *Climatic Change*, 87, 1, 21–42.

Cayan, D., Tyree, M., Dettinger, M., Hidalgo, H., Das, T., Maurer, E., Bromirski, P., Graham, N., and Flick, R., 2009: Climate Change Scenarios and Sea Level Rise Estimates for the California 2008 Climate Change Scenarios Assessment. California Climate Change Center, CEC-500-2009-014-F, 64 pages. Available at: www.hugohidalgoleon.com/files/papers/CEC-500-2009-014-D.PDF.

Congressional Budget Office (CBO), 2001. Causes and Lessons of the California Electricity Crisis. [Online] Available at:www.cbo.gov/ftpdocs/30xx/ doc3062/ CaliforniaEnergy.pdf.

Connell-Buck C. R., Medellin-Azuara J., Lund J. R., and Madani K., (2011), Adapting California's Water System to Warm vs. Dry Climates, *Climatic Change*, 109 (Suppl 1): S133-S149, doi: 10.1007/s10584-011-0302-7.

Dawson, C. W. and Wilby, R. L., 2001, Hydrological modeling using artificial neural networks. *Progress in Physical Geography* 25, 1, pp. 80–108.

Duan, Q. Sorooshian, S., and Gupta V., 1992. Effective and Efficient Global Optimization for Conceptual Rainfall-Runoff Models. *Water Resources Research* 28(4): 1015–1031, Paper number 91WR02985.

Duffy P., Bartlett J., Dracup J., Freedman J., Madani K., and Waight K., 2009." Climate Change Impacts on Generation of Wind, Solar, and Hydropower in California," California Energy Commission.

Franco, G., and Sanstad, A. H., 2006. *Climate change and electricity demand in California*. California Climate Change Center, CEC-500-2005-201-SF, [Online] February 2006. Available at:www.energy.ca.gov/ 2005publications/CEC-500-2005-201/CEC-500-2005-201-SF.PDF.

Gao, F., Guan, X., Cao, X-R., and Papalexopoulos, A., 2000. Forecasting Power Market Clearing Price and Quantity Using a Neural Network Method. *IEEE Power Engineering Society Summer Meeting* 2000.

Guégan, M., Uvo, C. V., and Madani, K. 2012. Developing a Module for Estimating Climate Warming Effects on Hydropower Pricing in California. *Energy Policy* 42: 261–271.

Horowitz, M. J., 2007. Changes in Electricity Demand in the United States from the 1970s to 2003. *The Energy Journal*, 28(3).

Kandel, A. Sheridan, M., and Mcauliffe, P., 2008. *A comparison of per capita consumption in the United States and California*. Staff paper from California Climate Change Center, CEC-200-2009-015, [Online] Available at: www.energy.ca.gov/2009publications/CEC-200-2009-015/CEC-200-2009-015.PDF.

Kauffman, E., 2003. Climate and Topography. Atlas of the Biodiversity of California. [Online] Available at: www.dfg.ca.gov/biogeodata/atlas/pdf/ Clim_12b_web.pdf [Accessed 31 March 2010].

Kingston, G. B., Maier, H. R., and Lambert, M. F., 2005. Calibration and validation of neural networks to ensure physically plausible hydrological modeling. *Journal of Hydrology*314:158–176.

Lu, X. Dong, Z. Y., and Li, X., 2005. Electricity market price spike forecast with data mining techniques. *Electric Power Systems Research* 73: 19–29.

Madani, K., 2009. Climate Change Effects on High-Elevation Hydropower System in California. *Ph.D. Dissertation*, University of California, Davis. Available at: http://cee.engr.ucdavis.edu/faculty/lund/students/MadaniDissertation.pdf.

Madani, K., 2011. Hydropower Licensing and Climate Change: Insights from Cooperative Game Theory. *Advances in Water Resources* 34 (2): 174–183. doi: 10.1016/j.advwatres.2010.10.003.

Madani, K., and Lund, J. R., 2007. Aggregated Modeling Alternatives for Modeling California's High-elevation Hydropower with Climate Change in the Absence of Storage Capacity Data. *Hydrological Science and Technology*, 23(1-4): 137–146.

Madani, K., and Lund, J. R., 2009. Modeling California's high-elevation hydropower systems in energy units. *Water Resources Research* 45, W09413. doi:10.1029/2008WR007206.

Madani, K., and Lund, J. R., 2010. Estimated impacts of climate warming on California's high-elevation hydropower. *Climatic Change* 102, 521–538. doi:10.1007/s10584-009-9750-8.

Madani, K. Vicuña, S., Lund, J., Dracup, J., and Dale, L., 2008. Different approaches to study the adaptability of high-elevation hydropower systems to climate change: the case of SMUD's upper American river project. In: Babcock RW, Walton R (eds) Proceeding of the 2008 world environmental and water resources congress, Honolulu, Hawaii. ASCE.

Medellín-Azuara, J., Harou, J. J., Olivares, M. A., Madani, K., Lund, J. R., Howitt, R. E., Tanaka, S., Jenkins, M. W., and Zhu, T., 2008. Adaptability and Adaptations of California's Water Supply System to Dry Climate Warming. *Climatic Change*, 87 (Suppl 1): S75–S90.

Miller, N. L., Hayhoe, K., Jin, J., and Auffhammer, M., 2008. "Climate, extreme heat, and electricity demand in California." *J Appl Meteorol Clim* 47(6):1834–1844.

Moser, S., Franco, G., Pittiglio, S., Chou, W., and Cayan D., 2009. The future is now: an update on climate change science impacts and response options for California. California Climate Change Center, CEC-500-2008-071, [Online] Available at: www.energy.ca.gov/2008publications/CEC-500-2008-071/CEC-500-2008-071.PDF.

McKinney, J. et al., 2003. California Hydropower System: Energy and Environment. [Online] Available at: www.energy.ca.gov/reports/2003-10-30_100-03-018.PDF.

National Oceanic and Atmospheric Administration (NOAA) – National Climatic Data Center, 2009. State of the Climate National Overview Annual 2008 [Online] (Updated 31 June 2009) Available at: www.ncdc.noaa.gov/ sotc/?report=national&year=2008&month=13.

Pew Center on Global Climate Change, 2009. Climate TechBook, chap: Hydropower. [Online] Available at: www.pewclimate.org/docUploads/Hydropower 10%2009 _FINAL_cleanPDF.pdf.

Rosenfeld, A., 2006. *Summing Up Energy Symposium: The 'Rosenfeld Effect'*. California Climate Change Center, CEC-999-2006-005, [Online] Available at: www.energy.ca.gov/2006publications/CEC-999-2006-005/CEC-999-2006-005.PDF.

Tanaka, S. T. Zhu, T., Lund, J. R., Howitt, R. E., Jenkins, M. W., Pulido, M. A., Tauber, M., Ritzema, R. S., and Ferreira I. C., 2006. Climate warming and water management adaptation for California. *Climatic Change* 76(3–4): 361–387.

Tanton, T., 2008. *California's Energy Policy – A Cautionary Tale for the Nation*. Competitive Energy Institute [Online] Available at: http://cei.org/cei_files/ fm/active/0/Tanton_California Energy Policy.pdf.

Union of Concerned Scientists, 2006. Global Warming and California's Electricity Supply - A fact sheet from the Union of Concerned Scientists. [Online] Available at: www.ucsusa.org/assets/documents/global_warming/ ucs_electricity_final.pdf .

Vicuña, S., Leonardson, R., Hanemann, M. W., Dale, L. L., and Dracup, J. A., 2008. Climate change impacts on high elevation hydropower generation in California's Sierra Nevada: A case study in the Upper American River. *Climatic Change*, 87 (Suppl 1), pp.123–137, doi: 10.1007/s10584-007-9365-x.

Vicuña, S., Dracup, J. A., and Dale, L., 2011. Climate change impacts on the operation of two high-elevation hydropower systems in California, *Climatic Change*, 109 (Suppl 1): 151–169.

Zarezadeh, M., Naghavi, A., Ghaderi, S. F., 2008. Electricity price forecasting in Iranian electricity market applying Artificial Neural Networks. *IEEE Electrical Power & Energy Conference* 2008.

Zhang, G., Patuwo, B. E., and Hu, M. Y., 1998. Forecasting with artificial neural networks: The state of art. *International Journal of Forecasting*, 14 (1): 35–62.

Zhao, J. H., Dong Z. Y., and Li, X. 2007. Electricity market price spike forecasting and decision making. *IET Gener. Transm. Distrib., 2007,* 1(4): 647–654.

Zhu, T., Jenkins, M. W., and Lund, J. R., 2005. Estimated impacts of climate warming on California water availability under twelve future climate scenarios. *Journal of the American Water Resources Association (JAWRA)*, 41(5): 1027–1038.

Acronyms

ANN	Artificial Neural Network
ARIMA	Autoregressive Integrated Moving Average
ASCE	American Society of Civil Engineers
CalISO	California Independent System Operator
CalPX	California Power Exchange
CBO	Congressional Budget Office
CCCC	California Climate Change Center
CCE	Competitive Complex Evolution
CPI	Consumer Price Index
EBHOM	Energy-Based Hydropower Optimization Model
ECP	Electricity Consumption Per Capita
ESI	Electricity Supply Industry
GCM	Global Climate Model
GFDL	Geophysical Fluid Dynamics Laboratory
GHG	Greenhouse Gas
GW	Gigawatts
GWh	Gigawatt-hours
HEESA	Hydro-Environmental and Energy Analysis
IPCC	Intergovernmental Panel on Climate Change
KWh	Kilowatt-hour
Logsig	Logistic sigmoid
MLP	Multi-Layer Perceptron
mm	Millimeter
MSE	Mean-Squared Error
MW	Megawatts
NCAR	National Center for Atmospheric Research
NCDC	National Climatic Data Center

NN	Neural Network
NOAA	National Oceanic and Atmospheric Administration
NOCAL	Northern California Region referring to Sacramento area
NSM	No-Spill Method
OASIS	Open Access Same-time Information System
PCM	Parallel Climate Model
PG&E	Pacific Gas & Electric
RMSE	Root Mean-Squared Error
SCE	Southern California Edison
SCE-UA	Shuffle Complex Evolution – University of Arizona
SDG&E	San Diego Gas & Electric
SOCAL	Southern California region, referring to the area around Riverside
SRES	Special Report on Emissions Scenarios
Tanh	See Tansig
Tansig	Hyperbolic tangent
USGS	U.S. Geological Survey
WSPC	Water Science and Policy Center

Glossary

Nominal Price: "The price paid for a product or service at the time of the transaction. Nominal prices are those that have not been adjusted to remove the effect of changes in the purchasing power of the dollar; they reflect buying power in the year in which the transaction occurred." (Source: EIA, http://www.eia.doe.gov/glossary/index.cfm?id=N)

Normal Prices: Prices that are not price spikes, i.e., positive price values below the threshold defining price spikes.

Predictor: A neuron in the input layer of an artificial neural network.

Predictand: A neuron in the output layer of an artificial neural network.

APPENDIX A:
Artificial Neural Network

Background and Motivation: ANNs to Model Electricity Prices

Artificial neural networks (ANNs) are networks of interconnected neurons that were developed in an attempt to reproduce the powerful human brain's architecture (Hsieh and Tang 1998). They are powerful machine learning models that have been successfully developed for different purposes, namely for nonlinear modeling (e.g., Kingston et al. 2005) and classification (e.g., Olsson et al. 2004). They provide an appealing solution for relating input and output variables in complex systems (Dawson and Wilby 2001) and have been widely applied in different fields, such as hydrological modeling (e.g., Dawson and Wilby 2001; Kingston et al. 2005; Olsson et al. 2004), electricity load forecasting (e.g., Azadeh et al. 2006; Ortiz-Arroyo et al. 2005; Hippert and Taylor 2010), and electricity price short-term forecasting (e.g., Ranjbar et al. 2006; Zarezadeh et al. 2008; Gao et al. 2000).

In recent years there has been active research to develop accurate short-term price forecasting tools for the energy market (e.g., Zhao et al. 2007; Lu et al. 2005; Amjady and Keynia 2010a; Yamin et al. 2004; Zarezadeh et al. 2008). Electricity price is a nonlinear, time-variant, and volatile signal owning multiple periodicity, high frequency components, and significant outliers—i.e., unusual prices (especially in periods of high demand) due to unexpected events in the electricity markets (Amjady and Hemmati 2006). California's electricity supply industry turned into a competitive, deregulated market in the 1990s (CBO 2001). This deregulation created competition among electricity producers and retailers who need price forecasts to develop their bidding strategy in the electricity market (Lu et al. 2005; Amjady and Hemmati 2006). Optimal decisions are now highly dependent on market electricity price (Amjady and Keynia 2010a). For instance, electricity generation scheduling is based on profit maximization in the unregulated environment; whereas, it was based on cost minimization—to satisfy the electricity demand and all operating constraints—in the earlier regulated environment (Zarezadeh et al. 2008).

Dealing with short-term price forecasting, ANNs have shown a good ability to forecast normal electricity prices (Zhao et al. 2007). One of the main advantage of ANNs over traditional methods such as regression and time series or autoregressive integrated moving average (ARIMA) is that they are more adapted to long-term patterns, as they can cope with high nonlinear behavior of the target signal (Amjady and Hemmati 2006). However, one main problem encountered in most studies is the inability of the models to deal with price spikes in the electricity market (e.g., Zhao et al. 2007; Lu et al. 2005; Amjady and Keynia 2010a; Yamin et al. 2004). Generally, price spikes are abnormal market clearing prices that include *abnormal high prices,* which are prices much higher than normal prices (Zhao et al. 2005). Price spikes are highly erratic and are caused by a number of complex factors and unexpected events such as transmission network contingencies, transmission or congestion, and generation contingencies (Zhao et al. 2007). According to Lu et al. (2005), almost all the existing techniques require that price spike signals be filtered out in order to forecast normal prices with rather high accuracy.

To the best knowledge of the authors, research on ANNs has exclusively focused on short-term price forecasting following market needs. No ANN model has been developed for long-term electricity price forecasting accounting for climate change scenarios, nor for estimating impacts of future climate on any other variable.

ANN Model Types

A typical ANN consists of a number of neurons (also called nodes) that are organized into a specific arrangement (ASCE 2000). One way of classifying neural networks is by the direction of information flow and processing, i.e., *feedforward* and *recurrent* networks (ASCE 2000). In a feedforward network (Figure A-1), information flows unidirectionally from an input layer toward an output layer. In between the input and output layers there can be one or several hidden layers processing information before it reaches the output layer. In this case, neurons are only connected between different layers, but not to other neurons belonging to the same layer. In a recurrent network, information flows in both directions—inputs toward outputs and vice versa—and nodes belonging to the same layer can be interconnected. Recurrent networks allow modeling dynamic systems by making feedback possible in the network, but it is also possible to treat explicitly dynamic systems with feedforward networks by including lagged inputs (Maier and Dandy 2000).

Feedforward networks (also known as multilayer perceptron, or MLP, models) are commonly used for prediction and forecasting applications in hydrological problems (ASCE 2000; Kingston et al. 2005) and in short-term electricity price forecasting (e.g., Ranjbar et al. 2006; Zarezadeh et al. 2008). Feedforward networks have, in general, a faster processing speed than recurrent networks (Maier and Dandy 2000), and Hornik et al. (1989) showed that with a single hidden layer they can approximate any nonlinear function, given that sufficient degrees of freedom (i.e., hidden neurons) are provided.

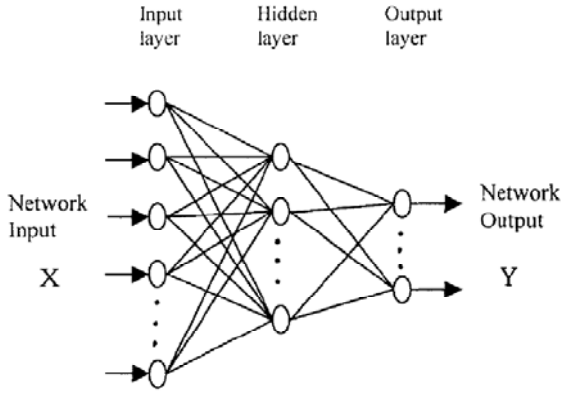

Source: ASCE 2000

Figure A-1: Schematic Diagram of a Feedforward Three-Layer ANN

Figure A-2 shows a schematic diagram of a neuron j. This neuron transforms an input vector $X = (x_1, \ldots, x_i, \ldots, x_n)$ into a single output y_j. Neuron 'j' is characterized by a set of weights

represented by a vector $W_j = (w_{1j}, \ldots, w_{ij}, \ldots, w_{nj})$, a bias b_j, and an activation function f. The inputs to the neuron can be causal variables (i.e., inputs to the system if the neuron is in the input layer), or they can be outputs from neurons belonging to previous layers. The activation function determines the response of the neuron as follows: $y_j = f(X * W_j + b_j)$. Sigmoid functions, namely logistic sigmoid ('logsig') or hyperbolic tangent ('tanh' or 'tansig'), are commonly used in the hidden layers (ASCE 2000). They return a nonlinear output response which makes them a useful tool to map nonlinear processes and are usually combined to a linear activation function in the output layer (ASCE 2000).

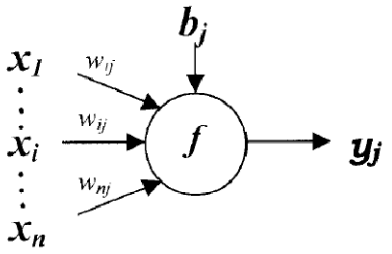

Source: ASCE 2000

Figure A-2: Schematic Diagram of a Neuron "j"

For a model to represent reality as accurately as possible, the model has to be trained and optimized. Training, or calibrating, an ANN model is the process of adjusting its parameters (i.e., weights) to minimize a predefined error function (Kingston et al. 2005). A data sample is presented to the model, and the error is calculated by comparing the simulated and the observed target intensities.

Local or global search optimization algorithms may be used to train the ANN (Maier and Dandy 2000). Local search methods scan the error surface in a single direction; whereas, global search methods scan the error surface in different directions simultaneously (Kingston et al. 2005). Back-propagation algorithm is among the most widely applied methods to train an ANN in hydrological modeling (Maier and Dandy 2000) and in electricity price short-term forecasting (e.g., Ranjbar et al. 2006; Zarezadeh et al. 2008). The radial basis function method and the conjugate gradient method are both examples of other local search algorithms (ASCE 2000).

One of the major drawbacks of local-type search optimization methods is that they are not designed to handle the presence of multilocal optima (Duan et al. 1992). It is therefore not guaranteed that the user will obtain the global optimum, as the ANN may get stuck in one of the local minima of the error surface (Kingston et al. 2005). Global search methods have the ability to escape local minima in the error surface and shall, in principle, find the optimal weight configurations (Maier and Dandy 2000). Genetic algorithms and Shuffle Complex Evolution algorithms are examples of global search methods that have been applied in the hydrological field (Kingston et al. 2005). See Maier and Dandy (2000), ASCE (2000), and Duan et al. (1992) for a more exhaustive review of training methods.

During the training phase, the ANN has to be adjusted to minimize the error function. The optimal ANN architecture is commonly determined through a trial-and-error procedure, by trying out a different number of hidden layers and nodes (ASCE 2000; Maier and Dandy 2000). Increasing the size of the ANN increases the number of free parameters (weights). An ANN should contain enough parameters to improve its capacity to map a complex relationship between the inputs and outputs (Dawson and Wilby 2001). However, increasing the size of the network over a certain threshold may produce the opposite effect if the ANN starts overfitting the data, annihilating its ability to generalize trends (Dawson and Wilby 2001). This phenomenon appears when the ANN performs well during the training period but produces poor results if a new data sample is presented to the ANN (Hsieh and Tang 1998). Cross-validation procedure, also referred to as *cross-training*, is commonly used to prevent overfitting (Maier and Dandy 2000). It consists of dividing the data sample into three sets—usually called the training, validation, and test sets—and then using them independently to check when the ANN is optimized. The ANN is considered to be optimized when the training set minimizes the error function and the error starts increasing in the validation phase (ASCE 2000). It has also been suggested in literature that if the number of training samples exceed a specific threshold, which is defined by a ratio between the number of training samples and the number of connection weights, overfitting will not arise. These ratios can vary consistently in literature (Maier and Dandy 2000), but they should be interpreted as follows: the higher the number of training samples, the lower the probability of overfitting the data.

ANN Model Set Up

The method used to design the ANN was inspired from the protocol for implementing the ANN Rainfall-Runoff model defined by Dawson and Wilby (2001) and modeling suggestions from Maier and Dandy (2000). The modeling process steps will be explicitly detailed as far as possible, so that the validity of the model and results can be assessed. The following procedure was used:

1. Selection of the adequate predictors and predictands and data collection
2. Data analysis and preprocessing
3. ANN selection: choice of an appropriate network type and training algorithm
4. Network training: choice of the architecture and training set
5. Evaluation of ANN performance

Data Collection: Predictors and Predictand Selection

Hourly prices were selected as the only predictand. Real-time hourly energy prices for 2005–2008 were collected from the California ISO (CalISO) Open Access Same-time Information System (OASIS) website (http://oasishis.caiso.com/). In April 2009 a new market design was implemented: instead of looking at three main price zones, CalISO started using locational marginal pricing that produces prices at 3,000 different pricing nodes around the California grid. Therefore the datasets from after April 2009 are considerably different from those in the previous system, so data could not be gathered easily for 2009. CalISO serves more than

30 million consumers with electricity, so these hourly prices are considered to be representative for California's energy market.

Electricity price is driven by many factors in a competitive energy market (Ranjbar et al. 2006). Research works applying ANNs to short-term price forecasting have chosen, among others, the following predictors: historical hourly prices, system loads, lagged hourly prices, and day of the week, as they are often easily accessible (e.g., Ranjbar et al. 2006; Zarezadeh et al. 2008). Gao et al. (2000) also considered fuel costs, power import/export data and other weather variables. In the present research, the following inputs were chosen: temperature, demand, season, month, day of the week, hour, lagged hourly temperatures for the three previous hours, and a "degree-day" temperature input. The season is expected to account for the annual price variability, the hour for the daily periodicity, and the day of the week for the weekly periodicity—that is, to distinguish workdays from weekends.

Hourly temperature data for the period 2005–2008 were extracted from the website of the University of California Statewide Integrated Pest Management Program (UC IPM) (www.ipm.ucdavis.edu/WEATHER/wxretrieve.html). These data were available for several pest stations across California, but not further north nor further south than Fresno and Colusa Counties, respectively. It was decided to extract hourly data from three different pest stations and to define their average as the representative temperature for California.

Hourly electricity load data were also collected from the CalISO OASIS website (http://oasishis.caiso.com/) for 2005–2008. Demand was estimated using temperature data, based on the work of Franco and Sanstad(2006). Using daily demand of electricity from 2004 for the area services by the CalISO, Franco and Sanstad found out that there is a high correlation between the daily demand and the average daily temperature measured in four locations of California. They approximated the relationship by the U-shaped third-degree polynomial plotted in Figure A-3, indicating the minimum daily demand for $T_{min} = 53{,}5°F$. Estimating hourly electricity demands through this function implies that the hourly demand follows the same pattern as the mean daily demand. This seems to be a reasonable assumption for this work, since we are interested in the big picture. However, future research may consider mapping hourly prices that contain many peaks, which might result from periods of peak demand, more properly.

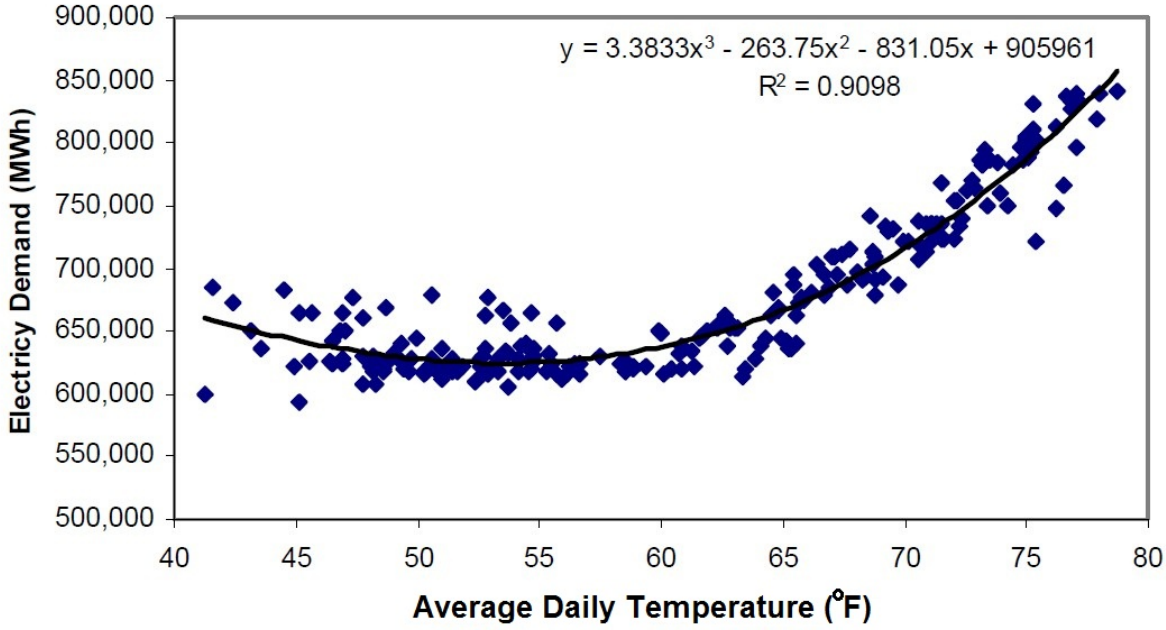

Source: Franco and Sanstad 2006

Figure A-3: Electricity Demand in the CalISO Area as Function of Average Daily Temperatures, 2004

Data Analysis and Preprocessing

Data Analysis

ANNs rely on the quantity and quality of the calibration data (Kingston et al. 2005). A preliminary data analysis was performed to better understand the varying nature of hourly prices, and to determine if there were any major abnormal trends. Temporary irregularities in the energy market or extreme weather conditions may, for instance, lead to substantial variations in energy prices, while being the result of single events; hedging the generalization capacity of ANNs.

Table A-1 shows the main statistical characteristics of the set. The dataset has a mean of $57/megawatt-hour (MWh) and a standard deviation of around $37/MWh. Around 80 percent of the data are in the range $25–$90, but the hourly prices are highly volatile, with prices up to $400/MWh, which is seven times the average price.

Table A-1: Dataset Statistical Characteristics Before Preprocessing

Prices in $/MWh				Price Percentiles in $/MWh				
Average	Standard Deviation	Minimum	Maximum	10th	25th	50th	75th	90th
56.77	36.52	0.00	399.99	24.23	37.78	50.85	67.18	89.91

The hourly price time-series for 2005–2008 is plotted in Figure A-4, where two "abnormal" trends are noticed (circled in the figure) with exceptionally high prices. Figure A-5 is plot of monthly average prices in each year. The same two periods of higher-than-normal prices can be observed. The first one happened in 2005, where prices started increasing in July, reached a maximum average value of $80/MWh in October, and only dropped to normal levels in January 2006. The second period of higher-than-normal prices happened in the first half of 2008 and peaked to a monthly average value of more than $100/MWh in June 2008. A specific investigation of these two periods was conducted, and is described in the following paragraphs.

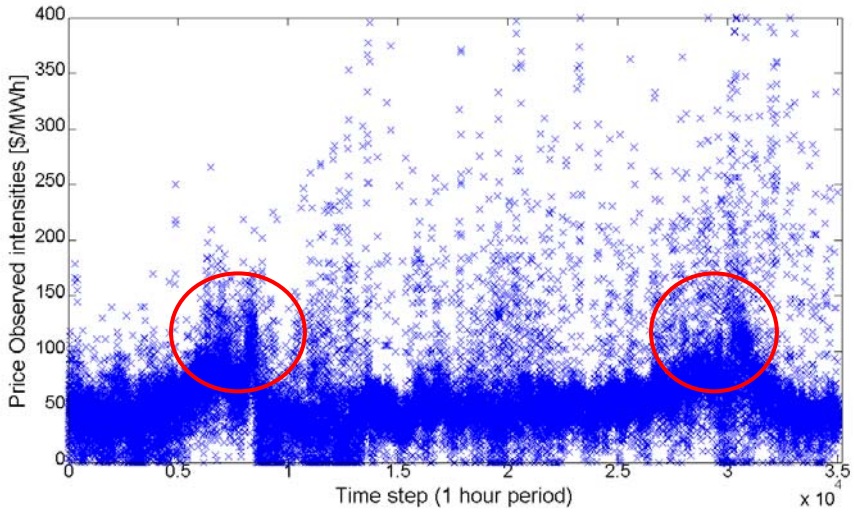

Source: Authors

Figure A-4: Real-time Hourly Prices Observed for the Time Series 2005–2008

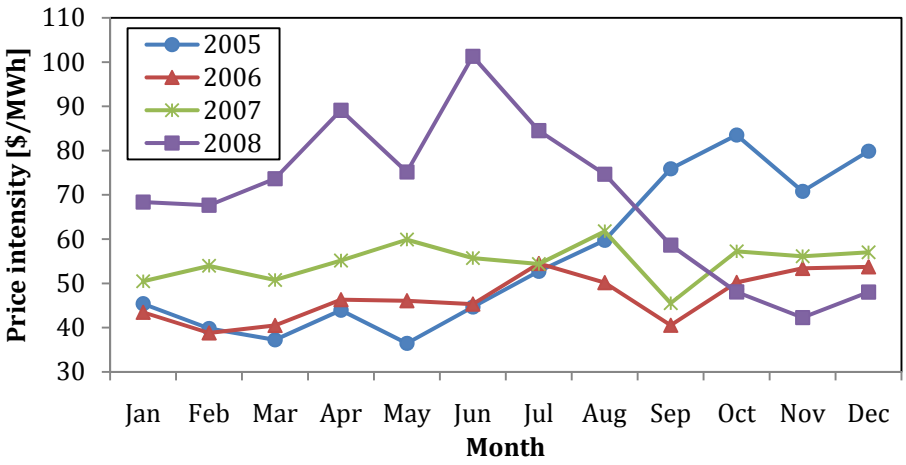

Source: Authors

Figure A-5: Average Hourly Prices Per Month for Each Year 2005–2008

In 2005, national natural gas prices increased substantially over levels seen in 2004 (CalISO 2006), resulting in increasing production costs for electricity. This steady rise began in January and later on prices peaked immediately after Hurricanes Katrina and Rita hit the U.S. Gulf Coast (CalISO 2006). The most destructive wave of the hurricanes occurred the last week of August in southeast Louisiana and caused severe destruction along the Gulf Coast, from central Florida to Texas. In particular, national gas production and transportation infrastructures in the Gulf of Mexico region were destroyed (CalISO 2006). After this event, Western markets—which had not been directly affected by the hurricanes—started trading gas at a discount of approximately $2/mmBtu (million British thermal units) compared to national prices (Department of Market Monitoring – CalISO 2006). In December 2005, a cold snap, coupled with limitations to the Gulf Coast transportation and production infrastructure, resulted in a second peak, with California prices reaching their highest levels since December 2000 (CalISO 2006).

The climatic conditions of 2008 were investigated, as extreme temperatures can lead to an increase in electricity demand, and drought conditions can lead to a reduction in generation from hydropower units. According to the National Oceanic and Atmospheric Administration (NOAA) (2009), summer and fall 2008 were warmer than average in California, as it experienced its sixth warmest summer and third warmest fall on record; whereas, temperatures in winter were slightly below normal. California experienced its driest spring (March to May) on record, and also received below-normal precipitation in summer and fall 2008 (NOAA 2009). At the same time, the snowpack was referred to as among the healthiest in more than a decade in some parts of the Western United States, with most locations near to above average (NOAA 2009).

From these facts, it is hard to assess if there was a shortage of supply, as the abundant snowpack runoff may have compensated for the drought. However, the 2008 Annual Report from CalISO (2009) states that "monthly average hydroelectric production in 2008 was below

2007 levels for most months and well below the monthly production levels for 2005 and 2006." Furthermore, the same report from CalISO (2009) explains that the primary driver of the high electricity prices in 2008 was the spike in worldwide fossil fuel costs. Natural gas, which is the primary fuel for California's energy supply, reached its highest price level since Hurricanes Katrina and Rita affected much natural gas infrastructure in 2005. These high natural gas prices, coincident with low hydroelectric production in California in the first half of that year, resulted in high production costs of electric power in 2008 and the need for additional electricity imports from the Pacific Northwest and Southwest (CalISO 2009). The senior vice-president and chief customer officer of Pacific Gas & Electric (PG&E) also declared that "The combination of skyrocketing natural gas prices, increased electricity demand and lower supplies of hydroelectric power are having a significant impact on the cost of electricity" (PG&E 2008).

As the main focus of this paper is to investigate the relation between prices and climate, prices are plotted against temperature in Figure A-6. The top graph is a plot of the raw hourly data, while the bottom one shows the average price corresponding to each degree Fahrenheit. From the top graph, no obvious conclusion can be drawn regarding the relationship between the real-time prices and the temperature. This strengthens the need for a powerful modeling tool able to represent highly nonlinear relationships. The bottom plot in Figure A-6 shows that prices tend to increase for both low (>30°F, or >-1°C) and high (>90°F, or 32°C) temperatures, but more significantly for high ones. This corresponds to the great need for cooling in the long warm periods in California. In-between average temperatures are around the mean of the entire set, which is 57°F (14°C). Electricity prices in 2008 were higher than those in other years for most temperatures above 50°F (10°C), due to the reasons discussed earlier.

It is well known that the hour of the day has a significant influence on demand, and therefore on price. Figure A-7, which shows the hourly average prices in each season, was plotted to check this affirmation. From Figure A-7 one can see that the main difference between seasons occurs between hours 12 and 20. The high cooling demand in summer increases the price, peaking at hour 17, while the "no" or little heating demand in winter decreases the price.

Figure A-6: Hourly Prices Plotted Against Temperature (Top) And Average Hourly Prices Per Temperature (Bottom)

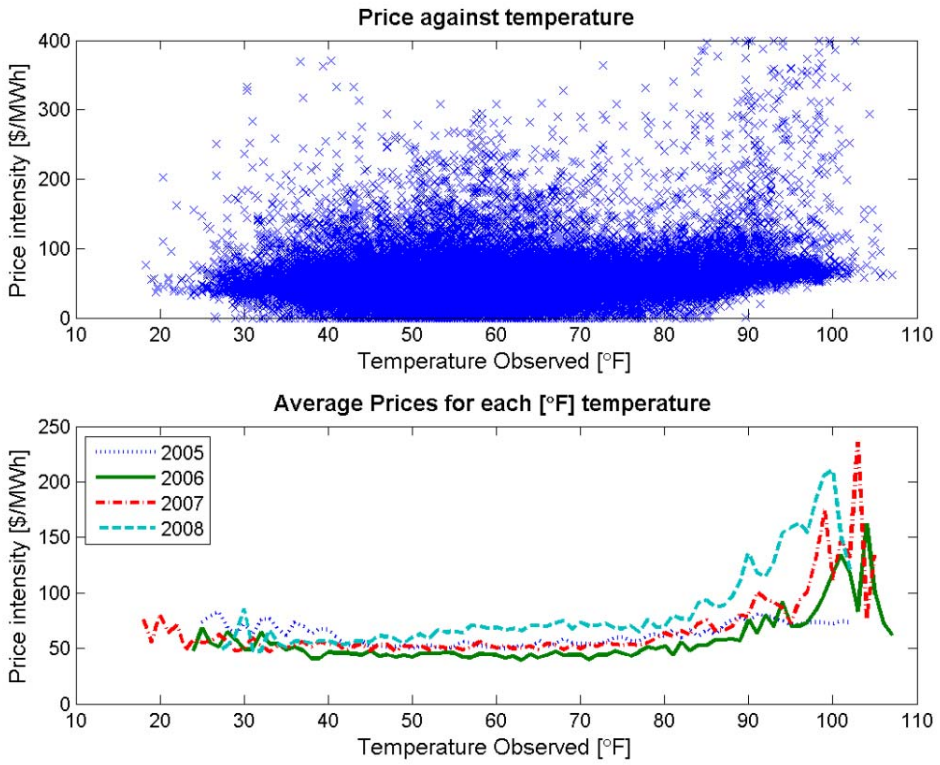

Source: Authors

Figure A-6: Hourly Prices Plotted Against Temperature (Top) And Average Hourly Prices Per Temperature (Bottom)

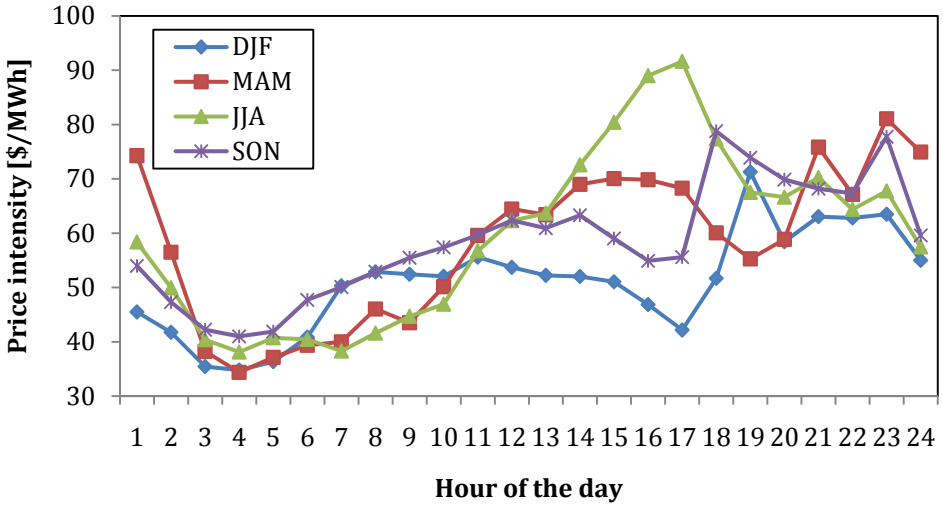

Source: Authors

Figure A-7: Hourly Average Prices in Each Season

Data Preprocessing

Bases on the data analysis results, the research team decided to exclude the period September to December 2005 from the input data to the ANN as they partly result form an extreme event (Hurricane Katrina) and would most probably hedge the training of the neural network. The price increase in 2008 was the result of a combination of several factors. It was decided to keep the 2008 data for two reasons: to keep a great quantity of data, and because soaring prices of fossil fuels together with dry periods are most likely to occur again in the future. However, an additional neuron in the input layer was introduced to account for this specific phenomenon. This input is equal to 1 for the period January to June 2008, and 0 otherwise.

Table A-2 shows the statistical characteristics of the preprocessed dataset. Negative price intensities were set to zero and the overall zero-depth probability is 1.30 percent.

Table A-2: Dataset Statistical Characteristics Before Preprocessing

Prices in $/MWh				Price Percentiles in $/MWh				
Average	Standard Deviation	Minimum	Maximum	10th	25th	50th	75th	90th
54.87	36.54	0.00	399.99	23.88	36.88	49.13	64.14	84.28

The last stage of the data preprocessing was the standardization of the hourly prices and temperatures, by subtracting the mean value of the set and dividing it by the standard deviation. Standardized temperature data ranged between -2.72 and 3.05 and standardized price data between -1.50 and -9.44. The output data (i.e., the hourly prices) were then scaled between 0.1 and 0.9 to avoid squashing when using the log sigmoid function in the hidden layer (and similarly between -0.9 and 0.9 when using the hyperbolic tangent activation function).

ANN Selection

A multilayer feedforward ANN was coupled with the global-search algorithm developed by Duan et al. (1992) called the "Shuffle Complex Evolution" (SCE-UA). A single hidden layer with a sigmoid activation function was chosen. The choice of the sigmoid function (tansig or logsig) and the number of hidden neurons were based on a sensitivity analysis detailed later in the paper. The activation function in the output layer is linear. Cross-validation was used as the stopping criteria to prevent overfitting the training dataset. The model was developed in FORTRAN by Juan Martin Bravo in application to river discharge analysis and was modified for this case study.

The general idea of the SCE-UA algorithm is to generate a population of random points from the feasible space of parameters that will evolve toward an optimal solution: the global minimum of the error surface. First, the population is divided into several communities (called complexes) that evolve independently. Within each community, only the part of the population with the best probability of converging toward a global solution is kept and stored in a "sub-complex" using the Complex Evolution Algorithm (CCE) (Duan et al. 1992). The points stored

in the sub-complex will become parents by generating offsprings toward an improvement direction. Each sub-complex will generate offsprings in different directions toward an optimum, based on its own "knowledge" of the error surface. The population is mixed regularly, in order to share the knowledge between the communities and to ensure survivability.

A set of optimum parameters will eventually be found, after several iterations of the procedure. None of the information from the sample is ignored, as each member of a community is a potential parent with the ability to participate in the reproduction process. The evolution process also ensures that the communities do not become trapped in unpromising regions. The SCE-UA method has good convergence properties over a broad range of problems, and it should have a high probability of finding the global optimum (Duan et al. 1992).

The flowchart of the SCE-UA algorithm, and further description of the algorithm's steps, can be found in Duan et al. (1992) and (1994).

Duan et al. (1994) established some guidelines on how to choose the algorithmic parameters in the SCE-UA model. The parameters were initialized to the recommended values (n is the number of parameters to optimize):

- Number of points in complex: m = 2n + 1
- Number of points in each sub-complex: q = n + 1
- Number of consecutive offspring generated by each sub-complex: α = 1
- Number of evolution steps taken by each complex: β = m = 2n + 1

Finally, the number of complexes is problem-dependent and was chosen based on sensitivity analysis detailed later in the paper.

Network Training

The cross-validation procedure was chosen to prevent overfitting/overtraining. The dataset was partitioned into three sets—calibration, test, and validation—in the following proportions: 50 percent, 25 percent, and 25 percent, respectively. Data was split randomly between the sets, but a control was performed to ensure a good distribution among the different sets by checking that extreme (or close to extreme) values of price and temperature were within the training set, and that means and standard deviations of all sets were similar. The training set should be representative of the entire population and include all ranges of intensities, because ANNs are unable to extrapolate (Maier and Dandy 2000).

Evaluation of ANN Performance

The results of the ANN modeling were assessed in terms of: correlation with the determination coefficientR^2, root mean square error (RMSE), the ANN's output price patterns, and the frequency distribution of prices. Because the dataset is large, it is important to assess the quality of the developed model not only based on R^2 value. Furthermore, it is important to keep in mind that in this research, the final desired output from the ANN model is to draw revenue curves for each month (for several climate change scenarios) that will serve as inputs to the EBHOM model. These revenue curves are nothing else than the integration over the price

frequency curves for each month (Madani and Lund 2009), so the frequency distribution of prices was directly assessed in terms of revenue curves.

ANN Model Set Up

ANN training was performed through a trial-and-error process. First, a sensitivity analysis was performed, to determine the best network architecture and the training algorithm parameters; it also included an assessment of the choice of some inputs. Several dataset breakdowns were then considered based on both deterministic and stochastic approaches. Finally, the research team performed a comparison of the different ANN models developed, to select the ANN model to be used as a long-term price forecasting tool.

Sensitivity Analysis

An ANN is a black-box model that has to be calibrated to determine the optimal architecture and parameters. The sensitivity analysis included assessment of the following parameters:

- Number of complexes for the SCE-UA optimization algorithm, and number of hidden neurons (nodes)
- Logsig vs. tansig activation function
- Relevancy assessment of the input selection

Number of Complex and Hidden Neurons

The optimal numbers of complex and hidden nodes were determined in the same way. The first models developed used only one complex and hidden neuron and were then independently increased to 2, 4, and 8 in the next models. Higher values were also tried, but the time required to run such models over the entire dataset exceeded 48 hours, which was considered excessive. Time is a limiting factor in the ANN model improvements. A single hidden layer was chosen, as it should be enough to model any nonlinear relationship (e.g., Hornik et al. 1989). Table A-3 showsR^2 values for the different models tried to estimate the adequate number of complex and hidden neurons. Correlation in terms of R^2 value improves with increasing number of complexes and hidden neurons, so they were both set to 8 for the next modeling steps.

Table A-3: Calibration Results Used to Select the Adequate Number of Complex and Hidden Neurons

Run	Number Complex	Hidden neurons	Activation function	R^2_{train}	R^2_{valid}	R^2_{test}
1	1	4	logsig	0.26	0.23	0.24
2	8	4	logsig	0.27	0.23	0.25
3	1	8	logsig	0.27	0.23	0.26
4	8	8	logsig	0.29	0.25	0.24
5	8	1	logsig	0.20	0.18	0.19
6	8	2	logsig	0.22	0.19	0.21
7	8	4	logsig	0.27	0.23	0.25
8	**8**	**8**	**logsig**	**0.29**	**0.25**	**0.24**

Logsig vs. Tansig Activation Function

A sigmoid-type activation function—usually logistic sigmoid (logsig) or hyperbolic tangent (tansig)—is commonly used in the hidden layer (Maier and Dandy 2000).A comparison of ANNs with identical architectures and these two activation functions (see Table A-4) led to the choice of tansig for the following reasons:

- Correlations are similar for both ANNs.
- The average price returned by the ANN using tansig function is closer to the average of historical prices. It also returns higher maximum price values.
- Tansig function was used in earlier research works applying ANNs to short-term electricity price forecasting (e.g., Ranjbar et al. 2006; Zarezadeh et al. 2008; Gao et al. 2000).

Table A-4: Results Used to Select the Adequate Activation Function in the Hidden Layer

Run	Activation Function	R^2_{sim}	Average Price ($/MWh)	Maximum Price ($/MWh)
Historic	-	-	54.87	399.99
9	Logsig	0.25	54.96	177.59
10	Tansig	0.25	54.93	217.39

Relevancy Assessment of the Selected Inputs

First, an ANN model using only a temperature input was tried, and then additional inputs (season, month, day, hour, temperatures in three earlier hours, and load) were included. The

correlation improves significantly when more predictors are considered (see Table A-5, where R^2_{sim} jumps from 0.08 to 0.23) because temperature only cannot represent accurately the high volatility of electricity prices. Among the other predictors, none were assessed during the sensitivity analysis, except the load input. ANN models should be able to determine single-handedly which inputs are critical, but it might increase processing speed if the inputs selected *a priori* have little importance (Maier and Dandy 2000).

Table A-5: Results Used to Select the Adequate Activation Function in the Hidden Layer

Run	Number Complex	Hidden neurons	Input neurons	Activation function	R^2_{train}	R^2_{valid}	R^2_{test}	R^2_{sim}	RMSE
11	8	2	**1**	logsig	0.09	0.07	0.08	0.08	0.070
12	8	2	**8**	logsig	0.25	0.21	0.23	0.23	0.065
13	16	4	**1**	logsig	0.09	0.07	0.09	0.09	0.070

Two approaches were imagined to estimate the impact of climate change simultaneously on electricity demand and prices. The first approach involved developing two ANNs in series, with the first one modeling demand using temperature and the other predictors, and the second one estimating prices based on the output demand from the first ANN. The second approach involved building a single ANN considering that demand is a linear function of temperature previously estimated by Franco and Sanstad (2006). A model using this demand function was compared to a model using historical hourly demand to estimate if results would be improved by using historical hourly demand data gathered from CalISO (http://oasishis.caiso.com/).

Using historical hourly demand data improved the R^2 correlation by only 0.03 (see Table A-6) which was not considered as a significant improvement. In terms of revenue curves, it is hard to assess which model is more accurate. In different months, different models fit the historical revenues better, as illustrated for the June and October months in Figure A-8.

Table A-6: Results Used to Choose the Demand Input to the ANN Between Historical Demand and the Demand Function Defined by Franco and Sanstad (2006)

Run	Demand specification	R^2_{train}	R^2_{valid}	R^2_{test}	R^2_{sim}	RMSE
14	Demand = f (T)	0.30	0.24	0.27	0.28	0.140
15	Real demand	0.33	0.29	0.31	0.31	0.136

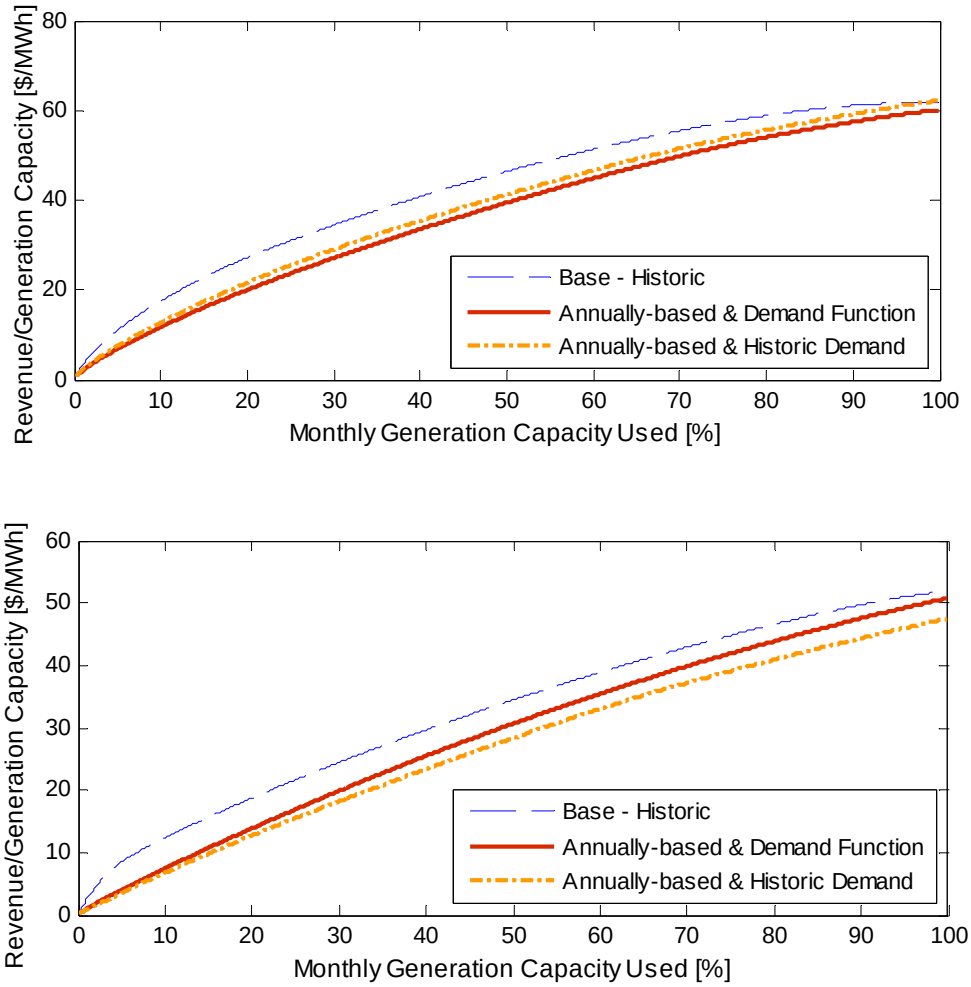

Source: Authors

Figure A-8: Revenue Curve Comparison Between Two Annually Based ANN Models Fed with Historical Hourly Demand Data or with Demand as a Function of Temperature Estimated by Franco and Sanstad (2006) for June (top) and October (bottom)

The research team chose to use the demand as a function of temperature, as estimated by Franco and Sanstad (2006), for a few reasons: virtually no accuracy would be gained by using direct hourly demand data from CalISO, training two ANNs in series could be time consuming, and there would be uncertainty in the estimation of demand from the first ANN model.

Comparison of ANNs Developed for Different Dataset Breakdown

Generally in a competitive energy market, hourly electricity price series contain multiple seasonalities, such as weekly and daily periodicities (Amjady and Hemmati 2006). It is very hard for a single ANN to map correctly the input/output relationship of such a signal in all time periods (Amjady and Keynia 2010b). In previous research, datasets have sometimes been partitioned along: periods of warm/cool days (e.g., Ranjbar et al. 2006), public holidays (e.g., Amjady and Keynia. 2010a), workdays/weekends (e.g., Gao et al. 2000), or stochastic components (e.g., Zhao et al. 2007). As part of the ANN calibration procedure, different data breakdowns have also been tried out in this work. A summary of the experiments and results obtained during training is given later in Table A-8; the results from the earlier sensitivity analysis detailed earlier are not included.

This section first presents common results to all experiments and then discusses each experiment and compares it to the others. Finally, two ANNs are elected for estimating future price representation.

General Comments on the ANN Results

General observations and comments can be drawn from the application of an ANN to model electricity prices for the selected inputs in this research. The results from the calibration of the ANN model over the entire dataset are used here for illustrative purposes (see Figures A-9–A-11) and apply to all the other ANN models developed during calibration. Figure A-9 shows the frequency of historical prices and ANN output prices, Figure A-10 plots the historical and ANN output prices against temperature, and Figure A-11 shows the hourly price time series for 2006 and 2008.

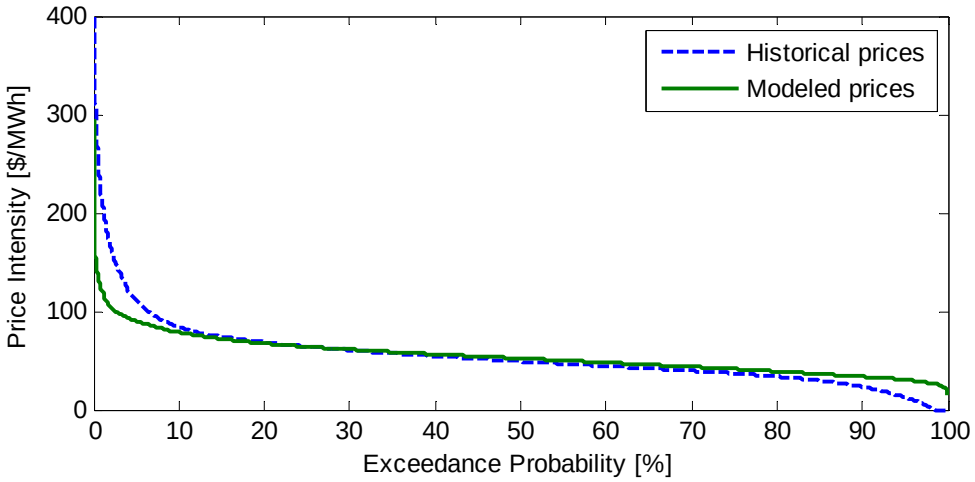

Source: Authors

Figure A-9: Frequency of Historical and Modeled Prices for an Annually Based ANN Trained on All Price Ranges from 2005–2008

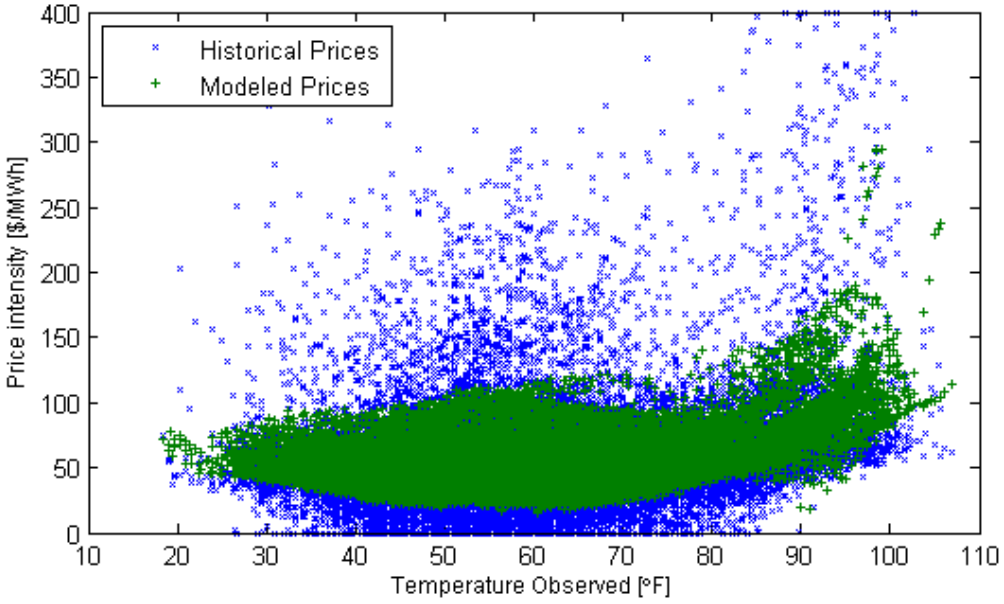

Source: Authors

Figure A-10: Modeled Prices for an Annually Based ANN Trained on All Price Ranges (Green +) and Historical Prices (Blue X) Against Temperature, 2005–2008

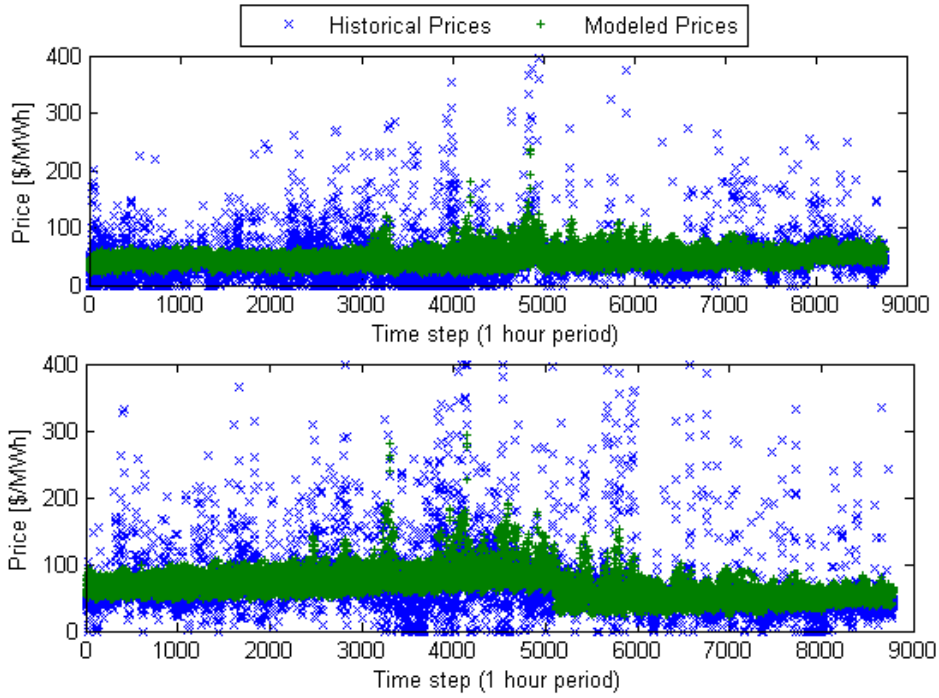

Source: Authors

Figure A-11: Price Time Series for 2006 (Top) and 2008 (Bottom) for an Annually Based ANN Model Trained on All Price Ranges from 2005–2008 (Green +) and Historical Price (blue x)

The ANN returns prices essentially in the range of $25–$100/MWh; lower and higher prices are poorly modeled, and no prices higher than 300$/MWh are returned (see Figure A-9). The frequency of prices belonging to the range $25–$100/MWh is very similar to the historical price frequency, as highlighted in Figure A-9. This pattern reflects the ability of the ANN to reproduce the historical price frequency where most data are available; around 80 percent of the data belong to the range $25–$100/MWh. The ANN cannot however model the very high prices because they are too rare. ANNs learn better on the (frequent) average data than on the (rare) extreme intensities (Olsson et al. 2004).

Price intensities start increasing significantly when temperatures exceed 80°F (27°C) (Figure A-10), and the highest price intensities are returned by the ANN in the summer (Figure A-11). This result was expected, as it corresponds to the high air-conditioning demand during summer in California. High prices (over $100/MWh) observed for middle-range temperatures (40°F–80°F, or 4.4°C–27°C) are not modeled (see Figure A-10). The inputs selected in this research are presumably not driving these high prices, so this result seems reasonable. These high prices can be considered as price spikes that are highly erratic in competitive energy markets and difficult to model using ANNs (Zhao et al. 2007), as discussed earlier.

From Figure A-11, one can see that there is a sudden price drop observed in the middle of 2008. This was expected, as a binary input was added to account for the specific conditions in the first half of 2008, as explained earlier.

Comparison of Dataset Breakdowns Based on Deterministic Variables

Inspired by previous works, several dataset breakdowns have been considered during ANN calibration. To save time, training was carried out only on parts of the dataset (e.g., for two hours of the day when an hourly data breakdown was considered). Based on the experimental results given in Table A-7, further investigation was decided or not. The following data breakdowns were tried, and Table A-8 shows the range of R^2 and RMSE values obtained for the simulations:

- Seasonally based: Summer and Autumn
- Monthly based: January, April and July
- Hourly based: Hours 14 and 24
- Daily based: Tuesday and Saturday
- Workday-/Weekend-based
- Yearly based: 2007

Table A-7: Range of R^2 and Root Mean Square Error (RMSE) Values for Data Breakdowns over Different Time Periods

Data breakdown	$R^2_{simulation}$	RMSE
Seasonally based	0.22–0.43	0.126–0.145
Monthly based	0.22–0.41	0.128–0.143
Hourly based	0.25–0.26	0.125–0.150
Daily based	0.24–0.36	0.116–0.142
Workday-/Weekend-based	0.28-0.33	0.121-0.144
Yearly based	0.20	0.136

Table A-8: Summary of the Results from ANN Calibration for the Data Breakdown Experiments

Network Architecture				Training Algorithm			Results					
Price range - Dataset breakdown	Inputs	Hidden layers	Hidden neurons	Activation function	Complex	Points per complex	Points per sub-complex	R^2_{train}	R^2_{valid}	R^2_{test}	R^2_{sim}	RMSE*
All	11	1	8	Tansig	8	51	50	0.30	0.24	0.27	0.28	0.140
January	9	1	8	Tansig	8	2*Npar+1	Npar+1	0.26	0.20	0.25	0.24	0.128
April	9	1	8	Tansig	8	2*Npar+1	Npar+1	0.42	0.33	0.39	0.39	0.143
July	9	1	8	Tansig	8	2*Npar+1	Npar+1	0,44	0,38	0,37	0,41	0,138
October	9	1	8	Tansig	8	2*Npar+1	Npar+1	0.25	0.20	0.18	0.22	0.132
Summer	10	1	8	Tansig	8	51	50	0.46	0.39	0.40	0.43	0.145
Autumn	10	1	8	Tansig	8	51	50	0.33	0.13	0.08	0.22	0.126
Hour 14	10	1	8	Tansig	8	2*Npar+1	Npar+1	0.30	0.24	0.20	0.25	0.150
Hour 24	10	1	8	Tansig	8	2*Npar+1	Npar+1	0.28	0.21	0.24	0.26	0.125
Tuesday	10	1	8	Tansig	8	2*Npar+1	Npar+1	0.28	0.24	0.17	0.24	0.142
Saturday	10	1	8	Tansig	8	2*Npar+1	Npar+1	0.41	0.24	0.33	0.36	0.116
Weekend-based	10	1	8	Tansig	8	51	50	0.38	0.27	0.30	0.33	0.121
Workday-based	10	1	8	Tansig	8	51	50	0.29	0.25	0.28	0.28	0.144
Year 2007	11	1	8	Tansig	8	2*Npar+1	Npar+1	0.22	0.16	0.20	0.20	0.136
″Normal prices″	11	1	8	Tansig	8	51	50	0.39	0.37	0.38	0.38	0.079
″Medium prices″	11	1	8	Tansig	8	51	50	0.36	0.36	0.34	0.36	0.069
″Low prices″	11	1	8	Tansig	8	51	50	0.10	0.09	0.04	0.08	0.035
″High prices″	11	1	8	Tansig	8	51	50	0.17	0.15	0.15	0.16	0.249

*RMSE: Root Mean Square Error

The different data breakdowns are compared in the next paragraphs.

Hourly based and daily based models

The hourly-based model was discarded from further analysis because it has a low $R^2_{simulation}$ range value and average RMSE value.

The correlation range for the daily based model simulations is $R^2_{simulation} = 0.24 - 0.36$ and for the workday-/weekend-based model$R^2_{simulation} = 0.28 - 0.33$.The partition between workdays and weekends, requiring only two individual models, was preferred to a daily data breakdown and the daily based models were abandoned. The division between weekends and workdays has already been used for short-term price forecasting (e.g., Gao et al. 2000) and will be assessed in detail later.

Hourly and daily based models have not been assessed based on other performance criteria (e.g., frequency distribution) because it would require building each individual model to extract monthly patterns, which was considered too time consuming.

Yearly based model

The model developed for year 2007 has the lowest determination coefficient among all experiments, with $R^2_{simulation} = 0.20$, and its RMSE value is not significantly reduced compared to the model built for all four years of data. Figure A-12 is a comparison of the revenue curves between this model and the model using the entire dataset for the months of June and December. Generally, monthly revenue curves developed for the 2007 model are further away from the historical data (or do not have a significantly better fit) than the model using the four years of data. It was therefore decided to exclude the yearly based model from further analysis.

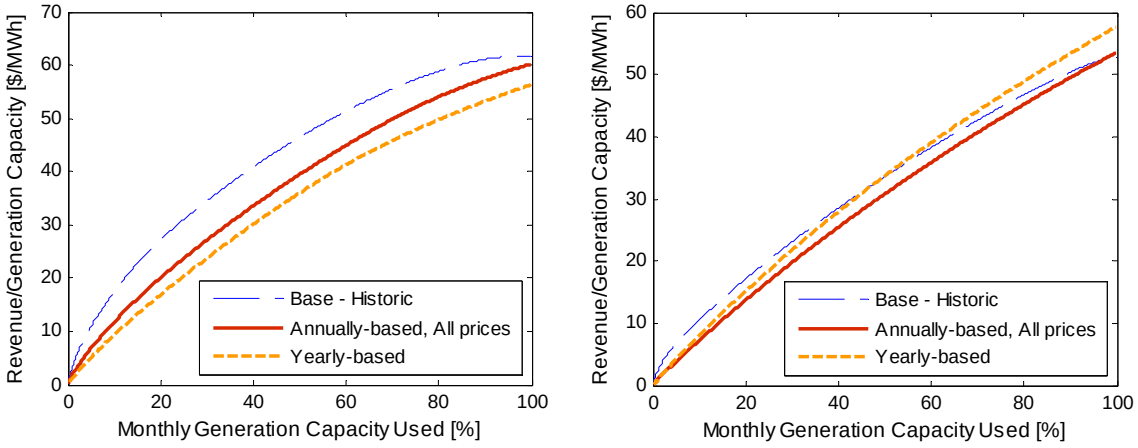

Source: Authors

Figure A-12: Comparison of the Revenue Curves for Yearly Based ANN Model Calibrated on 2007 Data and an Annually Based ANN Calibrated on all Data for June (left) and December (right)

Monthly based, Seasonally based, Workday-/Weekend-based

Figure A-13is a comparison of April's and July's revenue curves for four ANN models: seasonally based, monthly based, workday- and weekend-based models combined in parallel, and base model using all the data. The best fit for the revenue curves can be observed for monthly models and the summer model. The workday-/weekend-based model produced a better fit than the base model for most months. It was decided to keep only one model for the next steps of this research, and the monthly based models were elected, for the following reasons:

- Generally, those models produced the best fit for the revenue curves—especially for the month of April, where the other data partitions did not fit as well.
- This partition seemed the most appropriate to capture the monthly variability of prices, which is of interest in this research.
- $R^2_{simulation} = 0.22 - 0.41$ and RMSE=0.13–0.14 are among the best errors from the experiments together with the seasonal models.

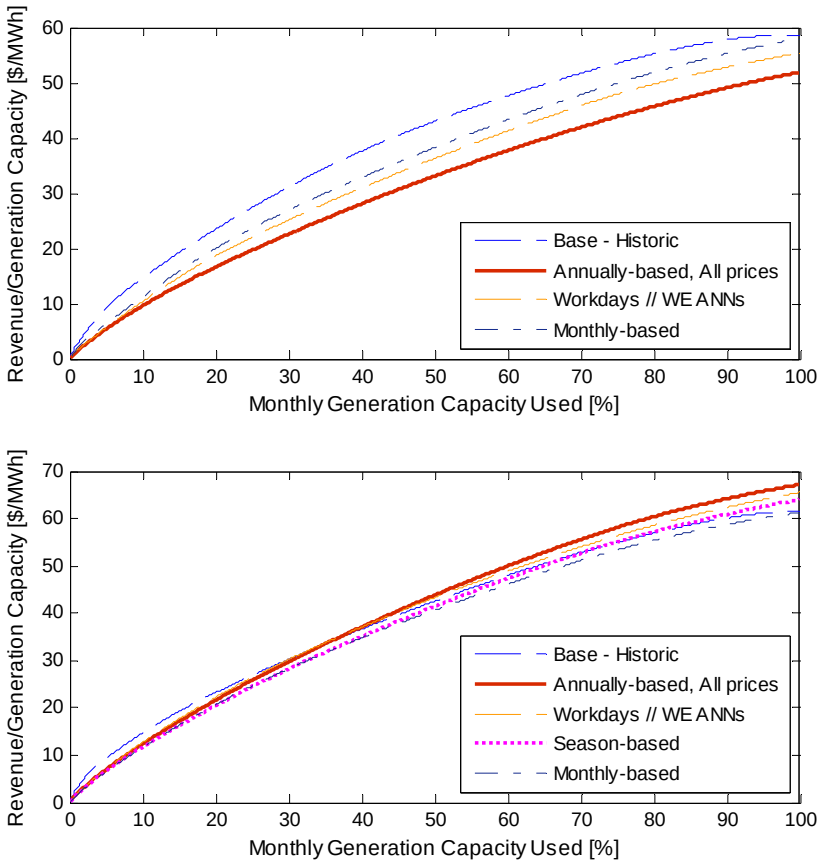

Source: Authors

Figure A-13: Revenue Curves for Four ANN Models: Base (Calibrated on All Data), Workday- and Weekend-Based Models Combined In Parallel, Seasonally Based and Monthly Based Models for April (top) and July (bottom)

Comparison of Dataset Breakdowns Based on Stochastic Variables

Additional dataset breakdowns were tried. This section presents the motivations for the partitions considered, and their implementation is detailed later.

The first partition was inspired by an experiment made by Olsson et al. (2004) for rainfall intensity classification. They first divided their dataset into different categories based on rainfall intensity. Then they tried to use a stratified sample for ANN calibration, designed to contain an identical number of intensities in each category. This may improve the ANN training, as the learning capacity of ANNs is commensurate with the quantity of data available (Olsson et al. 2004). This method was tried in the present research, since previous experiments have not been able to capture low price intensities (below $25/MWh) and high prices (above $125/MWh). In light of these results, the research team extracted a non-representative subsample designed to contain a similar number of price intensities in predefined price ranges.

The two following experiments were inspired by the work from Lu et al. (2005) and Zhao et al. (2007), who spotlighted that ANNs were unable to model price spikes because they are highly erratic, several orders of magnitude higher than the average price, often under-represented compared to normal prices, and most likely not driven by the inputs selected in the present work. With respect to the use of ANN models, this is a delicate issue. ANNs are trained better on the range of intensities that is the most frequent in the calibration set (Olsson et al. 2004). Therefore, scattered outliers will be poorly modeled. According to Lu et al. (2005), almost all the existing techniques for short-term price forecasting require that the price spike signals be filtered out, in order to forecast normal prices with rather high accuracy.

As defined by Lu et al. (2005) high price spikes are prices exceeding the threshold P_v:

$$P_v = \mu \pm 2\delta \qquad \textit{(Eq. 1)}$$

where μ is the mean of historical market price and δ is the standard deviation of the prices. In the present case study, price spikes correspond to prices exceeding $128/MWh, including 3.7 percent of the price population and representing 12.9 percent of cumulated price intensities. Many high-intensity prices happened in 2008 but probably are not really price spikes, as these resulted from a global increase in electricity prices. Their intensity is still "abnormally" high, so it was decided to make no distinction between those and other price spikes. Very few price spikes seemed to have occurred in 2005, but this is partly because four months of data were removed. Most spikes occurred in spring and summer.

Based on the previous comments, the following data partitions were considered:

- A stratified dataset considering five price ranges.
- Division of the set between "normal prices" (below the threshold P_v) and price spikes.

- Division of the set between '"low prices" (including the 10 percent lowest price intensities), "Medium prices" (prices between low prices and the threshold P_v), and price spikes.

Stratified dataset breakdown

Five categories of prices p (given in [$/MWh]) were defined on the basis of the cumulative distribution of prices: 0 <p ≤ 25; 25 < p ≤ 50; 50 < p ≤ 75; 75 < p ≤ 100; 100 <p. Each category contained 1,000 data samples, giving a total of 5,000 data samples, 15 percent of the original dataset. Then the set was divided into training, test, and validation sets, as usual for calibration. The optimized ANN for eight hidden neurons gave$R^2_{training} = 0.29$ and$R^2_{simulation} = 0.28$.

Figure A-14 shows the prices plotted against temperature. Prices below $20/MWh and above $150/MWh are still not captured. Visually, the agreement between historical and modeled prices is not improved for high temperatures, compared to the earlier models, e.g., the annually based model calibrated on all prices. This ANN model calibrated on a stratified sample was abandoned, as it did not capture the low and high prices as wished.

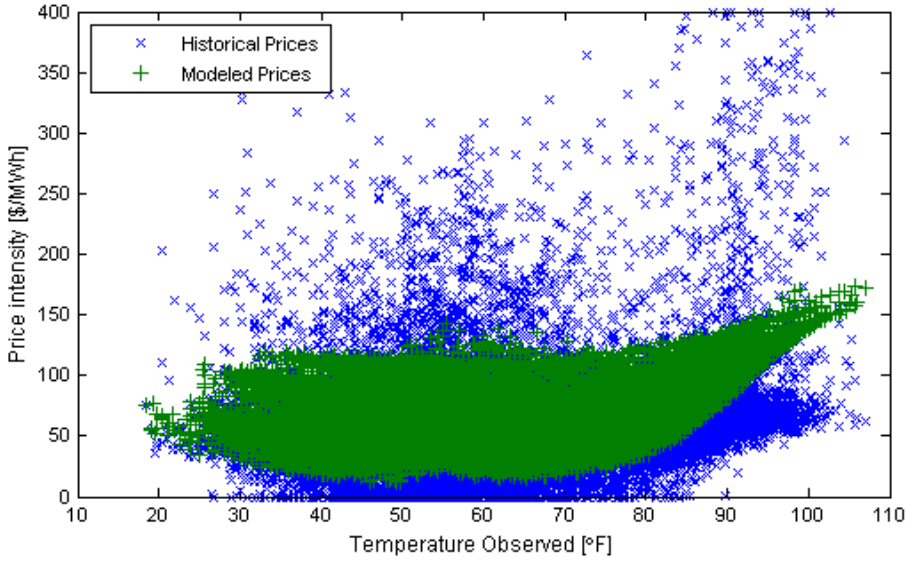

Source: Authors

Figure A-14: Price Obtained from the ANN Trained over a Stratified Sample (2005–2008) Against Temperature

"Normal prices" model

The correlations obtained from the "normal price" model are very much improved compared to the ANN developed for the entire dataset. The simulation for the optimal parameters gives $R^2_{simulation} = 0.38$ and RMSE = 0.08 (compared to $R^2_{simulation} = 0.28$ and RMSE = 0.14 for the annually based ANN model trained over all prices).

Figure A-15 shows the prices plotted against temperature. Prices below $20/MWh and above $90/MWh are still not modeled properly. Too few data belong to these ranges compared to the quantity of data available in the interval 20–90$/MWh to be modeled adequately by the ANN. This observation led to the next experiment considering a division between low, medium, and price spikes.

A second ANN was developed for the set of price spikes. As expected these could not be modeled accurately because there are too few data (1191 data samples), the spikes are very volatile, and they are probably not driven by the selected inputs. No further investigation to model price spikes was carried out, as it is beyond the scope of this work. Further research could consider applying a "damping scheme" as proposed by Yamin et al. (2004) or using similar reasoning.

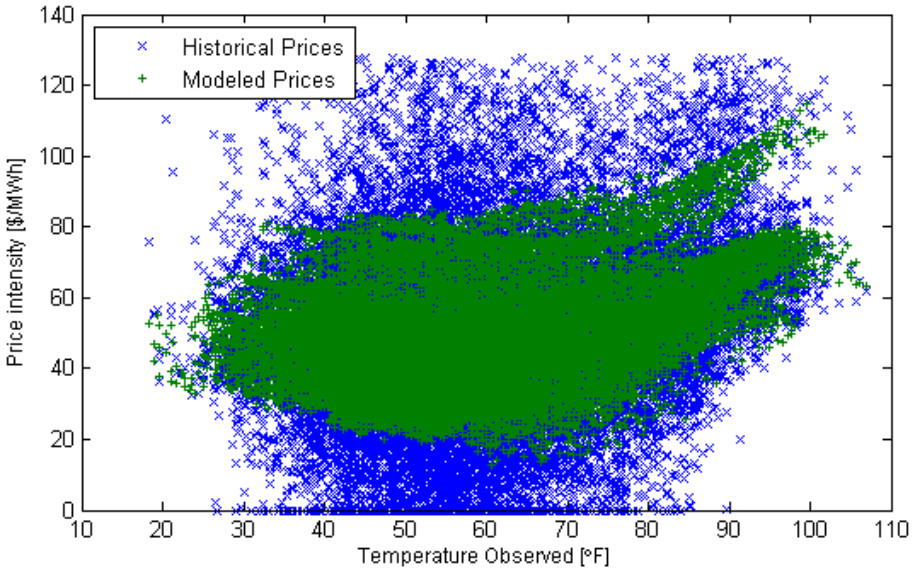

Source: Authors

Figure A-15: Prices from an ANN Model Trained over "Normal" Prices (below $128/MWh) Against Temperature (2005–2008)

Price spikes represent only 3.7 percent of the price population, but their summed intensities reach nearly 13 percent of the total. Two options were foreseeable to deal with price spikes: considering that a certain percentage of price spikes will occur in the future, or that there would not be any more spikes. The reliable choice depends on how the energy market is projected to evolve. Lu et al. (2005) showed that in an ideal competitive electricity market, price spikes should only occur when the demand exceeds the supply. However, most markets are not ideally competitive, and gaming behaviors probably influence the market (Lu et al. 2005). It has also been argued that suppliers take advantage of the vulnerability (storage difficulties, generation capacity constraints, and transmission congestion) of the electricity market by withholding their capacity so as to shift supply-and-demand curves

and force price spikes (Zhao et al. 2007). Therefore, if the market operation is expected to stay as it is today—which is the assumption we make in the present work—then price spikes should be kept unimpaired, as they will most likely continue to occur. If the market is envisaged to turn toward an "ideal" competitive market, or toward a highly supervised market that prevents spikes, then spikes should be removed.

The percentage of future energy spikes is assumed to be the same as in the Base case. Unimpaired price spikes were added to the modeled price set, and Figure A-16 shows the revenue curves for the models calibrated on all prices or on normal prices for June and September. The model developed for "normal prices" fits better historical data.

"Medium-price" and "low-price" models

Figure A-17 displays the plot of prices versus temperature for the medium-range prices, which gives $R^2_{simulation} = 0.36$ and RMSE = 0.07 (compared to $R^2_{simulation} = 0.38$ and RMSE = 0.08 for the "normal prices"). Surprisingly, these results are not far off from the results obtained for normal prices, and the correlation in terms of R^2 value is even lower. The same price trend as for "normal" prices is observed, except that the lower bound of the modeled prices is now higher; around $35/MWh. Truncating the 10 percent low prices did not help the ANN to reproduce the low range of the calibration set, and it increased the price set's average. ANNs usually return outputs where most data are available (Olsson et al. 2004); this may be at the origin of this phenomenon; otherwise, no other explanation has been identified to explain this trend.

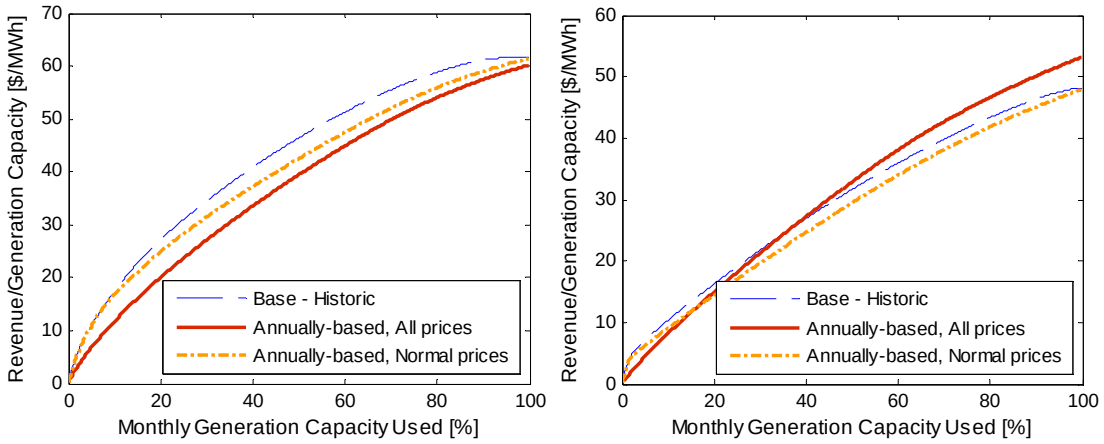

Source: Authors

Figure A-16: Comparison of the Revenue Curves for Two Annually Based ANN Models: One Trained on All Prices and One Trained on" Normal Prices" (Price Spikes Truncated) for June (Left) and September (Right). The Historic Proportion of Price Spikes in the Market Was Assumed to Remain Constant for the Second Model.

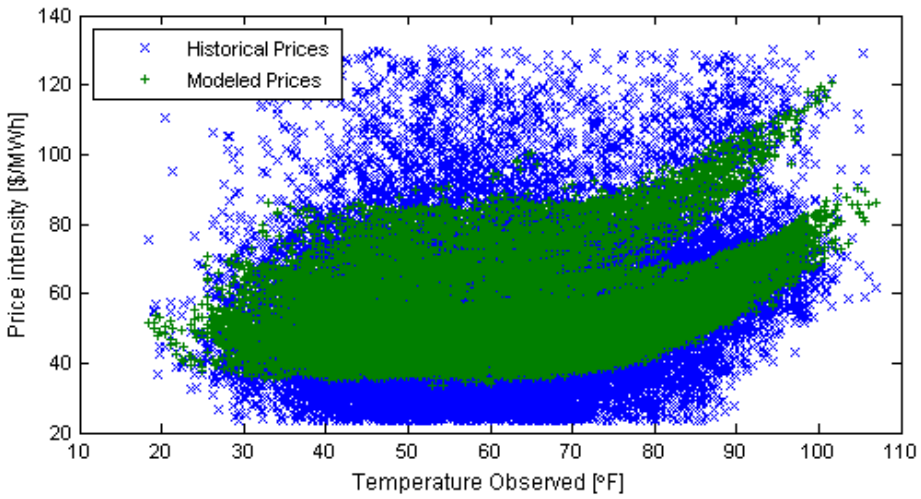

Source: Authors

Figure A-17: Prices from an ANN Model Trained over "Medium" Prices (Between $22 and $128/MWh) Against Temperature (2005–2008)

The second model developed for the set of the 10 percent lowest values returned prices mostly around the average of the calibration set (cf. Figure A-18) the correlation is low, $R^2_{\text{simulation}} = 0.08$. It is hard to assess if the ANN returned the prices follow an underlying relationship; this dataset breakdown was abandoned.

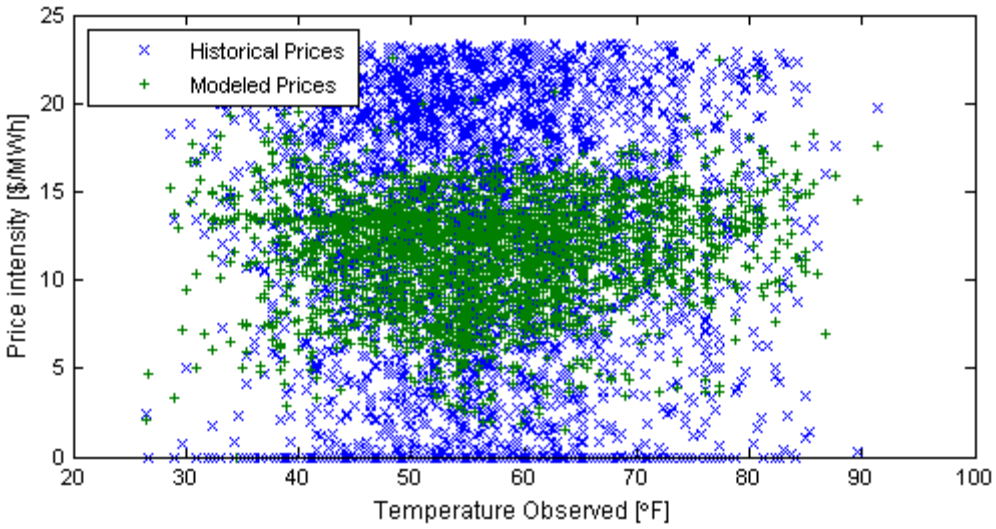

Source: Authors

Figure A-18: Prices from an ANN Model Trained over "Medium" Prices (Between $22 and $128/Mwh) Against Temperature (2005–2008)

Summary of the Findings and Choice of the Optimum ANNs

Among all the dataset breakdowns tried out in this research, two divisions stand out:

- Monthly based models
- Annually based model calibrated on the "normal" price (i.e., excluding price spikes)

Monthly models were elected because they visually fit well historical patterns and seem appropriate to capture the monthly variability of energy prices. The annual model trained for normal prices improves the determination coefficient but requires filtering out the spikes, assuming that all prices over a certain range are non-natural price spikes. The same proportion of spikes was assumed to occur in the future.

The two models are compared hereafter in terms of monthly price frequency distribution using revenue curves. The visual agreement between the revenue curves for January, April, and July (see FigureA-19) is very similar between the two models and historical data; April is the only month of the year for which the curves have a significant different pattern.

Both models were kept because it is not possible to know which one is the most accurate.

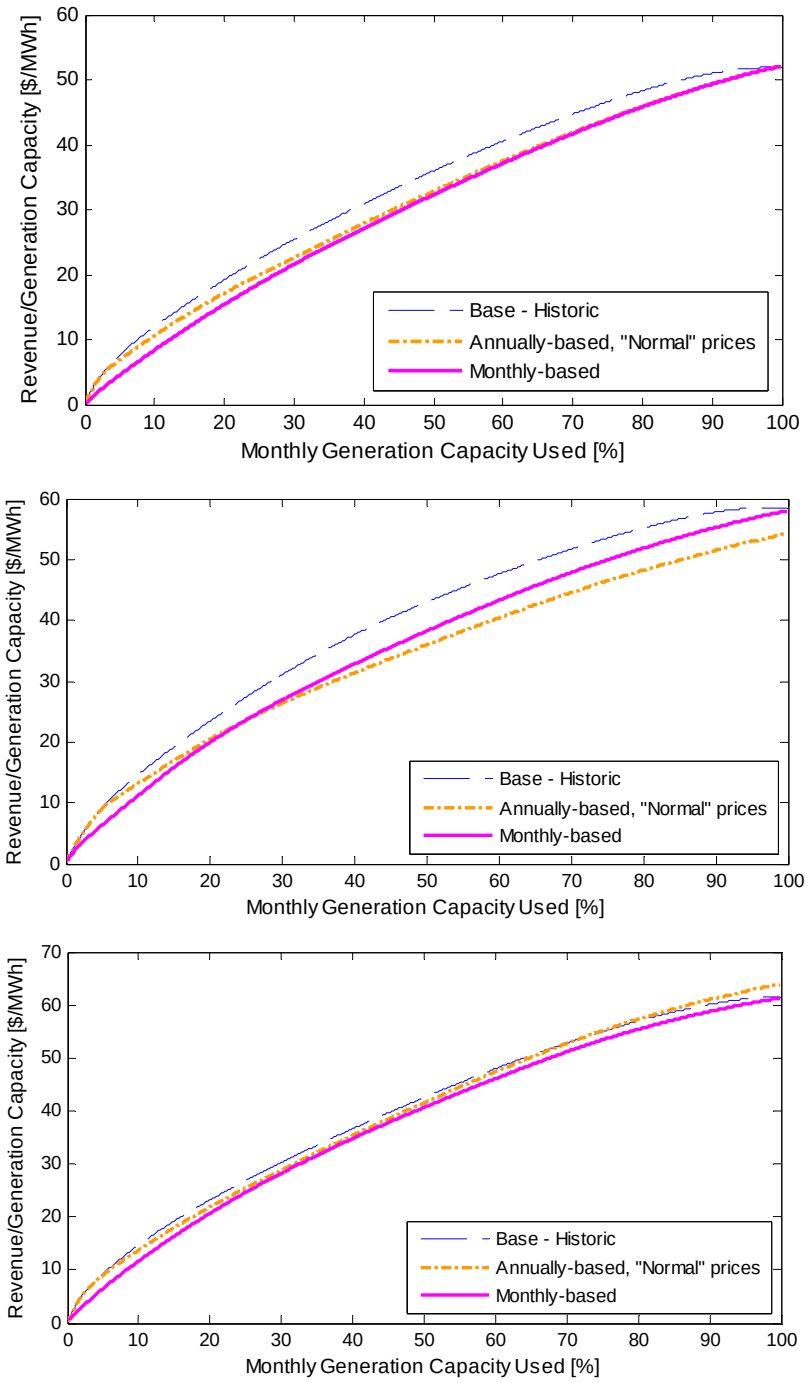

Source: Authors

Figure A-19: Comparison of the Revenue Curves for the Monthly Based ANNs and the Annually Based ANN Calibrated on "Normal Prices" (Price Spikes Truncated) for January (top), April (middle), and July (bottom)

Application of ANN to Long-Term Price Forecasting

Climate Warming Scenarios

This research estimated the impacts of climate warming by 2100 on hourly electricity prices based on five scenarios, shown in Table A-9 and adapted from the simulations of twenty-first century climates evaluated by Cayan et al. (2009). The study assumed that the statewide temperature increase is the average of the temperature increases in southern and northern California. This average value was considered to be representative of the high electricity-demand areas—the highly-populated areas in California which are of interest in this work. This study also assumed that the increase estimated by Cayan et al. (2009) is based on mean values for the historical period (1961–1990) and that the increase is based on mean values for (2005–2008).

Four scenarios consider a constant temperature increase throughout the year, and one high-forcing scenario (GFDL-A2-Seasonal) considers a higher increase in summer and a lower increase in winter, respectively, than in the rest of the year. As no more information was gathered about the temperature increases in spring and autumn, these values were assumed to be equal to the average annual temperature increase.

Table A-9: Climate Change Scenarios for California

			Far-Term Period (2070–2099) Temperature Change (°F) *		
Scenario Name	GCM	SRES	Winter (DJF)	Summer (JJA)	Spring (MAM) & Fall(SON)
GFDL-A2-Annual	GFDL	A2	+8,0	+8,0	+8,0
PCM-A2-Annual	PCM	A2	+4,6	+4,6	+4,6
GFDL-B1-Annual	GFDL	B1	+4,9	+4,9	+4,9
PCM-B1-Annual	PCM	B1	+2,8	+2,8	+2,8
GFDL-A2-Seasonal	GFDL	A2	+6,0	+10,5	+8,0

* The temperature change in spring and fall was assumed to be equal to the average annual temperature change.

Source: Adapted from Cayan et al. (2009).

Results

Table A-10 shows the results for each climate warming scenario and ANN model. The forecasted average price for all climate warming scenarios exceeds the Base case average price ($55/MWh). Monthly ANNs predict higher average price increases than the Annual Normal price ANN model for all scenarios; i.e. Monthly based ANNs estimate higher price increases than the Annual ANN.

Figure A-20 shows the forecasted price intensities plotted against temperature for climate warming scenario PCM-A2-Annual, for both ANN models (with monthly based models on the top and annually based model on the bottom). Figure A-21 is the same figure, but for scenario GFDL-A2-Annual. Prices increase for all scenarios for the highest temperatures relative to historical prices; high forcing scenarios lead to high price increases, and low forcing scenarios to lower price increases.

Table A-10: Price Distribution Statistics for Each Climate Warming Scenario and ANN Model

		Prices in $/MWh				Price Percentiles in $/MWh				
Climate scenario	**ANN model**	**Average**	**Standard Deviation**	**Minimum**	**Maximum**	**10th**	**25th**	**50th**	**75th**	**90th**
Base Case	-	54.87	36.54	0.00	399.99	23.88	36.88	49.13	64.14	84.28
GFDL-A2-Annual	ANN1	59.89	33.16	0.00	425.66	30.78	41.04	51.73	70.20	96.15
	ANN2	55.96	33.04	9.00	399.99	31.13	40.58	49.31	61.95	76.11
PCM-A2-Annual	ANN1	56.94	27.51	0.00	392.77	31.11	40.64	50.91	66.91	88.49
	ANN2	55.25	32.74	9.76	399.99	31.31	40.20	49.02	60.11	74.98
GFDL-A2-Seasonal	ANN1	61.55	35.28	0.00	425.66	31.20	41.69	52.38	71.93	99.75
	ANN2	56.67	33.07	9.00	399.99	31.64	41.15	49.87	63.24	76.89
PCM-B1-Annual	ANN1	55.82	25.09	0.00	384.30	31.42	40.55	50.64	65.44	85.00
	ANN2	55.03	32.57	10.73	399.99	31.67	40.24	48.98	48.98	74.42
GFDL-B1-Annual	ANN1	57.15	27.95	0.00	388.50	31.11	40.67	50.93	67.11	89.09
	ANN2	55.30	32.76	9.62	399.99	31.27	40.20	49.04	60.24	75.04

Revenue curves for one month from each season (January, April, July, October) were plotted for climate scenarios GFDL-A2-Annual and PCM-A2-Annual in Figure S A-22 and A-23, for ANN1 and ANN2, respectively. For both ANN models, all climate warming scenarios led to high increases in revenues in summer months, and more attenuated increases in spring and autumn. In winter, high forcing scenarios led to higher price drops relative to Base case if compared to low forcing scenarios. These patterns correspond to what was expected: increased need for cooling in warm months and decreased need for heating in winter months. For all climate scenarios, the annually based ANN returns similar revenue curves in April. April is the transition month between winter and spring seasons, so energy price patterns might be different between years, and it is difficult for the ANN to learn the input-output relationship.

The lower increases in revenue using an annually based ANN compared to those using monthly based ANNs probably result from the time scale of the ANN models. In the case of an annual model, temperature data samples from all twelve months of the year are fed to the ANN during calibration, and the trained ANN has knowledge of all historical temperature ranges. Most perturbed temperature samples for climate warming scenarios will not be out of range of the calibration temperature range, except for the extreme highest temperature. Monthly based models use a monthly calibration set; they are independent from each other and have no knowledge of the price/temperature relationship mapped in other months. The highest perturbed temperatures accounting for climate change of each monthly calibration set will be unknown by the corresponding ANN, but might be known by other monthly ANN models.

Generally, monthly models might overestimate future price intensities. For illustrative purposes, Figure A-24 shows the price distribution against temperature from the monthly based and annually based ANN models under the GFDL-A2-Annual scenario in March. The monthly model estimates very high price increases for the highest temperatures experienced in that month (T>95ºF); whereas, the annual model estimates more moderate price increases, which seem more reasonable. Historically, this temperature range was experienced in other months of the year—in spring for example—and was not responsible for such high prices. Having no knowledge of the rest of the year, monthly-based ANNs might mis-estimate the input/output relationship, and an annual (or seasonal) model may be more appropriate to deal with perturbed temperatures.

Another possible reason for the lower increases in revenue estimated by the Annual ANN model is that an ANN model learns from examples that are input during the training procedure. Since this model was trained only for normal prices, it will not return prices much higher than the ones fed during training. In the first experiment (monthly models for all prices range), since price spikes were not removed, the ANN will more likely return high price intensities.

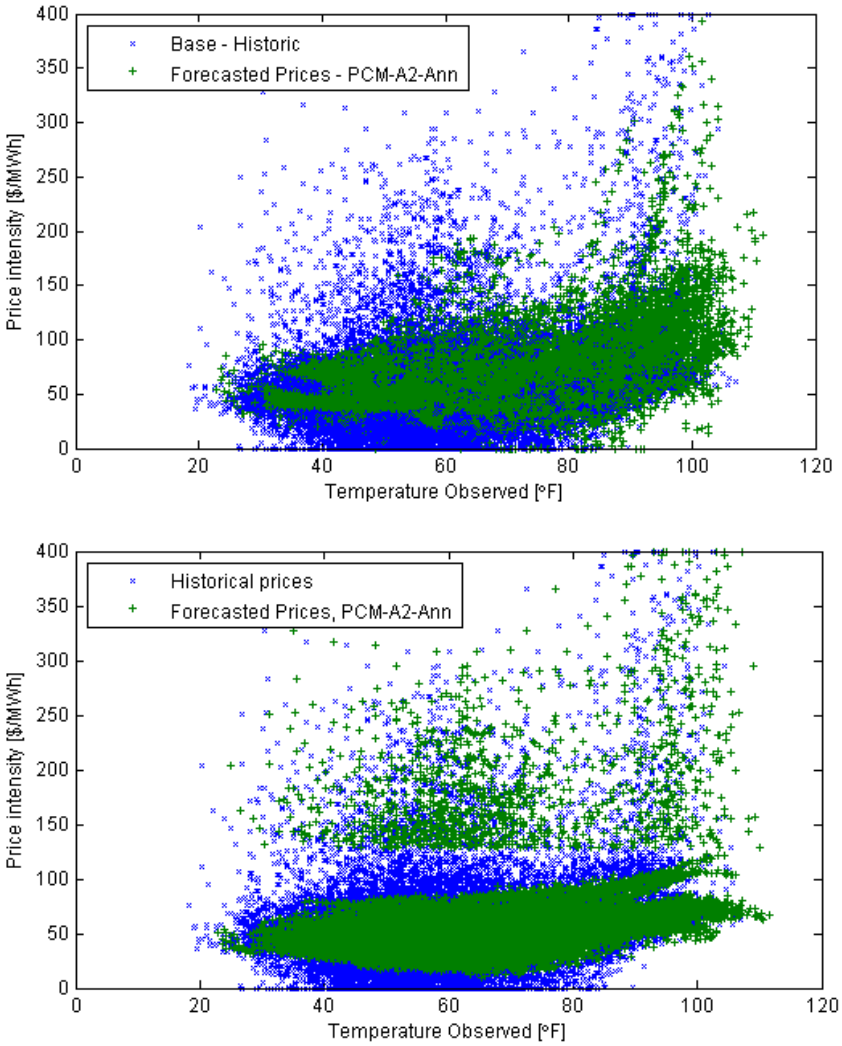

Source: Authors

Figure A-20: Simulated ANN Prices and Historical Prices (2005–2008) for a PCM-A2-Annual Climate Warming Scenario for Both ANN Models: Monthly Based ANNs (top) and Annually Based Model Trained for "Normal Prices" and Unimpaired Price Spikes (bottom)

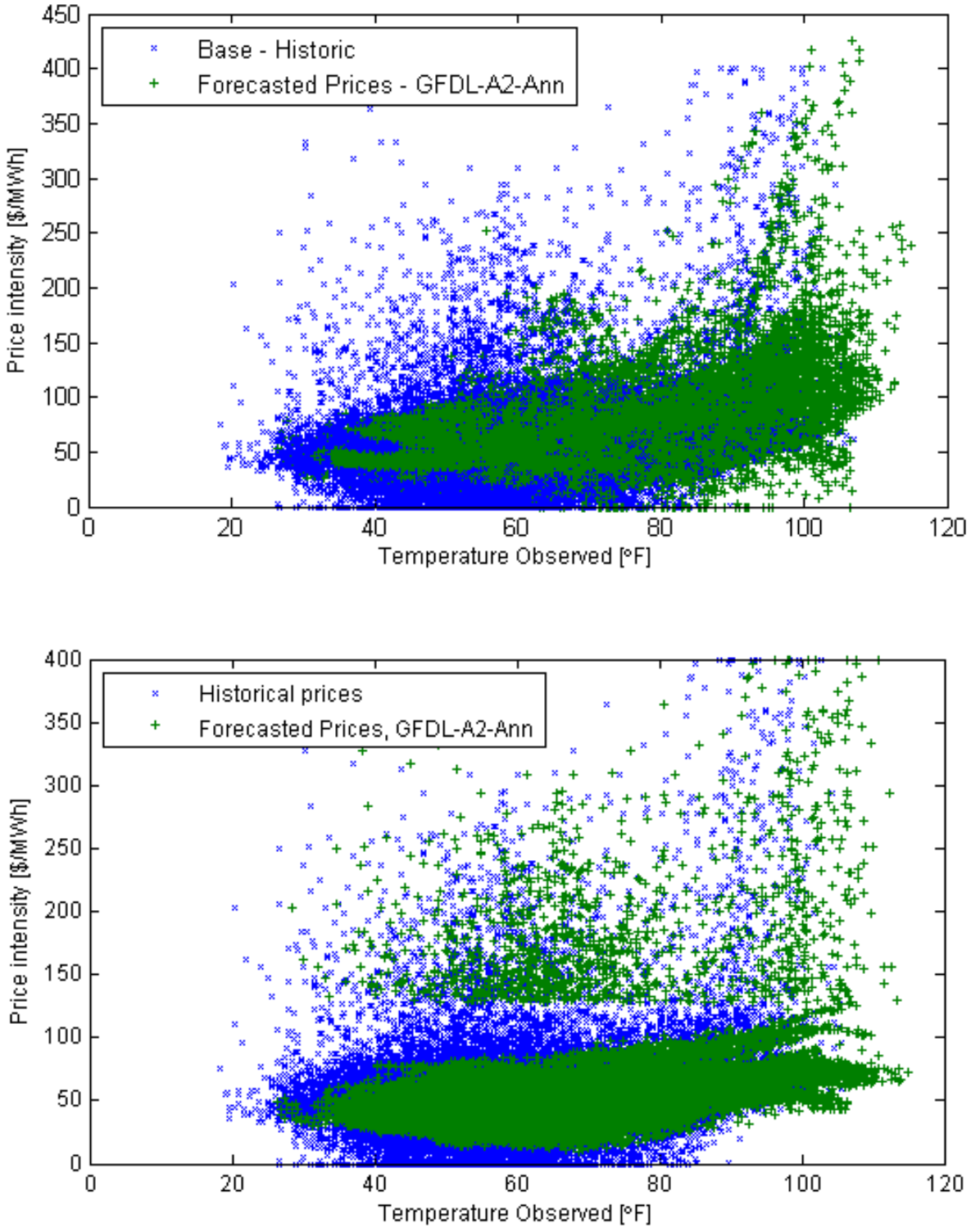

Source: Authors

Figure A-21: Simulated ANN Prices and Historical Prices (2005–2008) for a GFDL-A2-Annual Climate Warming Scenario for Both ANN Models: Monthly Based ANNs (top) and Annually Based Model Trained for "Normal Prices" and Unimpaired Price Spikes (bottom)

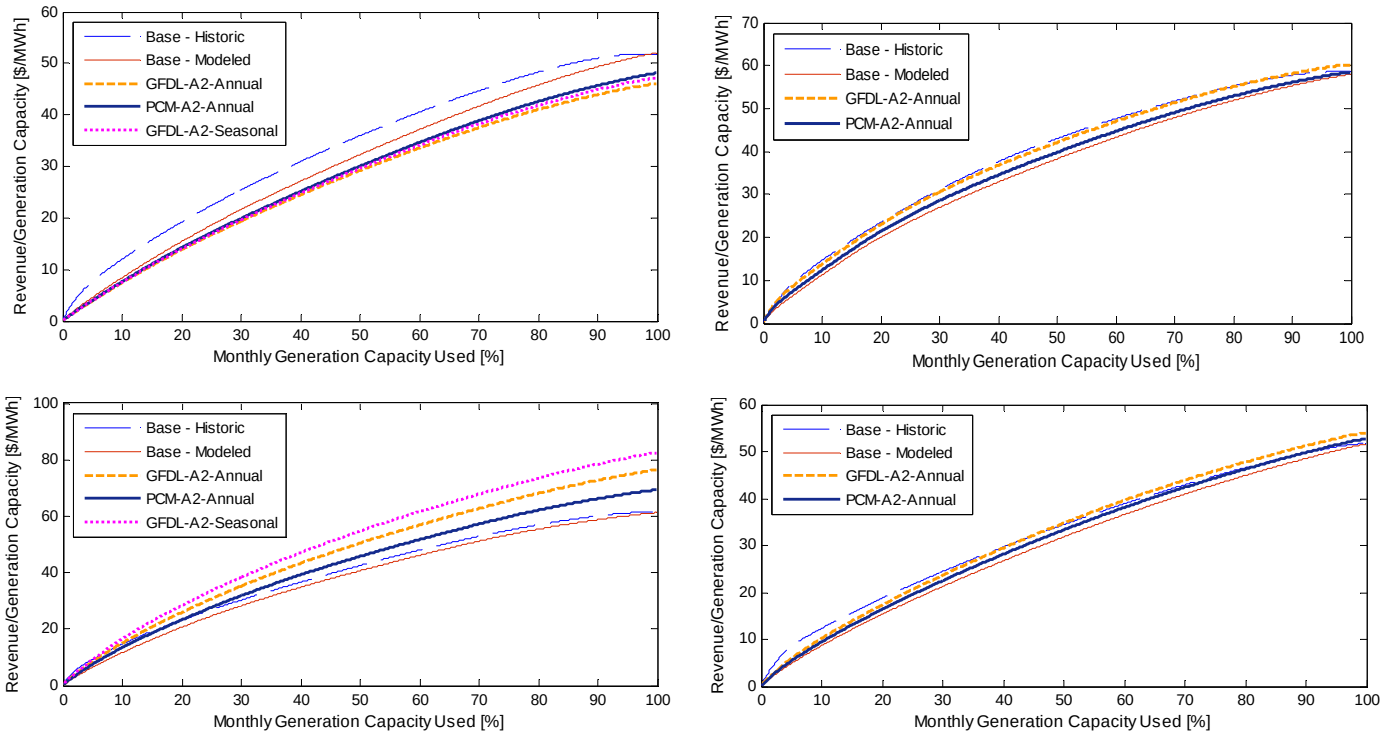

Source: Authors

Figure A-22: Monthly Revenue Curves Obtained from the Monthly-Based ANN Models for January (top-left), April (top-right), July (bottom-left), and October (bottom-right) for Different Climate Warming Scenarios

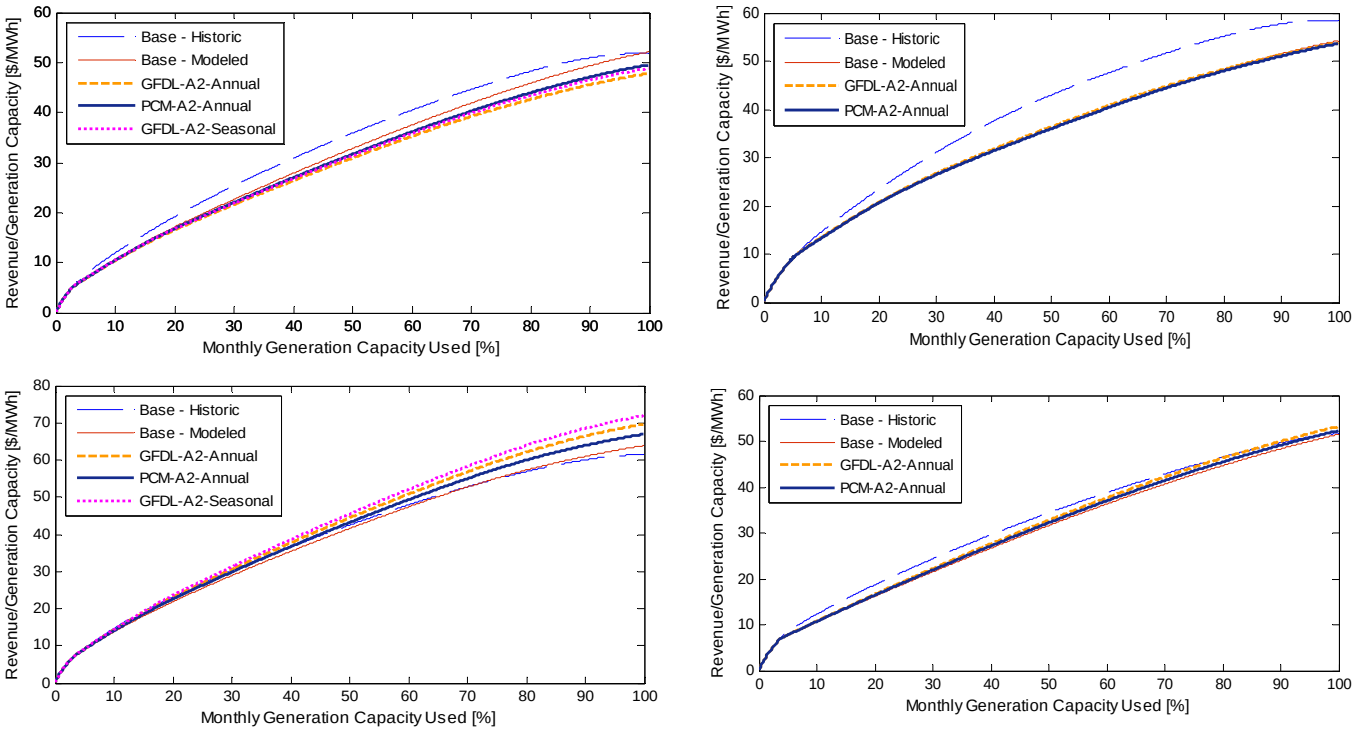

Source: Authors

Figure A-23: Monthly Revenue Curves Obtained from the Annually Based ANN Model Calibrated on Normal Prices, for January (Top-Left), April (Top-Right), July (Bottom-Left) and October (Bottom-Right) for Different Climate Warming Scenarios. (It Is Assumed That the Same Proportion of Price Spikes as in the Historical Price Set Occur Under Climate Scenarios.)

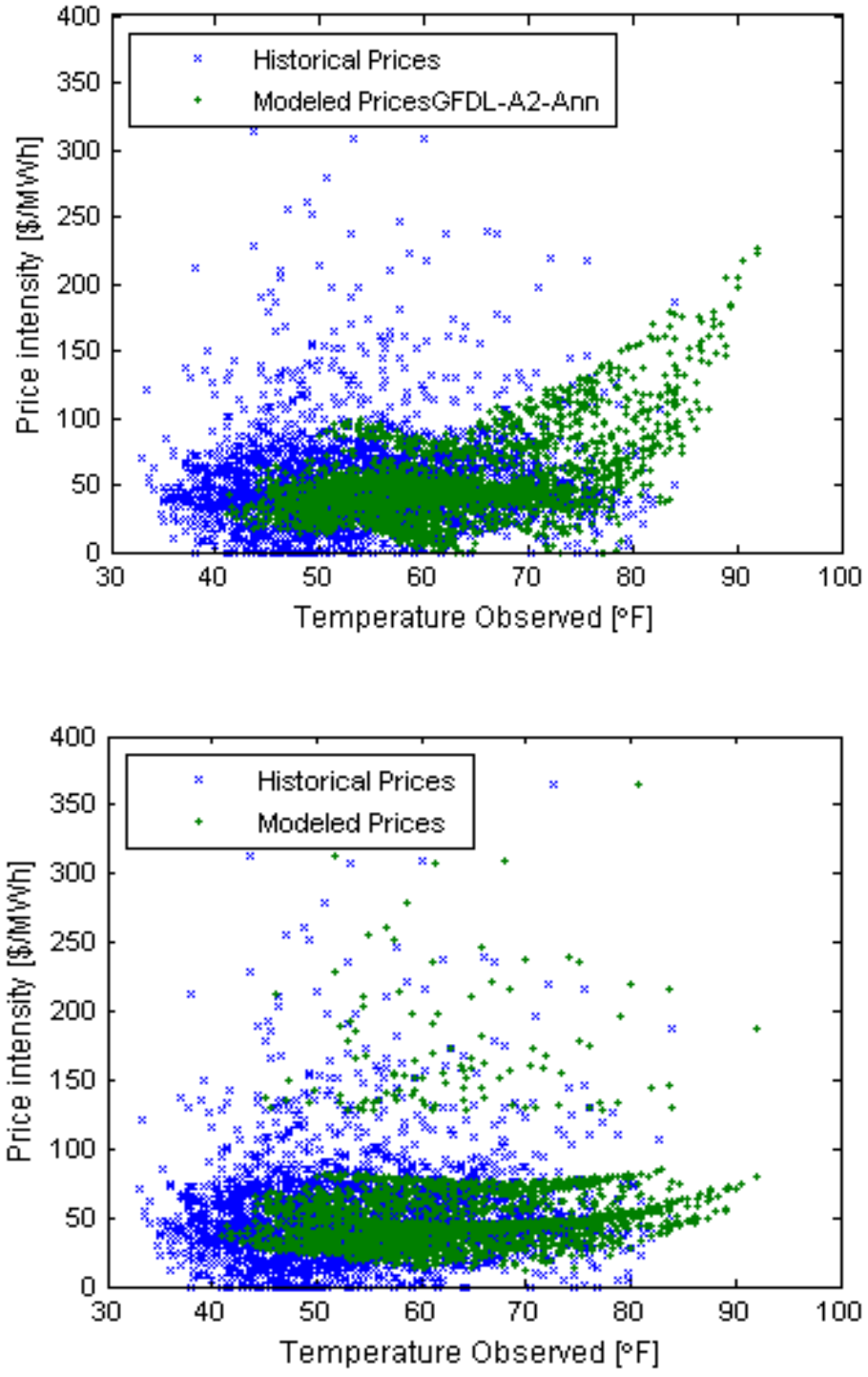

Source: Authors

Figure A-24: Results from Two ANN Models (Monthly Based Models (Top) and Annually Based Model for Normal Prices (Bottom)) for GFDL-A2-Annual Climate Warming Scenario for March.

Appendix References

Amjady, N., and Hemmati, M., 2006. Energy price forecasting - problems and proposals for such predictions. *IEEE Power Energy Mag. 4 (2)*, 20–29.

Amjady, N., and Keynia, F., 2010a. Electricity market price spike analysis by a hybrid data model and feature selection technique. *Electric Power Systems Research* 80, 318–327.

Amjady, N., and Keynia, F., 2010b. Application of a new hybrid neuro-evolutionary system for day-ahead price forecasting of electricity markets. *Applied Soft Computing 10*, 784–792.

ASCE, 2000. Artificial Neural Networks in Hydrology. I: Preliminary Concepts. *Journal of Hydrologic Engineering*, 5 (2).

Azadeh, A. Ghaderi, S.F, Tarverdian, S., and Saberi, M., 2006. Integration of artificial neural networks and genetic algorithm to predict electrical energy consumption. *Applied Mathematics and Computation 186*, 1731–1741.

California Independent System Operator – Department of Market Monitoring, 2006. 2005 Annual Report on Market Issues and Performance. [Online] Available at: www.caiso.com/17d5/17d59ec745320.pdf [Accessed 24 March 2010].

California Independent System Operator – Department of Market Monitoring, 2009. 2008 Annual Report on Market Issues and Performance. [Online] Available at: www.caiso.com/2390/239087966e450.pdf [Accessed 24 March 2010].

Cayan, D., Tyree, M., Dettinger, M., Hidalgo, H., Das, T., Maurer, E., Bromirski, P., Graham, N., and Flick, R., 2009: Climate Change Scenarios and Sea Level Rise Estimates for the California 2008 Climate Change Scenarios Assessment. California Climate Change Center, CEC-500-2009-014-F, 64 pages. Available at: www.hugohidalgoleon.com/files/papers/CEC-500-2009-014-D.PDF.

Congressional Budget Office (CBO), 2001. Causes and Lessons of the California Electricity Crisis. [Online] Available at: www.cbo.gov/ftpdocs/30xx/ doc3062/ CaliforniaEnergy.pdf.

Dawson, C. W., and Wilby, R. L., 2001, Hydrological modeling using artificial neural networks. *Progress in Physical Geography* 25, 1, pp. 80–108.

Duan, Q. Sorooshian, S., and Gupta V., 1992. Effective and Efficient Global Optimization for Conceptual Rainfall-Runoff Models. *Water Resources Research* 28(4): 1015–1031, Paper number 91WR02985.

Duan, Q., Sorooshian, S., and Gupta V., 1994. Optimal use of the SCE-UA global optimization method for calibrating watershed models. *Journal of Hydrology* 158: 265–284.

Franco, G., and Sanstad, A. H., 2006. *Climate change and electricity demand in California*. California Climate Change Center, CEC-500-2005-201-SF, [Online] February 2006. Available at: www.energy.ca.gov/ 2005publications/CEC-500-2005-201/CEC-500-2005-201-SF.PDF.

Gao, F., Guan, X., Cao, X-R., and Papalexopoulos, A., 2000. Forecasting Power Market Clearing Price and Quantity Using a Neural Network Method. *IEEE Power Engineering Society Summer Meeting* 2000.

Hippert, H. S., and Taylor, J. W., 2010. An evaluation of Bayesian techniques for controlling model complexity and selecting inputs in a neural network for short-term load forecasting. *Neural Networks* 23: 386–395.

Hornik, K., and Stinchcombe, M., and White, H., 1989. Multilayer feedforward networks are universal approximators. *Neural Networks*, 2(5): 359–366.

Hsieh, W. W., and Tang, B., 1998. Applying Neural Network Models to Prediction and Data Analysis in Meteorology and Oceanography. *Bulletin of American Meteorology Society*, 79(9).

Kingston, G. B., Maier, H. R., and Lambert, M. F., 2005. Calibration and validation of neural networks to ensure physically plausible hydrological modeling. *Journal of Hydrology* 314:158–176.

Lu, X. Dong Z. Y., and Li, X., 2005. Electricity market price spike forecast with data mining techniques. *Electric Power Systems Research* 73: 19–29.

Madani, K., and Lund, J. R., 2009. Modeling California's high-elevation hydropower systems in energy units. *Water Resources Research* 45, W09413. doi:10.1029/2008WR007206.

Maier, H. R., and Dandy G. C., 2000. Neural networks for the prediction and forecasting of water resources variables: a review of modeling issues and applications. *Environmental Modeling & Software* 15: 101–124.

National Oceanic and Atmospheric Administration (NOAA) – National Climatic Data Center, 2009. State of the Climate National Overview Annual 2008 [Online] (Updated 31 June 2009) Available at:www.ncdc.noaa.gov/ sotc/?report=national&year=2008&month=13.

Olsson, J. Uvo, C. B. Jinno, K. Kawamura, A. Nishiyama, K. Koreeda, N. Nakashima, T., and Morita, O., 2004. Neural Networks for Rainfall Forecasting by Atmospheric Downscaling. *Journal for Hydrologic Engineering,* ASCE.

Ortiz-Arroyo, D., Skov, M. K., and Huynh, Q., 2005. Accurate Electricity Load Forecasting with Artificial Neural Networks. In: International Conference on Computational Intelligence for Modeling, Control and Automation and International Conference on Intelligent Agents, Web Technologies and Internet Commerce (CIMCA-IAWTIC'06). IEEE 2005 (1): 94–99.

Pacific Gas and Electric Company (PG&E), 2008. News Release: Rising Natural Gas Prices and Lower Hydroelectric Power Supplies Expected to Increase Electricity Costs. [Online] Available at: www.pge.com/about/news/ mediarelations/newsreleases/q2_2008/080610.shtml.

Ranjbar, M., Soleymani, S., Sadati, N., and Ranjbar, A. M., 2006. Electricity price forecasting using Artificial Neural Network. In: IEEE, *2006 International Conference on Power Electronic, Drives and Energy Systems*.

Yamin, H. Y. Shahidehpour, S. M., and Li, Z., 2004. Adaptive short-term electricity price forecasting using artificial neural networks in the restructured power markets. *Electrical Power and Energy Systems* 26 (2004): 571–581.

Zarezadeh, M., Naghavi, A., Ghaderi, S.F., 2008. Electricity price forecasting in Iranian electricity market applying Artificial Neural Networks. *IEEE Electrical Power & Energy Conference* 2008.

Zhao, J. H., Dong, Z. Y., Li, X., and Wong K. P., 2005. A general method for electricity market price spike analysis. *Proc. IEEE Power Engineering Society General Meeting*, June 2005, pp. 563–570.

Zhao, J. H., Dong Z. Y., and Li, X. 2007. Electricity market price spike forecasting and decision making. *IET Gener. Transm. Distrib., 2007,* 1(4): 647–654.